

OXIDATION AND HYDROLYSIS REACTIONS IN SUPERCRITICAL WATER:
CHLORINATED HYDROCARBONS AND ORGANOSULFUR COMPOUNDS

by

RUSSELL PHILIP LACHANCE

Captain, United States Army

B.S. United States Military Academy, West Point, 1985

Submitted to the Department of Chemical Engineering
in Partial Fulfillment of the Requirements for the Degree of

MASTER OF SCIENCE
in Chemical Engineering

at the

MASSACHUSETTS INSTITUTE OF TECHNOLOGY

June 1995

© Massachusetts Institute of Technology 1995
All Rights Reserved

Signature of Author _____
Department of Chemical Engineering
May 12, 1995

Certified by _____
Professor Jefferson W. Tester
Thesis Supervisor

Accepted by _____
MASSACHUSETTS INSTITUTE OF TECHNOLOGY
Professor Robert E. Cohen

JUL 12 1995 Science
LIBRARIES

**OXIDATION AND HYDROLYSIS REACTIONS IN SUPERCRITICAL WATER:
CHLORINATED HYDROCARBONS AND ORGANOSULFUR COMPOUNDS**

by

RUSSELL PHILIP LACHANCE

Submitted to the Department of Chemical Engineering
on May 12, 1995 in Partial Fulfillment of the Requirements for the
Degree of Master of Science in Chemical Engineering

ABSTRACT

Supercritical water oxidation is an efficient and clean technology for the treatment of aqueous organic wastes. Many organic compounds and oxygen are virtually completely soluble in supercritical water, providing a single-phase medium for rapid oxidation of organic to CO₂, H₂O, and N₂. The scale-up and reliable operation of commercial-sized process equipment require a thorough understanding of hydrolysis and oxidation kinetics, reaction pathways, and mechanisms which were the focus of this study.

Methylene chloride (CH₂Cl₂) hydrolysis and oxidation were examined as part of a collaborative effort of several members of our research group. Experiments were done in an isothermal, isobaric, tubular plug-flow reactor over the range of 450 - 600°C, 4-9 seconds reactor residence time and sub- to superstoichiometric O₂/CH₂Cl₂ feed ratios, all at a pressure of approximately 246 bar. Major products of both hydrolysis and oxidation were carbon monoxide, carbon dioxide, formaldehyde, methanol, hydrochloric acid and molecular hydrogen. Trace quantities of one and two carbon chlorinated hydrocarbons were also detected. Conversion under hydrolysis conditions was very close to that under oxidation conditions. Significant corrosion of the Hastelloy C-276 preheater tubing was observed, most likely caused by the presence of aggressive Cl⁻ ions.

Supercritical water hydrolysis and oxidation of thiodiglycol ((HOC₂H₄)₂S) were performed over the range of 400 - 525°C at a pressure of approximately 250 bar. Two different organic feed systems were examined. One method employed the preheating of an organic solution in water, and a second method delivered pure organic metered from a syringe pump through a cooled nozzle into the mixing tee of the reactor. Under supercritical conditions, thiodiglycol degradation occurred rapidly with and without oxidant. Additional experiments were performed at subcritical temperatures to further explore hydrolysis degradation. Products identified include carbon monoxide, carbon dioxide, hydrogen, methane, ethylene, acetaldehyde, acetic acid, formic acid, thioxane, sulfuric acid, hydrogen sulfide, and elemental sulfur.

Thesis Supervisor: Jefferson W. Tester
Title: Professor of Chemical Engineering
Director, Energy Laboratory

**It should come as no surprise that this thesis is dedicated to my family;
Lisa, Zachary, Hannah, Chelsea and Baby-to-be.
You mean everything to me.**

Several acknowledgments must accompany this thesis, certainly much more than the few I mention below:

First, and foremost, my wife, Lisa, who not only pushed me, kicking and screaming, to complete this work, but flawlessly ran a household of five in addition to volunteer work and a business of her own. Lisa's work will probably never be appreciated through publication, but I'll be the first to tell you that she is an expert in her field.

My son, Zachary, my daughter, Hannah, and my youngest daughter Chelsea who continued to love me whether I was home or not. My children and their accomplishments bring me much more pride than any job I've ever had, and yet one would never know that based on the inequitable time spent with each.

Fellow students of Group Tester, who collectively taught me more than any other facet of graduate school and made research life a little more bearable. These students deserve special recognition:

Phil Marrone, who just about held my hand the entire two years, teaching me everything from proper experimental techniques to changing the name of the Macintosh hard drive and taking time to assist me whenever he possibly could.

Joanna DiNaro and Brian Phenix, who held my other hand as I stumbled through research. I was fortunate enough to take advantage of some of their many innovative ideas (usually with permission) not the least of which was the direct organic feed delivery system and the UV mixing tests of that system.

Matt DiPippo, who could have easily told me to get lost but helped on countless occasions with parts (most of which he knows about), great ideas and IBM expertise.

Randy Weinstein and Mike Kutney, who also continually offered helping hands and were great sources of levity, usually laughing with them and not at them.

Previous students of Group Tester such as MAJ Jerry Meyer, Gabe Worley, Rick Holgate, Fred Armellini, Rich Helling and Paul Webley whose experimental expertise has been inherited by present Tester students and is certainly much appreciated.

Professor Jeff Tester and Dr. Bill Peters, who were both patient enough and committed enough to advise me throughout this research, that was certainly no easy task.

Dr. K.C. Swallow, who selfless, immeasurable assistance was truly exemplary. K.C. did everything from personally analyzing some of my samples to meeting with me on a monthly basis. I can never thank her enough.

Celia Huey, Cadet David Sawyer and Bill Tiebert, who provided valuable services as undergraduate research assistants. It was my pleasure to work with them, and I believe I learned more from them than they did from me.

Members of the 10.978 seminar group, who, despite their lack of courtesy to seminar speakers, always seemed to make you consider issues that you would have otherwise missed.

Members of the U.S. Army ERDEC, especially Paul Bossle, Mike Ellzy and Steve Harvey, who were a tremendous help with TDG analyticals as well as possible reaction pathways.

Major Mike Turner, whose own TDG thesis work and advice over the phone were invaluable to the TDG research presented here.

The U.S. Army and my country, for giving me opportunities and experiences not found in any other job or place in the world.

Table of Contents

List of Figures	11
List of Tables	15
Chapter 1. Introduction and Background	
1.1 Introduction	17
1.2 Properties of Supercritical Water	18
1.3 SCWO Process	22
1.4 Objectives and Approach	25
1.5 Selection of Model Compounds	26
Chapter 2. Experimental Techniques	
2.1 Apparatus	29
2.2 Analytical Methods	40
2.3 System Operating Procedures	46
2.4 Data Reduction	50
2.5 Experimental Uncertainty	52
2.6 Evaluation of Direct Organic Feed System	53
2.7 Evaluation of Plug-Flow Criteria	59
Chapter 3. Experimental Studies of Methylene Chloride Hydrolysis and Oxidation in Supercritical Water	
3.1 Introduction	65
3.2 Literature Review	66

3.3 Experiments Performed	67
3.4 Kinetic Results	69
3.5 Product Distribution	74
3.6 Corrosion	81
3.7 Mechanistic Insights from Experimental Results	82
Chapter 4. Experimental Studies of Thiodiglycol Hydrolysis and Oxidation in Supercritical Water	
4.1 Introduction	87
4.2 Literature Review	88
4.3 Experiments Performed	97
4.4 Kinetic Results	100
4.5 Product Identification	116
4.6 Product Distribution	139
4.7 Mechanistic Insights from Experimental Results	144
Chapter 5. Conclusions and Recommendations	
5.1 Conclusions	149
5.2 Recommendations	152
Appendices	
A. Tabulated Experimental Data	155
B. Nomenclature	163
References	165

List of Figures

Figure 1.1	Density of Pure Supercritical Water	19
Figure 1.2	Solvation Properties of Pure Water at 250 bar	20
Figure 1.3	MODAR Process Flow Sheet	23
Figure 2.1	Schematic for Present MIT Isothermal, Plug-Flow Reactor Apparatus	30
Figure 2.2	Schematic for Revised PFR Apparatus with Direct Organic Feed	37
Figure 2.3	Cooled Nozzle and Mixing Cross Detail for Direct Organic Feed	38
Figure 2.4	UV Absorbance Traces for Continuous Monitoring Tests of Direct Organic Feed Mixing Assembly	55
Figure 2.5	Test of Direct Organic Feed System in PFR Apparatus	58
Figure 3.1	Hydrolysis and Oxidation Conversion of CH_2Cl_2 as a Function of Temperature	70
Figure 3.2	CH_2Cl_2 Conversion vs. Reactor Residence Time	73
Figure 3.3	Distribution of Carbon-containing Products	76
Figure 3.4	Molar Yield of Products vs. Temperature: CH_2Cl_2 Hydrolysis	78
Figure 3.5	Molar Yield of Products vs. Temperature: CH_2Cl_2 Oxidation	79
Figure 3.6	Plausible Reaction Network for CH_2Cl_2 Oxidation in SCW	84
Figure 4.1	TDG Hydrolysis Conversion versus Temperature Reported by Turner (1993)	92
Figure 4.2	Results from Scoping Runs: TDG Hydrolysis and Oxidation in SCW	101
Figure 4.3	Results from Reactor Bypass Runs: TDG Hydrolysis in SCW	101

Figure 4.4	Results from Direct Organic Feed Runs: TDG Hydrolysis and Oxidation in SCW	103
Figure 4.5	Results from Soluble Organic Feed Runs: TDG Hydrolysis and Oxidation in SCW.	106
Figure 4.6	Results from Soluble Organic Feed Runs: TDG Hydrolysis in Subcritical Water	108
Figure 4.7	Assumed First Order Arrhenius Plot for TDG Hydrolysis at Subcritical Temperatures	110
Figure 4.8	Normalized Decay Profile: TDG Hydrolysis in Subcritical Water	113
Figure 4.9	Normalized Decay Profile on a Logarithmic Basis: TDG Hydrolysis in Subcritical Water	113
Figure 4.10	Predicted Conversion of Three Different Models vs. Experimental Conversion: TDG Hydrolysis in Subcritical Water	114
Figure 4.11	TCD Gas Chromatograms for TDG Hydrolysis and Oxidation at 525°C, 260 bar, and Reactor Residence Time of 6.5 seconds	120
Figure 4.12	FID Gas Chromatograms for TDG Hydrolysis and Oxidation at 525°C, 260 bar, and Reactor Residence Time of 6.5 seconds	121
Figure 4.13	ECD Gas Chromatograms for TDG Hydrolysis and Oxidation at 525°C, 260 bar, and Reactor Residence Time of 6.5 seconds	122
Figure 4.14	HPLC Chromatograms from UV Detection at 208 nm for TDG Hydrolysis and Oxidation at 400°C, 260 bar, and Reactor Residence Time of 7.8 seconds	127
Figure 4.15	FID Chromatograms for TDG Hydrolysis and Oxidation at 400°C, 260 bar, and Reactor Residence Time of 7.8 seconds	128

Figure 4.16	Carbon Balances for TDG Hydrolysis and Oxidation in Sub- and Supercritical Water	134
Figure 4.17	Sulfur Balances for TDG Hydrolysis and Oxidation in Sub- and Supercritical Water	135
Figure 4.18	Trends for Unidentified 13 Minute Peak in FID Chromatograms	137
Figure 4.19	Trends for Unidentified 20 Minute Peak in HPLC Chromatograms	138
Figure 4.20	Percent of TDG Carbon Gasification versus Temperature during Hydrolysis and Oxidation Reactions	140
Figure 4.21	Variation of Product Yields with Temperature for TDG Supercritical Hydrolysis Reactions	142
Figure 4.22	Variation of Product Yields with Temperature for TDG Supercritical Oxidation Reactions	143
Figure 4.23	Plausible Reaction Pathways and Hierarchy of Products of TDG Reactions in Sub- and Supercritical Water	145

List of Tables

Table 2.1	Plug-Flow Evaluation Criteria	64
Table 3.1	Groupings of Oxidation Runs for Residence Time and Concentration Variations	69
Table 4.1	Physical Properties of TDG and HD	89
Table 4.2	Previous Batch Test Operating Conditions for TDG from Turner (1993)	90
Table 4.3	Previous Continuous-flow Operating Conditions for TDG from Turner (1993)	91
Table 4.4	CHCl ₃ -soluble Products Identified by GC/MS from 40% by volume HD Hydrolysis Reaction	94
Table 4.5	Product Yields of HD Pyrolysis Reported by Williams (1947)	95
Table 4.6	Analytical Results for Mustard Testing Reported by Downey et al. (1995)	96
Table 4.7	TDG Experiments Performed in this Study	97
Table 4.8	Summary of Compounds Tested as Possible Gas Phase Products	117
Table 4.9	Summary of Compounds Tested as Possible Liquid Phase Products	125
Table A.1	Experimental Data for TDG Hydrolysis and Oxidation Scoping Runs	156
Table A.2	Experimental Data for TDG Hydrolysis Runs with Reactor Bypass	157
Table A.3	Experimental Data for TDG Hydrolysis and Oxidation Runs with Direct Organic Feed	158
Table A.4	Experimental Data for TDG Hydrolysis Scoping Runs with Direct Organic Feed	159

Table A.5	Experimental Data for TDG Hydrolysis and Oxidation Runs with Soluble Organic Feed	160
Table A.6	Experimental Data for TDG Hydrolysis Runs at Subcritical Temperatures	161
Table A.7	Experimental Data for TDG Hydrolysis Runs at Subcritical Temperatures: Residence Time Variations	162

CHAPTER 1

Introduction and Background

1.1 Introduction

Supercritical water oxidation (SCWO) is an efficient and clean technology for the treatment of aqueous organic wastes. Supercritical water (SCW), defined as water at temperatures and pressures above its critical point of 374°C and 221 bar, has unique solvation properties which make it an attractive media for oxidation reactions. Significant decreases in the dielectric constant and hydrogen bonding of SCW creates a solvent very similar to a dense, non-polar gas. In this environment, organics and gases (e.g., O₂, N₂, CO₂, etc.) are completely miscible while inorganic salts have very low solubility. With no interphase mass transport limitations, organics and oxidants react rapidly and completely. The hydrocarbon products of these reactions are CO₂ and H₂O. Heteroatoms (F, Cl, S, P) are converted to mineral acids which can precipitate as salts in the presence of neutralizing base. Nitrogen is typically converted mostly to N₂ with some N₂O produced. A more detailed description of SCWO reactions can be found in a review by Savage et al. (1995) and its cited references.

The SCWO process brings together the organic contaminant with a suitable oxidant (pure oxygen, air or hydrogen peroxide) in a homogeneous supercritical water phase to achieve rapid destruction in residence times of 1 minute or less. A fundamental understanding of model compound hydrolysis and oxidation kinetics and mechanisms is essential to optimizing the preheating, reaction, and salt formation steps of the SCWO process design. To this end, members of our research group have used an isothermal, isobaric, plug-flow reactor system (first built in 1983) to obtain kinetic data and mechanistic information (Helling, 1986; Webley, 1989; Holgate, 1993;

Meyer, 1993). This lab-scale system has gone through several improvements over the past twelve years, but the overall steps remain essentially the same. Organic solutions (less than one percent by weight) and water saturated with oxygen are pumped separately through a preheater system at reaction pressure to attain the desired reaction temperature just prior to mixing. The oxidation reaction begins upon opposed-flow mixing of the two feeds and proceeds through a coiled, tubular reactor under well-defined conditions of temperature, pressure, initial concentration, and residence time. Liquid and gas flow rates are measured and liquid phase and gas phase products are identified and quantified by a variety of instrumental and chemical analytical techniques.

The underlying motivation for this study is twofold. First, this work represents another phase in our evolving research program aimed at providing kinetic data on important model compounds. So far, we have completed studies on CO, H₂, CH₄, CH₃OH, glucose and acetic acid. Interpretations of chemical pathways and rates during hydrolysis and oxidation of these model chemicals will assist the design and operation of SCWO processing units for treating toxic wastes. Second, under the sponsorship of the University Research Initiative of the U.S. Army Research Office we are interested in specific model compounds of relevance to the treatment of military wastes, particularly chemical warfare agents.

1.2 Properties of Supercritical Water

Water transforms into a single, homogeneous, supercritical phase when both its temperature and pressure exceed the critical values of 374.3°C and 217.6 atm (3200 psia). The density of water in this region is a strong function of temperature and pressure (see Figure 1.1). In fact, the density of supercritical water varies by over an

Figure 1.1 Density of Pure Supercritical Water. Data from the NBS/NRC Steam Tables, Haar et al., 1984.

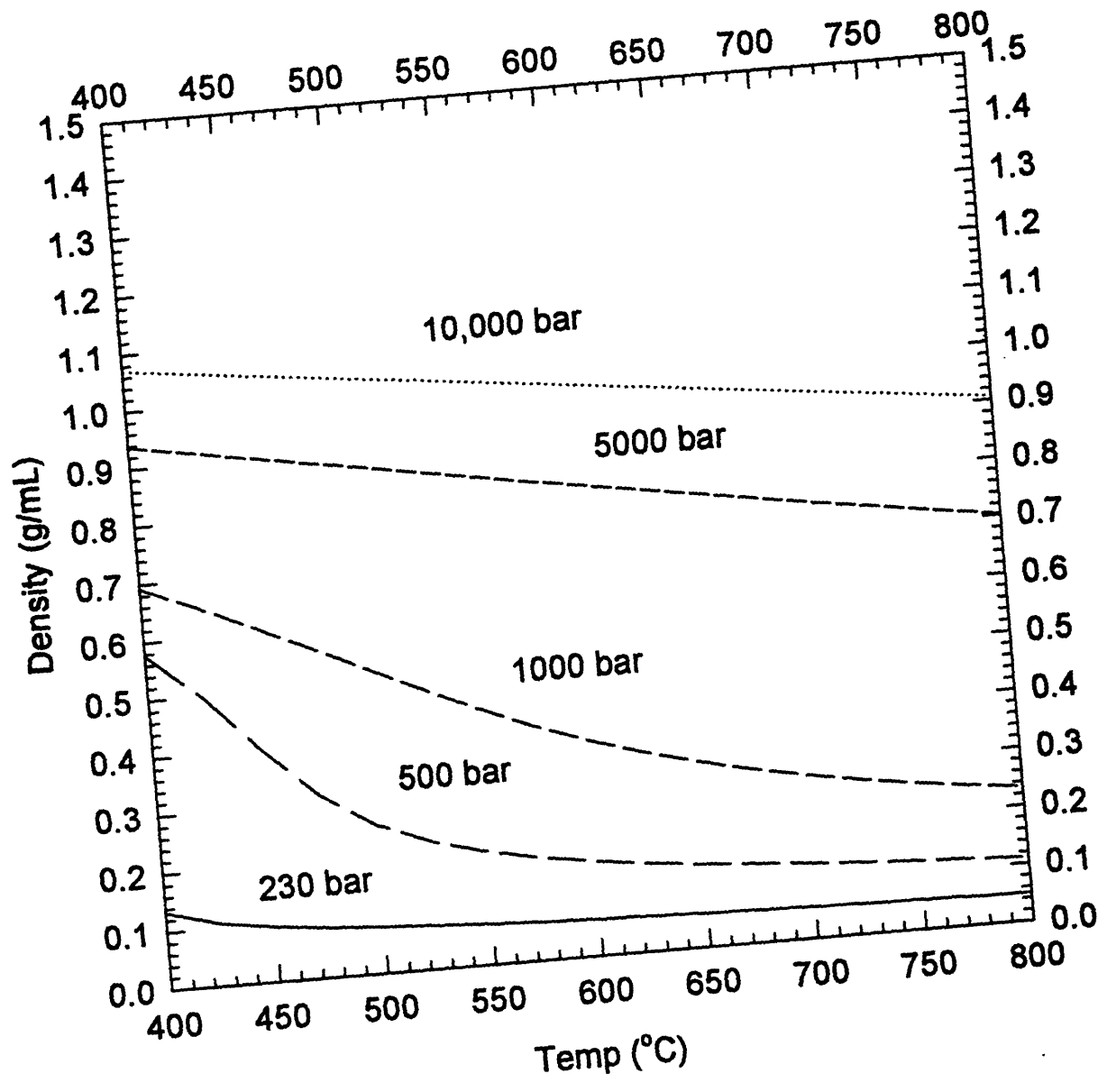
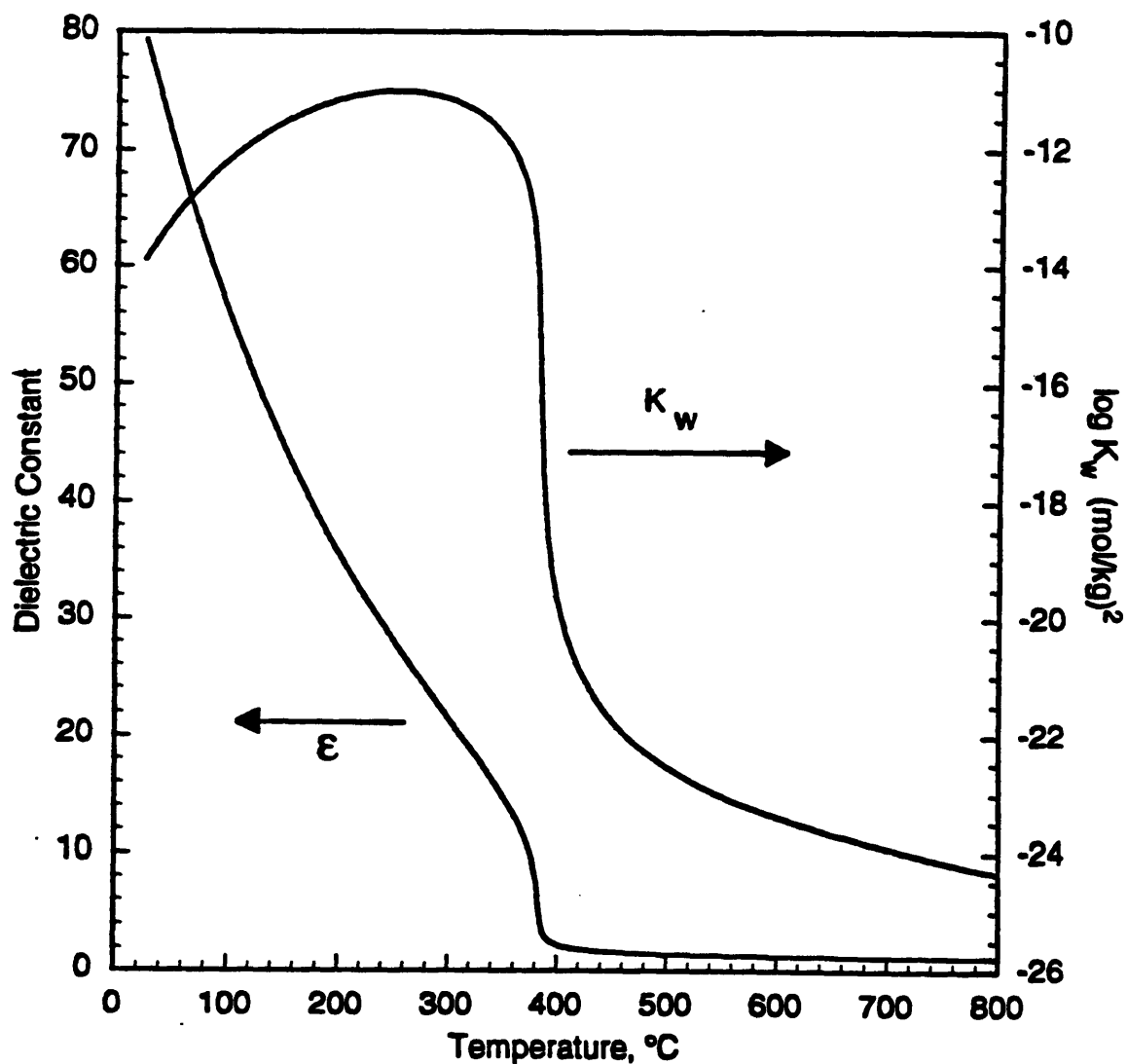


Figure 1.2 Solvation Properties of Pure Water at 250 bar. Properties shown are the static dielectric constant ϵ (Uematsu and Franck, 1980) and the ionic dissociation constant K_w (Marshall and Franck, 1981).



order of magnitude, between a liquid-like value ($\sim 1 \text{ g/cm}^3$ or higher) and a more gas-like value (approximately 0.1 g/cm^3 or lower). For a typical SCWO process, the pressures range from 230 to 250 bar and the temperatures range from 400 to 600°C corresponding to a fluid density range of about 0.13 to 0.07 g/cm^3 .

As seen in Figure 1.2, water's static dielectric constant at 250 bar decreases steadily from a room temperature value of 80 to a value in the supercritical region of 1 to 2 (Heger et al., 1980; Uematsu and Franck, 1980, Franck et al., 1990). This figure also traces the ionic dissociation constant ($K_w = [\text{H}^+][\text{OH}^-]$) from an ambient value of 10^{-14} to a value approaching 10^{-23} in the supercritical region (Marshall and Franck, 1981). Supercritical water also has a high diffusivity (Tödheide, 1972; Lamb et al., 1981) and low viscosity (Tödheide, 1972; Dudziak and Franck, 1966).

As a result of these dramatic property changes, supercritical water acts as a non-polar dense gas with solvation properties similar to a typical liquid hydrocarbon (Josephson, 1982). For example, organics like benzene and methylene chloride are highly soluble in SCW (Connolly, 1966), and “non-condensable” gases like oxygen and nitrogen (Japas and Franck, 1985), carbon dioxide (Tödheide and Franck, 1963) and methane (Krader and Franck, 1987) exhibit complete miscibility. On the other hand, the low solubility and dissociation of inorganic salts in SCW (Armellini et al., 1994) allow for their separation from the reactants and products of interest. The phenomenon of supercritical water thus makes for an effective means for oxidizing organic wastes; the reaction of oxidant and organic is not limited by mass transfer, undesirable heteroatoms are separated through precipitation, and the kinetics are fast and complete at temperatures of interest.

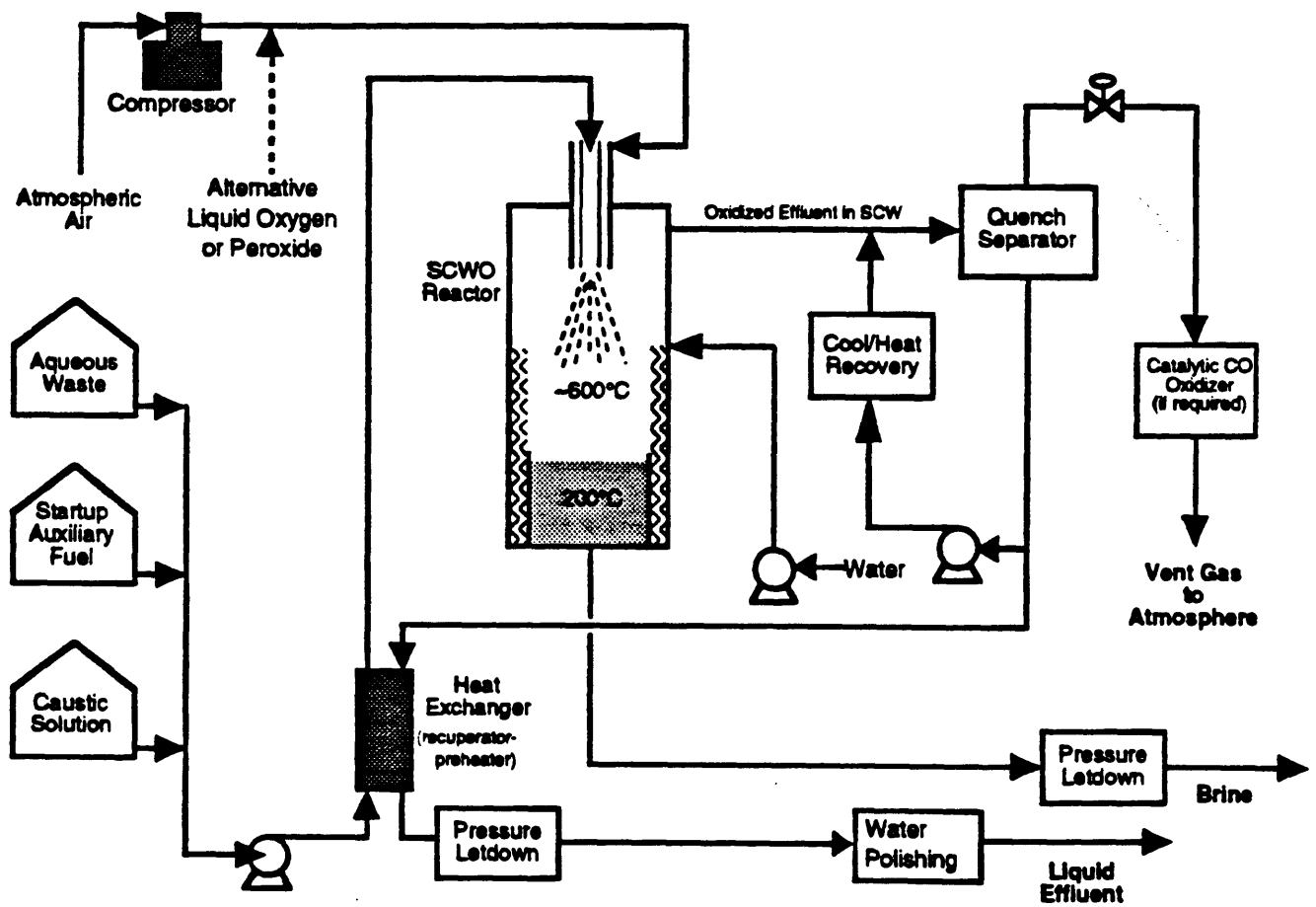
1.3 SCWO Process

A variety of SCWO reactors and process designs have been described and patented (some of the patents include Modell, 1982, 1985; Modell et al., 1993; Hong, 1991; Huang, 1992; Huang et al., 1992; Titmas, 1986). A thorough description of the SCWO process can be found in three different reviews by Modell, 1989; Thomason et al., 1990; and Tester et al., 1993. The process flowsheet given in Figure 1.3 corresponds to a vessel-type reactor concept where salt is removed in a concentrated brine at subcritical temperatures. The seven major steps of SCWO processes are: feed preparation and pressurization; preheating; reaction; salt formation and separation; quenching, cooling and heat recovery; pressure letdown; effluent water polishing.

Feed preparation and pressurization is accomplished by considering the reactant heating value, its heteroatom content, the available oxidant and means of pressurizing both waste and oxidant feeds. The SCWO process operates with an optimum heating value for the organic waste which can be adjusted by diluting a high-heating value waste or adding auxiliary fuels to make the destruction of low-heating value wastes more economical. If the waste contains heteroatoms (Cl, F, P, or S), neutralizing base is usually included in the feed stream. The oxidant can be compressed air or oxygen or hydrogen peroxide based on safety and process cost considerations. The aqueous organic waste and oxidant are then pumped from atmospheric pressure to the desired supercritical pressure.

Preheating of waste and oxidant feed streams can be achieved by heat exchange with the hot process effluent. This helps the initiation of the oxidation reaction and makes efficient use of plant energy production through heat integration.

Figure 1.3 MODAR Process Flow Sheet. Adapted from Barner et al., 1992.



The *reaction* begins by mixing the aqueous waste with oxidant. The heat produced from this exothermic reaction increases the mixture temperatures to 550°C-650°C which accelerates the reaction rate and reduces the required residence time. More refractory compounds can be further processed in a second stage reactor or through a recycle.

Salt formation and separation occurs as the mineral acids (from heteroatoms) mix with caustic forming inorganic salts which rapidly crystallize under shock-like conditions in the reactor's supercritical water media. The more dense salts separate from the SCW and fall to the bottom of the reactor. This precipitate can then be removed as solids or redissolved in cold water and removed as a liquid brine.

In *the quenching, cooling and heat recovery stage*, the gaseous effluent exiting the top of the reactor is first mixed with cold water to redissolve any small amount of entrained salt. Then the effluent, now consisting of SCW, carbon dioxide and possibly some nitrogen, is further cooled to atmospheric temperatures. The energy recovered from the effluent can be used for a variety of needs including compression of the oxidant and pumping and preheating the feeds.

After *pressure letdown, phase disengagement* is accomplished in multiple stages to minimize valve erosion and maximize separation. The gas phase consists primarily of carbon dioxide and oxygen (when oxidant is in excess of stoichiometric requirements). Molecular nitrogen may also be present if air is the oxidant or if the waste contained nitrogen atoms.

Effluent water polishing is included as a final step to remove any trace metal concentrations found in the original waste or formed from the corrosive nature of supercritical brines.

The attractive properties of SCW along with an efficient SCWO process design lead to several advantages over conventional waste treatment technologies. The entire SCWO process can be completely enclosed, and it is a procedure that destroys contaminants as opposed to simply extracting them and/or containing them. SCWO uses only moderate temperatures to process wastes quickly and efficiently with innocuous reaction products.

1.4 Objectives and Approach

Objectives

The primary objective of this work was to obtain and analyze kinetic data on the hydrolysis and oxidation of selected model compounds in supercritical water under well-defined conditions. To increase our understanding of important mechanisms and chemical pathways, we wanted to explore the effects of two specific heteroatom bonds, C-Cl and C-S.

Approach

The approach to accomplishing the objectives was taken in the following steps:

- 1. Select Model Compounds.** A discussion of this topic is given in Section 1.5.
- 2. Choose Operating Conditions.** The operating conditions for experiments with each compound were chosen based on a literature search of related reactions and the results of initial scoping runs. The conditions for methylene chloride experiments were temperatures of 450 - 600°C, reactor residence times of 4 - 9 seconds, initial organic concentrations of $0.24\text{-}0.9 \times 10^{-3}$ mol/L and initial oxygen concentrations of $0.5\text{-}2.1 \times 10^{-3}$ mol/L, all at a pressure of 246 bar. The conditions for thiodiglycol (TDG) experiments were temperatures of 100 - 600°C, subcritical reactor residence times of 38 - 180

seconds with an initial organic concentration of 2.5×10^{-3} mol/L, supercritical reactor residence time of 6 seconds with an initial organic concentration of 0.5×10^{-3} mol/L and a stoichiometric oxidation O_2 /TDG feed ratio of 7, all at a pressure of 250 bar.

3. Develop Chemical Analysis Methods. Accurate and sensitive methods of identification and quantification were developed for each compound and their possible degradation products. More details on this topic are provided in Sections 2.2, 3.5 (methylene chloride) and 4.5 (thiodiglycol).

4. Conduct Experimental Kinetic Measurements. Detailed results are presented in Chapter 3 for methylene chloride and Chapter 4 for thiodiglycol.

5. Analyze and Correlate Data. An analysis of the results is presented in Chapter 3 for methylene chloride and Chapter 4 for thiodiglycol.

6. Develop Global Kinetic Rate Expression and Mechanism. This topic is addressed in Chapter 3 for methylene chloride and Chapter 4 for thiodiglycol.

1.5 Selection of Model Compounds

The central objective of this particular study is to examine the supercritical water hydrolysis and oxidation reactions of two model organics containing Cl and S heteroatoms. The interest in the C-Cl bond stems from the number of toxic chlorinated organics that require hazardous waste treatment. The C-Cl chemistry is also important in the treatment of several chemical warfare agents. Similarly, the C-S bond is found in several toxic wastes as well as the mustard family of chemical warfare agents.

Methylene chloride (CH_2Cl_2) was chosen to represent a simple C-Cl bond in a chlorine-containing organic. It has a simple C_1 structure with two C-Cl bonds. Methylene chloride is also considered a waste itself. It is popular in industry because of its nonflammability, low boiling point and properties as a strong non-polar solvent. Recent concern over methylene chloride's effects on public health and the environment,

coupled with its popularity in the chemical industry have turned it into an important hazardous waste to avoid, collect and remediate. Its label as a real-world contaminant and its simple structure make it an excellent choice as a model compound for SCWO.

Thiodiglycol (TDG), $(\text{HOC}_2\text{H}_4)_2\text{S}$, was chosen to represent the C-S bond. Although TDG does not have a simple structure, it does have several other attractive characteristics. Most importantly, TDG is an excellent simulant for the chemical warfare agent, HD sulfur mustard, $(\text{ClC}_2\text{H}_4)_2\text{S}$. TDG is not only a key ingredient in mustard production but it is also a primary hydrolysis product of mustard found in degrading stockpiles and in the decomposing residue of agents employed on battlefields. The hydrolysis of mustard can occur under ambient conditions following the simple reaction



With the growing international concern over the difficult task of decontaminating and remediating aging chemical warfare stockpiles, some countries are beginning to look at SCWO as an alternative efficient and effective technology. A first step before conducting SCWO reactions of actual chemical agents is to gain fundamental knowledge through reactions with an appropriate simulant. TDG serves as an excellent simulant for the mustard vesicant with the correct C-S bond arrangement. An alternative to TDG would be dimethylsulfoxide (DMSO), $(\text{CH}_3)_2\text{SO}$. In fact, MODAR, Inc. performed destruction efficiency studies of DMSO through SCWO in their pilot-scale apparatus (Thomason et al., 1990). Although this might be a simpler compound for the study of C-S chemistry, it is not the best choice to simulate sulfur agents. DMSO contains a sulfoxide bond which may be easier to oxidize than the reduced sulfide bond found in mustard agents.

CHAPTER 2

Experimental Techniques

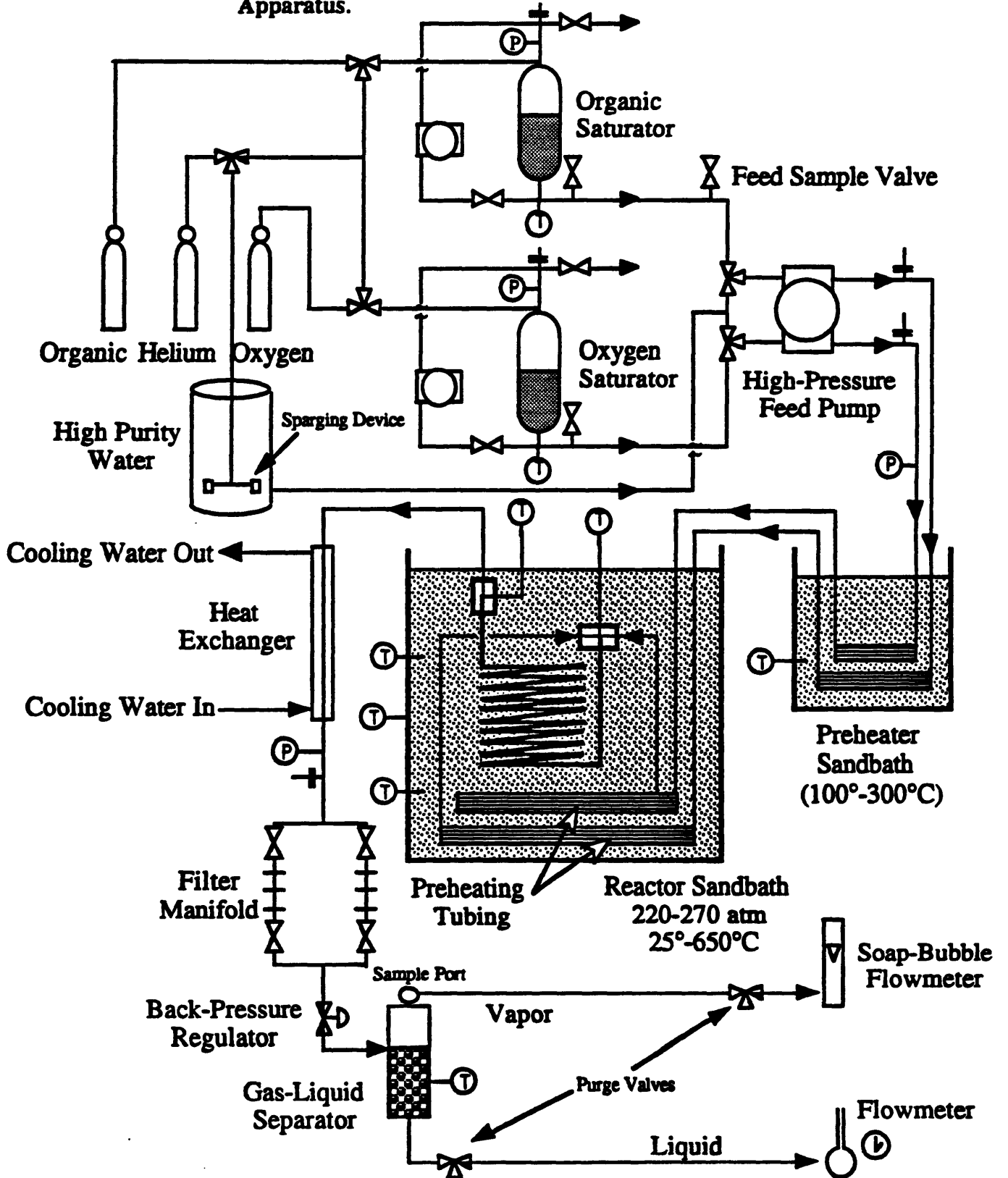
2.1 Apparatus

Experiments were conducted in an isobaric, isothermal plug-flow apparatus that is essentially the same system used and upgraded by several investigators at MIT since 1983 (Helling, 1986; Webley, 1989; Holgate, 1993; Meyer, 1993). For all methylene chloride experiments and most thiodiglycol experiments, the traditional organic solution feed technique was used and a diagram of the appropriate system configuration is shown in Figure 2.1. For sixteen thiodiglycol experiments, a new organic feed delivery technique was designed and tested. For these experiments, the apparatus configuration was changed considerably (see Figure 2.2). The two designs are described separately below.

2.1.1 Soluble Oxygen and Organic Feed Methods

Feed solutions are delivered to the reactor from two, three-liter, stainless steel tanks (saturators) (Hoke 8HD3000, maximum pressure 1800 psig). The oxygen solution is prepared by adding approximately 2500 mL of high purity water (all water used was purified using a Barnstead NANOpure system) to the oxygen saturator and pressurizing it with compressed oxygen from a cylinder (Airco), adjusting the pressure to achieve the desired concentration. A single-head, positive displacement pump (LDC Analytical/Milton Roy minipump) provides agitation by circulating the water throughout the saturator. This recirculation pump operates overnight at its maximum flow rate (~7.5 mL/min.) to turn the saturator volume over at least twice, helping to

Figure 2.1 Schematic for Present MIT Isothermal, Plug-Flow Reactor Apparatus.



achieve equilibrium. With this system, the maximum oxygen concentration in the reactor is limited to approximately 0.03 wt% (0.01 mol/L) by the pressure rating of the saturator and the maximum flow rate of the feed pump. Hence, kinetics are only investigated over a limited range of organic feed concentrations. Higher concentrations, however, would lead to reactor non-isothermality with the significant reaction exotherms typical of oxidation reactions. When the organic is gaseous at ambient conditions, the procedure for preparing feed solution is the same as for oxygen solutions. For the organics studied here, which were liquids at ambient conditions, feed solutions were prepared in a two-liter volumetric flask, loaded into the organic saturator and pressurized with 1 bar of helium. Methylene chloride's volatility and low solubility in water (1.32 g/100 mL of water at 25°C) made preparing accurate feed compositions difficult. After evaluating several different techniques, the best method (and the one used for all experiments) employed a Hamilton liquid syringe to add the desired amount of pure methylene chloride to the water. The flask was vigorously shaken until the organic phase disappeared (dispersing the organic was never a problem since the amount of methylene chloride added was always an order of magnitude below its solubility limit). Thiodiglycol does not have the volatility or water solubility problems of methylene chloride but its viscous nature made it difficult to handle with syringes or pipettes. Experiments revealed that thiodiglycol solutions were best prepared by weighing the desired amount of thiodiglycol in a weight boat on a Mettler AE100 balance, and subsequently adding it to the flask of water. All liquid feed solutions were not prepared or loaded until we were within one hour of the beginning of the experiment in order to preserve their integrity (i.e., reduce losses due to volatility in the case of methylene chloride).

Each feed was delivered to the reactor in separate lines by a single, high-pressure, variable-speed, duplex pump (LDC Analytical/Milton Roy minipump with a maximum flow rate of 7.5 mL/min. per pump head, 15 mL/min. combined). For

hydrolysis experiments, high purity water was pumped through the oxygen side from a separate feed tank. During the thiodiglycol study, two diffusing stones, made of fused crystalline alumina grains and attached to a helium line, were installed in the bottom of the high purity water tank. Prior to each experiment, the water was sparged with helium for at least one hour to remove residual oxygen. A fine metering valve (Swagelock Model # SS-4MG) controlled the helium flow. A one-time measurement with a dissolved oxygen probe showed that this method of sparging reduced the oxygen concentration from approximately 8 ppm to less than 100 ppb. System pressure was maintained by a back-pressure regulator (Tescom Model 26-3220 for most experiments, a GO Model #BP-66 was used for some of the thiodiglycol experiments) positioned just prior to the gas-liquid separator. Pressure was measured both upstream and downstream of the reactor. A pressure transducer (Dynisco μ PR690, 0-690 bar) was positioned near the exit of the heat exchanger and a pressure gauge (Omega Engineering, 0-517 bar) was positioned just downstream of the feed pump. During an experiment, these devices read essentially the same pressure within the natural variability of system pressure (most likely due to pump pulsations) and the readability of the pressure gauge (combined effects being ± 3 -7 bar), verifying that the pressure drop across the system was negligible relative to the normal operating pressure of 250 bar. High purity water from a separate feed tank (pressurized with approximately 1 bar helium) is pumped at pressure through the entire system during heatup of the reactor. Feeds are switched to the oxygen and organic solutions in the saturators once desired reactor conditions have stabilized for at least 30 minutes.

Both solutions pass separately through 5 ft. of 1/16 in O.D., 0.01 in. wall, 316 stainless steel tubing in the preheater fluidized sand bath (Techne Model SBL-2). This particular sand bath was not turned on during any organic solution feed experiments to prevent the premature breakdown of the organic. The feeds then enter the main fluidized sand bath (Techne Model FB-08) by first passing through an additional

preheating section of 3.0 m (heated length 2.8 m), 1/16 in. O.D., 0.01 in. wall, Hastelloy C276 tubing. The solutions are mixed (opposed-flow mixing) in a Hastelloy C276 high-pressure cross fitting (High Pressure Equipment #60-24HF4) at the top of the reactor. The bottom port of that inlet cross was connected to the reactor and the two horizontal ports were used for the opposing feeds. The fourth port housed a 1/16 in., Inconel-sheathed, type K thermocouple (Omega Engineering) positioned in the fluid to measure the mixing temperature. The same type thermocouple is located in the fluid at the exit of the reactor, housed in a Hastelloy C276 high pressure tee fitting (High Pressure Equipment #60-23HF4). Additional external thermocouples (type K) are located outside the top and bottom of the reactor in the fluidized sand. Ordinarily all thermocouple measurements, including a fifth thermocouple built into the sand bath itself, are within a few degrees Celsius of each other. There were a few experiments where the inlet temperature was significantly less than the other recorded temperatures (5-12°C for lower temperature experiments (400-450°C) where increased flow rates were used to maintain the same reactor residence time). This problem was possibly the result of poor fluidization of the sand. Nevertheless, based on heat transfer arguments presented in Holgate (1993), the temperature that best represents the majority of the reactor is the exit temperature which is consistently in good agreement with the three external thermocouple readings of the sand. All system thermocouple readings are recorded every two minutes during an experiment using a HOTMUX temperature data logger from DCC Corporation that interfaced with an IBM-compatible 286 computer.

The reactor is an Inconel 625 tubing coil, 4.71 m long, 6.35 mm O.D. x 1.71 mm I.D., which corresponds to a calculated internal volume of 10.82 cm³. The total calculated internal volume is 11.11 cm³ which includes the volume of the entrance and exit fittings. Reynolds numbers in the reactor are maintained above the critical value for laminar flow (2100), which ensure transition or turbulent flow conditions. Upon exiting the reactor, the mixture passes through a short riser section having an internal

volume of 0.51 cm³ which is above the level of fluidized sand and is then rapidly quenched in a water-cooled, countercurrent shell-and-tube heat exchanger. A reactor bypass was employed in certain hydrolysis experiments for both methylene chloride and thiodiglycol. The bypass took the place of the reactor and consisted of a 17.25 in. 316 stainless steel tube (1/4 in. O.D., 1/16 in. I.D.) which connected the mixing cross directly to the heat exchanger. The internal volume of this connection was less than 10% of the reactor volume and was well suited for studying degradation of organics in solution during preheating.

For the thiodiglycol experiments, a filter manifold, similar to the one used in the University of Texas continuous-flow reactor system (Turner, 1993), was installed after the heat exchanger. The manifold consisted of two parallel sets of three series-connected Nupro Model SS-4TF in-line filters. Each set of filters had a high pressure needle valve (High Pressure Equipment # 20-11LF4) upstream and downstream which allowed each one to be isolated for replacement during operation. Each set of filters contained sintered stainless elements of different pore sizes arranged in descending order (15, 7, and 2 micron). The purpose of this improved filter system was to remove solid particles typically found in reactor effluents of thiodiglycol hydrolysis experiments. The unfiltered particles would clog the back pressure regulator which caused pressure and flow control problems. The filter manifold improved system performance somewhat, but both sets of filters had to be used simultaneously and filter elements had to be replaced at least every other experiment.

The cooled effluent finally passes through the back pressure regulator and the resulting two phases are separated in a gas-liquid separator (1/2 in. O.D. 316 stainless steel tube partially filled with glass beads). It is assumed the two streams are in equilibrium when they are separated. A soap-bubble flowmeter is used to measure the

gas flow and the liquid flow rate is measured by recording the time required to fill a volumetric flask.

The present apparatus described above includes several modifications from previous designs that are summarized below:

1. The system high-purity water feed tank was modified by installing diffusing stones attached to a helium line and a venting system which allowed for sparging of all water used in the apparatus.
2. A low pressure feed sample valve was installed on the organic line just before the feed pump. This allowed for more accurate sampling of the organic feed solution and was particularly helpful for measurements with the volatile organic, methylene chloride.
3. A filter manifold (described in detail above) was added just before the back pressure regulator to remove particles from the effluent and maintain the performance of the back-pressure regulator.
4. Several improvements were made to the gas-liquid separator assembly to better resolve the composition of the gas phase (particularly in cases of low gas flow rates) and liquid phase more quickly. For the gas phase, the internal volume of the line to the soap-bubble flow meter was reduced, the gas sampling port was moved closer to the top of the separator and a three-way valve was installed to allow purging of the line prior to sampling. Also, the overall length of the separator was reduced to decrease the hold-up volume of the gas phase. The resulting gas phase hold-up volume was decreased to approximately four times less than the previous system. For the liquid phase, a three-way valve was installed at the bottom of the separator to allow draining of the liquid prior to sampling.
5. As mentioned above, the temperature measurement system was automated with a data logger reading thermocouple signals every two minutes,

converting those to temperature readings and saving and printing the data. Previously, all nine thermocouples in the system were manually read and recorded every ten minutes.

6. The voltage to the sand baths and the recirculation pumps was boosted from 208 volts as supplied to 240 volts by a transformer. This significantly improved the performance of the recirculation pumps and the sand baths which were all rated at 240 volts.

2.1.2 Direct Organic Feed Method

To keep thiodiglycol from degrading in the preheater coil, an alternate feed system was designed and tested. The objective of this technique was to deliver pure organic to the head of the reactor at temperatures much less than supercritical water (thus avoiding thermal breakdown) and at the proper flow rate to explore the same range of concentrations as previous studies. The concept was first developed by co-workers in the lab as a way of introducing organics with water solubility problems (benzene in particular). The foundation of this feed delivery system is a syringe pump. The model used for experiments in this study was an Isco Model #260D with a flow rate range of 1 $\mu\text{L}/\text{min}$. to 100 mL/min . at pressures from ambient to 414 bar. The pump dispenses liquids at a constant flow rate (adjusting to the varying system pressure) by slowly moving a piston in a cylinder containing pure organic (maximum capacity of 265 mL) which displaces the appropriate volume of liquid.

Several modifications were made to the overall apparatus (see Figure 2.2) in order to accommodate this direct organic feed system. Oxygen was delivered in the same manner as described in Section 2.1.1, but the line from the organic saturator was closed and pure water flowed in the organic delivery line downstream from the feed pump. A pulse damper (SSI LO-Pulse) was installed immediately after the feed pump

Figure 2.2 Schematic for Revised PFR Apparatus with Direct Organic Feed.

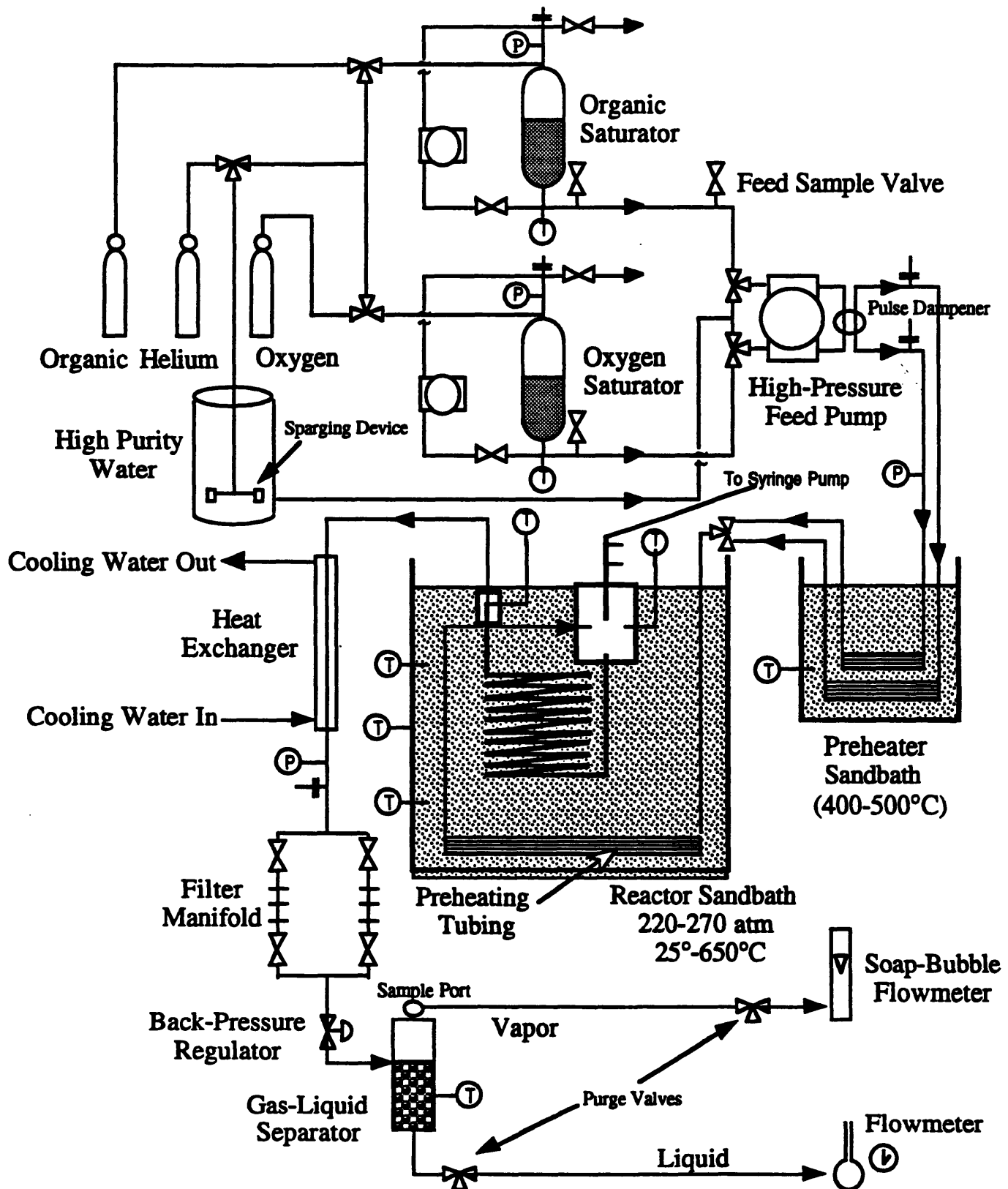
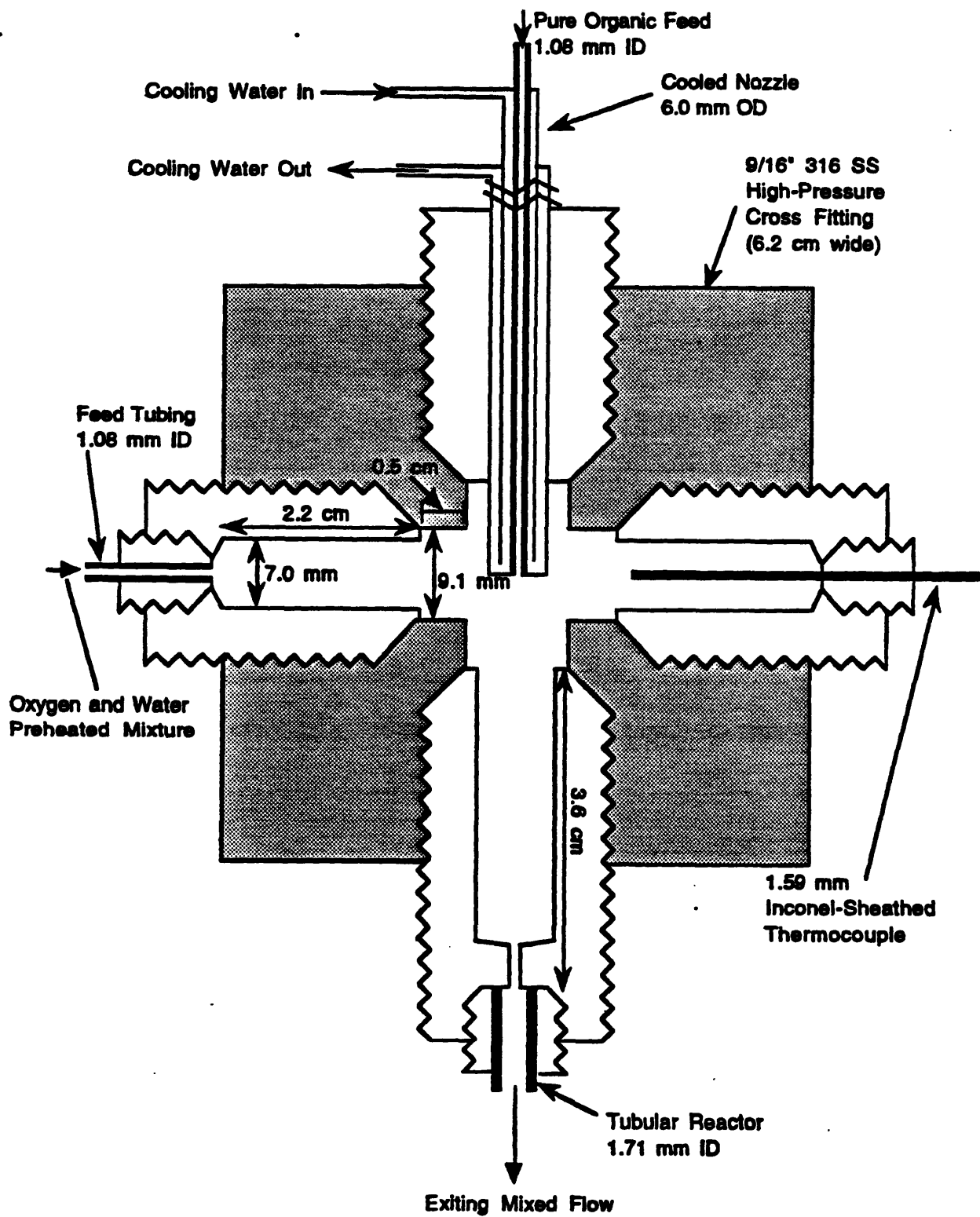


Figure 2.3 Cooled Nozzle and Mixing Cross Detail for Direct Organic Feed.

to reduce system pulsations which would interfere with uniform mixing of the water and oxygen flow with the pulse-less organic micro-flow (a term used to best describe the extremely slow organic flow of this system). Unfortunately, the pulse damper used did not have a significant effect (pulsations were still ± 50 -100psig). Perhaps using two pulse dampers in series or one for each pump head or a more expensive model may have given better results. A new preheater sand bath was used (Tecam SBS-4 from a sister lab) which had a faster heating rate and a higher maximum temperature. This preheater sand bath was energized for all direct organic feed experiments because it was merely preheating water and oxygen. Upon exiting the preheater sand bath, the two lines were joined in a Swagelock 1/8 in. 316 stainless steel tee, and the lines between the two sand baths were wrapped in insulation tape. In the main sand bath, the single water oxygen feed entered a second preheating coil that was 21 ft. of Hastelloy C276 tubing (1/16 in. O.D., 0.01 in. wall). The water-oxygen stream mixed with the organic stream in a 9/16 in. high pressure 316 stainless steel cross (High Pressure Equipment # 20-24LF9) (see Figure 2.3, Cooled Nozzle and Mixing Cross Detail for Direct Organic Feed).

The design of the mixing cross and the cooled nozzle used for direct organic delivery to the cross was originally developed by Armellini (1993) in our lab for injecting relatively cold salt solutions into supercritical water in his study of shock crystallization phenomena. The cooled nozzle consisted of three concentric tubes; the inner and outer tubes were made of Hastelloy C276 and the middle tube, which was only exposed to high purity cooling water, was made of 316 stainless steel. The tip of the nozzle was a 1/4 in. disk punched out of a 1/16 in. sheet of Hastelloy C276 metal. A 1/16 in. hole was drilled out of this disk and the disk was electron-beam welded to the 1/16 in. O.D. inner tube and the 1/4 in. O.D. outer tube. The 1/8 in. O.D. middle tube was then lowered over the inner tube and sealed in place with Swagelock tees and reducing unions. The inner tube was united with another 1/16 in O.D. tube that ran to

the syringe pump. The high purity cooling water was supplied from a five gallon Nalgene bottle, pressurized with 1 bar of helium. A fine metering valve (Swagelock Model # SS4MG) controlled the cooling water flow rate. Typical cooling water flow rates ranged from 2.0 to 3.0 g/min. As depicted in Figure 2.3, the cooling water flowed into the nozzle along the inner tube, reversed directions at the tip of the nozzle and flowed out along the outer tube.

The tip of the cooled nozzle was positioned in the center of the cross, down from the top fitting. The supercritical water and oxygen stream entered the cross from a horizontal side port. A 1/16 in. O.D. Inconel-sheathed thermocouple occupied the other side port and the reactor was connected to the cross at the bottom port. To reduce the void volume and improve mixing in this relatively large cross, zirconia beads (approximately 1/16 in.O.D.) were packed into the cross through the side port used to support the thermocouple. The measured void volume of the beads was about 40% which reduced the calculated internal volume of the cross from 4.48 cm³ to 2.48 cm³ (the internal volume of the thermocouple fitting did not have zirconia beads). Unfortunately, this volume was still a significant part of the total reactor volume (18.5% of a total volume of 13.42 cm³). The parts of the overall apparatus that are downstream of the reactor remained the same as described in Section 2.1.1 above.

2.2 Analytical Methods

2.2.1 Gas Phase Analysis

The gas phase from all experiments was analyzed using three separate gas chromatographs (GCs). Gas samples from early methylene chloride experiments were also analyzed on a fourth separate GC described in section 2.2.2 below. Two GCs

were Hewlett Packard (HP) 5890 Series II. One was equipped with separate thermal conductivity (TCD) and flame ionization (FID) detectors and a packed column inlet and capillary column, split/splitless injection port. The other HP GC was equipped with a second FID, an electron capture detector (ECD) and two, capillary column, split/splitless injection ports. Both HP GCs were interfaced to a Hewlett Packard Vectra computer with HP Chem Station software for data acquisition and analysis. The third GC was a Perkin Elmer Sigma 1B GC with TCD and FID detectors and two packed column inlets.

The HP TCD was used to detect O₂, N₂, CO₂, C₂H₄, C₂H₆, CH₄, C₂H₂, CO and H₂S (order of elution). This detector was also sensitive to SO₂ but it was not found in any sample. The original method was first developed by Helling (1986) and Webley (1989) for a different GC. Two packed columns were employed, a 12 ft. x 1/8 in. stainless steel column packed with 80/100 Poropak T (Column I) and a 8 ft. x 1/8 in. stainless steel column packed with 60/80 mesh molecular sieve 5A (Column II), and connected by an air-actuated switching valve. The carrier gas and reference gas were high grade (in this case, high grade is a purity of five 9s, i.e., ≥ 99.999% pure) helium with a carrier gas flow rate of 20 mL/min. The inlet temperature was 60 °C and the detector temperature was 100 °C with the sensitivity of the TCD set on low. Oven temperature program was 60 °C for 7 minutes, ramp 40 °C/min. to 100 °C and hold at 100 °C for 6 minutes (7 minutes for thiodiglycol samples). The switching valve was employed such that samples pass through Column I and then Column II; immediately after O₂ and N₂ elute, the valve (and order of the columns) is switched so CO, CH₄, H₂S and SO₂ pass through both columns and Column I a second time while CO₂ and other gases only pass through a single column (Column I). A small C₂H₄ peak can be lost at high CO₂ concentrations; otherwise, this method provides rapid separations and well-resolved peaks.

The Perkin Elmer TCD was used to quantify hydrogen and helium. Residual amounts of helium in the effluent were the result of using helium throughout the system. The HP GC was not sensitive to hydrogen because of similarities between the thermal conductivities of hydrogen and helium (carrier and reference gas). For this reason, nitrogen was used as the carrier and reference gas with a carrier gas flow rate of 40 mL/min. The same columns were used but the switching valve was not employed. The oven temperature program was isothermal at 60 °C for 7 minutes. Actual pure gases were used to volumetrically calibrate both TCDs.

The ECD was used in the methylene chloride and thiodiglycol experiments. The ECD was purchased because of its excellent sensitivity and selectivity for chlorinated species, but it also proved to be fairly sensitive and selective for sulfur gases. In both cases, the inlet was operated in the split mode using a 20 µL injection size for methylene chloride studies and a 200 µL injection size for thiodiglycol studies. A DB-624 capillary column was used to separate chlorinated species while a DB-1 capillary column with cryogenic cooling was used to separate sulfur species. In both cases, high grade helium was the carrier gas and high grade nitrogen was the makeup and anode purge gas. An intricate, quantitative calibration method was developed for some chlorinated species using the ECD, but sulfur species were merely identified and not quantified with this detector.

An FID was used during the thiodiglycol experiments which provided improved sensitivity for hydrocarbon gases. The method employed an inlet operating in the splitless mode and an injection size of 20 µL. A GS-Q PLOT column with cryogenic cooling provided good separation of C₁-C₄ hydrocarbon gases. Helium was used as the carrier gas and nitrogen was used as the makeup gas. Time did not permit the difficult job of quantitatively calibrating this method but it still provided valuable information for species identification.

The gas phase of methylene chloride experiments was further analyzed for formaldehyde (HCHO) and methanol. The gaseous effluent flow was redirected through a glass impinger (containing a known amount of water) for a fixed period of time. The liquid solution was then analyzed as described below. The presence of Cl₂ gas was also checked by using an ortho-toluidine colorimetric test.

2.2.2 Liquid Phase Analysis

Methylene Chloride Experiments: The primary method for methylene chloride determination used an electrolytic conductivity (Hall) detector (ELCD) in a Tracor 585 GC. The ELCD is particularly sensitive and selective for chlorinated species. This method was also used for early gas samples prior to employing the ECD. Liquid compounds were vaporized and separated on a DB-624 column with helium as the carrier gas. During the methylene chloride study, the ELCD performance degraded and an FID method was developed. Separation for the FID was accomplished with a DB-1 column using helium as the carrier gas and nitrogen as the makeup gas. An HP autosampler was purchased and used for the analysis of several methylene chloride samples. The improved injections from the autosampler resulted in better, reproducible quantification of all liquid samples. A third GC method employed the second FID to quantify methanol. In this case, an SPB-1 column provided separation also with helium carrier gas and nitrogen makeup gas.

Formaldehyde in the liquid phase was detected and quantified using a colorimetric test known as the chromotropic acid method (Bricker and Vail, 1950; West and Sen, 1956; Altshuller et al., 1961). This method reacts aqueous formaldehyde (in the presence of excess sulfuric acid) with a 1% solution of chromotropic acid in

concentrated sulfuric acid to form a violet color. The original formaldehyde concentration determines the intensity of the color which was calibrated using a spectrophotometer (Shimadzu UV160U) set a 580 nm. This method gave a linear response to formaldehyde concentrations between 0.05 and 2.00 ppmw (by weight). Compounds that were known interferences to color development were not present at relevant concentrations in effluent samples.

A chloride specific combination ion electrode (Orion Research, Inc.) measured HCl concentrations. Interfering ions, as listed in the electrode manual, were not present in any samples. All analytical methods were calibrated regularly with liquid solution standards. For methylene chloride itself, standards in methanol were purchased from a professional lab (Accu Standard) to ensure precise quantification.

Thiodiglycol Experiments: Thiodiglycol (TDG) concentrations were first determined using an FID with separation provided by a DB-1701 column. This method was problematic with TDG retained in the column and the inlet liner. As a result, significant amounts of residual TDG would elute even with injections of just pure water, making accurate quantification difficult. The problems with GC analysis of TDG were verified by analytical chemists from the U.S. Army Edgewood Research, Development and Engineering Center (ERDEC), an organization with a wealth of experience in the analysis of TDG and related compounds. Upon their recommendation, an isocratic, high performance liquid chromatography (HPLC) method was adopted for thiodiglycol quantification; a method which was originally developed by ERDEC (Bossle et al., 1993).

The HPLC procedure calls for separations using an ion-exclusion column (Interaction ORH-801 column with guard column was used here) with an isocratic, 100 nM perchloric acid mobile phase (Rainin HPXL solvent delivery system used).

However, this particularly weak ionic-strength mobile phase of very dilute perchloric acid resulted in poor separation performance for several compounds of interest (e.g., formic acid, acetic acid). During the TDG study, the mobile phase was changed to 0.002 M H₂SO₄ (as recommended in the column manual) which drastically improved column performance. The final, optimized method used a mobile phase flow rate of 0.5 mL/min., a column temperature of 65°C (Timberline column heater) and ultra-violet (UV) absorbance detection at 208 nm and 290 nm (Rainin Dynamax UV-1 UV/visible detector). Samples were injected using a six-port, sample loop injector (Rheodyne Model #7125). Different sample loop sizes were used depending on the desired sensitivity (5 µL, 20 µL, 100 µL, 1.0 mL). The entire HPLC system was interfaced to a Macintosh IIsi with Rainin DYNAMAX software for data acquisition and analysis. Peaks from liquid chromatograms were identified by matching retention times with those of standard solutions of pure compounds. Following positive identification, the HPLC was calibrated using at least four different concentrations of the pure compound to cover the range of concentrations typically found in effluent samples. Integration by peak area generally gave better results than peak height and was used for all quantifications.

Sulfate ions in solution were measured using a turbidimetric method (Greenberg et al., 1992). Samples were mixed with barium chloride in an acetic acid medium, forming barium sulfate crystals of uniform size which would absorb UV light at 420 nm. The linear range of this method for sulfate concentration was 10-40 ppmw (by weight) using the standard buffer solution. A different buffer spiked with sodium sulfate was used for concentrations from 1-10 ppmw. Effluent samples from oxidation experiments were typically diluted twenty times in order to fall within the linear range. Initial tests on hydrolysis samples generally gave the same results as a system blank which was at the low end of sensitivity for this method (about 1ppmw). As a result,

subsequent hydrolysis samples were not analyzed for sulfate. Interfering compounds as cited in the reference, were not present in any samples.

A one-time GC/FID analysis was also performed on several thiodiglycol effluent samples. Injections for this method were separated on an SPB-1 column with high grade helium as the carrier gas and high grade nitrogen as the makeup gas. One sample from each experiment was analyzed with this technique with all analyses occurring on the same day, approximately three weeks after the last experiment.

2.3 System Operating Procedures

Details of the typical procedures for thiodiglycol experiments are presented here. The procedures for methylene chloride experiments were essentially the same excluding the application of a few modifications described above (items 1, and 3-6 listed at the end of Section 2.1.1). System preparation and conditioning, feed preparation and sample collection and analysis are the major steps described. The procedures were different for each organic feed technique.

2.3.1 Procedures for Soluble Organic Feed

The experimental system was prepared the night before an experiment by verifying the proper operation of the feed pump and the back pressure regulator and checking for leaks. In the case of thiodiglycol, this period usually included replacing all filter elements and repairing back pressure regulator seals. The organic saturator was drained and purged with approximately two volumes of 1 bar helium, and the oxygen solution was also prepared at this time. The oxygen saturator was loaded with about 2500 mL of high purity water and the headspace of the saturator was purged with roughly 7 bar

of oxygen three times. The desired oxygen pressure was then regulated to the saturator and overnight recirculation began by pumping.

The day of the experiment would begin by calibrating the pressure transducer and opening the valve for the heat exchanger cooling water. For thiodiglycol experiments, the system water sparging would also begin. The next step was to begin water flow and pressurize. After measuring the cold flow rate, the sand bath would be turned on along with the computer and printer to record temperatures. During heatup, calibrations of the GCs and HPLC were verified, blanks were injected (both air and system blanks), and flow rates were recorded. The organic feed was prepared just as the reactor reached the desired temperature. In the case of thiodiglycol, the concentration of the feed was verified before loading it into the saturator. Generally, three feed samples were taken for each experiment; one from the feed flask before loading into the saturator and two from the system organic feed sampling valve (one before and one after the run). All feed samples were collected in 15 mL amber glass sample vials, capped with zero headspace and stored in a 4°C refrigerator until analysis. The organic solution was loaded into the saturator, pressurized with 1 bar of helium and the organic line was purged by draining about 100 mL of feed solution from the sample valve. Hydrolysis experiments began by switching the organic feed to the pump from water to organic solution. For oxidation experiments, the pump oxygen feed was also switched from water to saturated oxygen solution. Ambient pressure was then recorded from a mercury barometer along with the sand bath airflow rate and sand bath setpoint.

During the run, liquid flow rates were generally recorded every 10 minutes along with system pressure, oxygen and organic saturator pressures. Gas flow rates were taken every five minutes when possible. The first gas sample was taken after draining the liquid from and purging the headspace of the gas-liquid separator,

generally 45-60 minutes after switching to organic feed. As described in Section 2.3, a gas sample consisted of two 200 μL syringe injections, each into separate GCs with TCDs, and a third syringe injection of different sizes into a third GC but alternating between an FID and ECD detector. The GC analysis and subsequent oven cool-down took 15-20 minutes which allowed for a total of four to eight gas samples per experiment. Mole fractions for each gas were determined from volume fractions (volume of an individual gas divided by the sum of the volumes for all gases). Final gas compositions were typically averaged over four to six gas samples, discarding any suspicious injections due to low injection volume, poor peak elution or large peak integration discrepancies.

The first liquid sample was generally taken between 60-90 minutes after switching to organic feed. For each experiment, a total of three samples were taken at evenly-spaced intervals, usually after every other flow rate measurement. Liquid samples of the effluent, which flowed through the separator, were collected in 120 mL amber glass vials, capped with zero headspace, and stored in a 4°C refrigerator until sample analysis. The size of each liquid sample was greater than eight separator volumes, which were collected continuously, thus ensuring a well-mixed and accurate representation of the liquid effluent. All liquid samples were generally analyzed within 24 hours (it required this long to complete a thorough HPLC analysis of all samples) with the following exceptions. Samples were allowed to collect for up to seven days before sulfate analysis. FID analysis of select liquid samples were performed all at one time, approximately three weeks after the last experiment. As a result of continually improving the HPLC analytical method, some liquid samples (all which remained in the refrigerator) were re-analyzed at various times over the course of days to months. Where possible, an attempt was made to determine the degradation of these samples. In general, the sample integrity appeared to be preserved. Samples with particulates were filtered through 0.2 micron disposable filters (Gelman Sciences Acrodisk) before

analysis. Tests of this filtration procedure were conducted on aqueous solution standards and indicated no significant effect on accurate quantification. Analyses for all methylene chloride experiments were more consistent than for TDG. Initial GC analyses of all liquid samples were performed here within hours of an experiment. Only samples which gave suspicious results were re-analyzed at a later date. Samples were allowed to collect for up to seven days before chloride and formaldehyde analysis.

2.3.2 Procedures for Direct Organic Feed

System preparation the night before an experiment was identical to the procedures described above with the following exception. Instead of purging the organic saturator which was not used for these experiments, the entire internal volume of the syringe pump was flushed with high purity water three times, draining the final time through the entire downstream plug-flow apparatus so as to purge all lines of pure organic. The syringe pump was then filled with water and allowed to sit overnight to dissolve any residual organic. The procedures on the day of the run began as above with transducer calibration, heat exchanger cooling water flow and system water sparging. In addition, the valve for the nozzle cooling water was opened and the water flow rate was measured. During system water sparging, the syringe pump was drained and further purged with a continuous flow of about 5 bar of nitrogen to remove residual liquid in the syringe itself as well as the filling and draining lines, valves and filter. Approximately 20 mL of organic was then loaded and purged, and about 15 mL of organic was loaded for the experiment. After at least one hour, sparging was stopped and water flow was initiated.

Several different techniques were explored for accurately flowing the organic to the system. The objective was to verify that the system was receiving the correct organic concentration under ambient temperature and high pressure conditions before

heating the reactor. The best technique began by flowing organic at 2 mL/min for one minute to quickly fill the line to the reactor. Organic flow was then reduced to the appropriate $\mu\text{L}/\text{min}$ rate and system pressure was increased. It appeared as though increasing system pressure slightly forced the organic back up the cooled nozzle as evidenced by organic concentrations of the effluent going to zero. To quickly correct this problem, organic flow was increased until about 1.5 mL were dispensed and then flow rate was reduced. Liquid effluents were measured after one hour of continuous flow, at which time the desired concentration was usually achieved. This measurement was the only feed analysis performed. Due to the variability of liquid concentrations using this feed technique (see Section 2.6), the feed concentration for each experiment was calculated from the flow rate setting on the syringe pump. Once the organic concentration was verified, both the main sand bath and the preheater sand bath would be turned on along with the temperature recording equipment. As with the previous procedure, calibrations were verified, blanks injected and flow rates were recorded during heatup. For this feed delivery technique, the start of a hydrolysis experiment was specified by the time the reactor reached its temperature setpoint since organic was continuously flowing during heatup. The run procedures along with sampling techniques from this point on were the same as described above.

2.4 Data Reduction

Data reduction calculations for this study are the same as those cited by Helling (1986), Webley (1989), Holgate (1993) and Meyer (1993) and are explained in detail in those theses. A summary of important assumptions and calculations is provided below.

The gas and liquid effluents are assumed to be in equilibrium once they exit the gas-liquid separator. The total molar flow rate for each species in the gas phase has not only a gas phase contribution but also a liquid phase contribution that corresponds to the amount

dissolved in the liquid effluent. The gas phase contribution is determined by GC analysis, but the liquid phase contribution is determined by a Henry's Law equilibrium calculation. The liquid-phase concentration of each gaseous species dissolved is related to the measured gas-phase volume (mole) fraction by Henry's law:

$$y_i \phi_i P = H_i(T, P) x_i \quad (2.1)$$

where

- y_i = gas-phase mole fraction of species i
- ϕ_i = gas-phase fugacity coefficient
- P = total pressure
- $H_i(T, P)$ = Henry's law constant
- x_i = liquid-phase mole fraction of species i

and x_i is the desired quantity. Since the evaluated phases are at ambient temperature and pressure, ϕ_i is set to unity. Henry's law constants under ambient conditions are functions of temperature and were obtained for oxygen (Benson et al., 1979), carbon monoxide (Rettich et al., 1982), hydrogen, helium, nitrogen, carbon dioxide (with a correction for the dissociation of carbonic acid), ethylene, acetylene, and hydrogen sulfide (Wilhelm et al., 1977), and methane and ethane (Rettich et al., 1981). The calculated liquid-phase contribution to the total molar flow rates of effluent gaseous species was usually small, although the high equilibrium solubility of carbon dioxide and hydrogen sulfide in water made their contribution significant. Estimating the concentration of hydrogen sulfide was verified by a wet chemistry test which measures S^{2-} in solution (Greenberg et al., 1992). Despite the difficulty of this analysis, the measured quantity was in good agreement with the calculated result.

Inlet concentrations were calculated using flow rates of the two feed streams, given by a volumetric flow rate measurement of the effluent and a feed pump calibration

(Webley, 1989). Organic concentrations in the saturator were measured and converted to reactor inlet concentrations by calculating a water density change from expansion on heating and adding the flows of the two feed streams. Reactor inlet O₂ concentrations were calculated in a similar manner but from a saturator concentration that was calculated not measured. The liquid-phase mole fraction of oxygen in the saturator solution was calculated from Henry's law (Equation (2.1)). For this case of a high-pressure (8 to 110 bar), non-ideal gas phase, the fugacity coefficient, ϕ_i , was calculated from the Peng-Robinson equation of state with parameters found in Reid et al. (1987). Values of the fugacity coefficient typically ranged from 0.911 to 0.993. A Poynting-type correction accounted for the pressure dependence of the Henry's law constants as,

$$H_i(T, P) = H_i(T, P_o) \exp[\bar{V}_{i,\infty}(P - P_o) / RT] \quad (2.2)$$

where the assumed constant, infinite-dilution partial molar volume ($\bar{V}_{i,\infty}$) for oxygen was obtained from Brelvi and O'Connell (1972) with atmospheric pressure used as the reference pressure (P_o). A typical value of the Poynting-type correction used in TDG oxidation studies was 1.08. Tests of this method were conducted with the reactor operating at ambient temperature. The calculated gas feed concentration agreed with the measured effluent concentration within 2%, adding credence to the technique.

2.5 Experimental Uncertainty

Experimental errors listed in this study are estimates based on uncertainties in measured values. All measured quantities are given as approximate, normal, 95% confidence intervals (intervals of two standard deviations as used here). Measurement uncertainties are propagated to uncertainties in derived quantities using standard propagation-of-error formulas (Aikens et al., 1984). Descriptions of error calculations are provided below.

Typically, the liquid and gas flow rates for an experiment were taken as the average of five to fifteen flow rate measurements. The 95% confidence intervals for these quantities were taken as two standard deviations of the data. Similarly, the composition of the gas phase was calculated as the average of four to eight gas samples, with the confidence interval equal to two standard deviations. For most of the experiments, the analytical results of three liquid samples of each run were averaged to obtain the concentration of liquid products in the liquid effluent, again with two standard deviations as the confidence interval. In a few cases, however, an accurate analysis of only one sample was possible (e.g., the re-analysis of a few thiodiglycol effluent samples). The confidence interval for this case was considered to be equal to the representative confidence interval for the specific analytical technique as derived from reproducibility studies (e.g., $\pm 5\%$ for HPLC analysis).

Rigorously, a Student's t distribution should be used to obtain confidence intervals, rather than the normal distribution. However, the t distribution approaches the normal distribution as the number of data points gets large. In our case, enough experimental measurements were typically made so that the difference between the two distributions was negligible.

2.6 Evaluation of Direct Organic Feed System

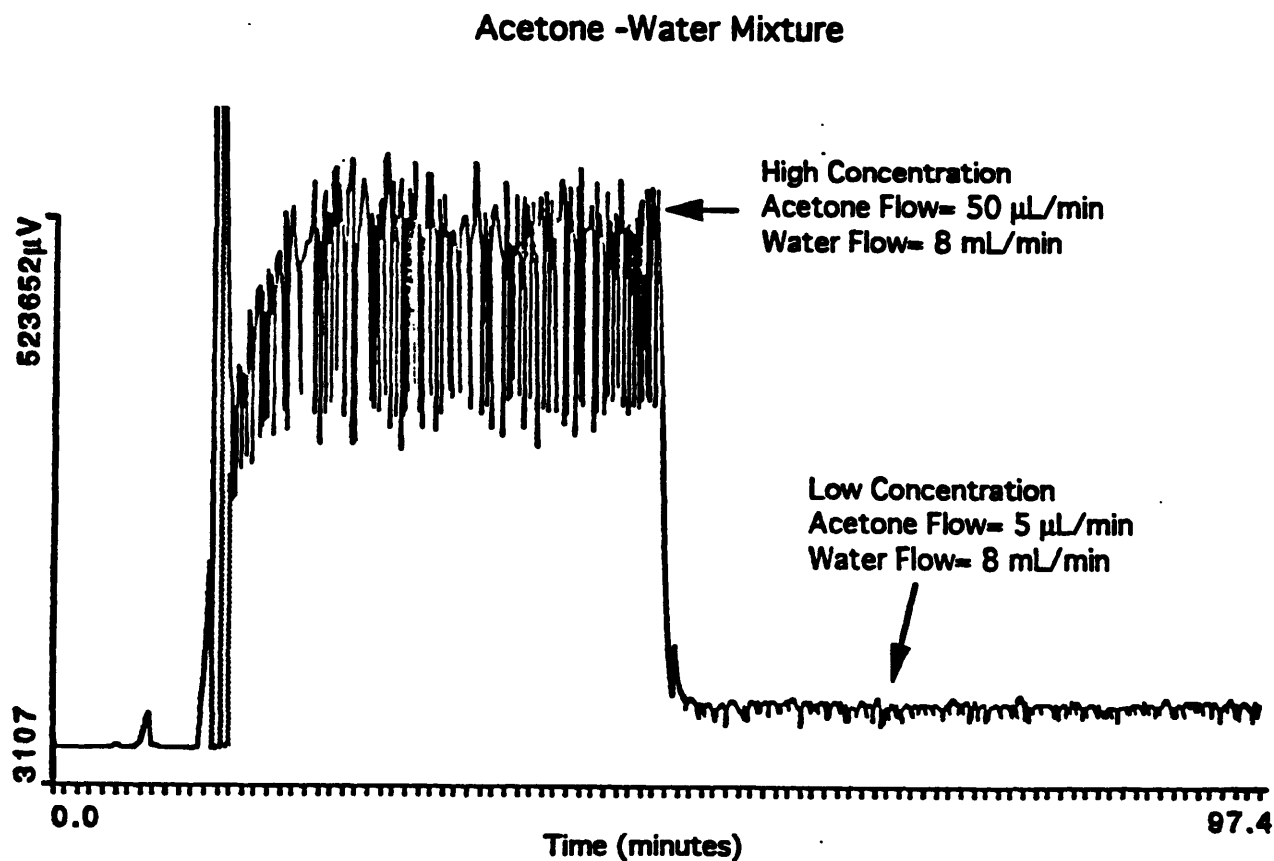
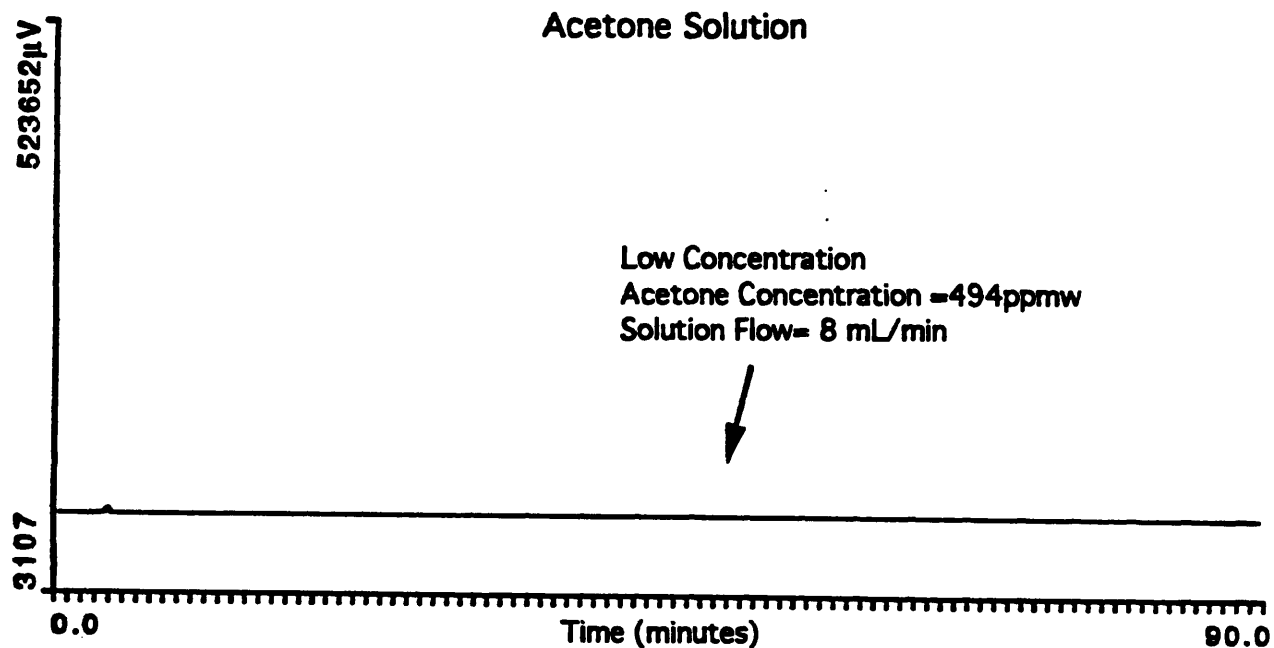
Several preliminary cold and hot flow tests were performed to make an initial evaluation of the new direct organic feed system. The syringe pump was tested separately; the syringe pump was attached to the cooled nozzle and mixing cross and tested; and the entire assembly was attached to the plug-flow (PFR) apparatus and tested.

The accuracy of the syringe pump itself was determined by flowing methanol into a volumetric flask of water for a specified time and measuring the concentration by GC/FID analysis. Solutions made by the syringe pump were generally within at least $\pm 2\%$ of the target. This test was particularly difficult to perform because of the difficulty in handling the tubing from the syringe pump to the flask without interfering with the flow of methanol. Also, the effects of liquid surface tension seemed to be magnified for this micro-flow of methanol.

The combined assembly of the syringe pump, cooled nozzle, and mixing cross was tested outside of the PFR apparatus using two different techniques. These tests were performed to make initial evaluations of organic and water mixing by continuous monitoring and point sampling of the effluent. For continuous monitoring, a UV detector was attached to the effluent of the mixing cross which continually measured the absorbance of a UV-sensitive tracer in a dilute solution flowing past the UV lamp. An HPLC pump (Rainin) provided high purity, filtered and degassed water flowing at 8 mL/min. to the water port in the mixing cross. The syringe pump delivered the organic at various flow rates to the cooled nozzle. The reactor port of the mixing cross was reconfigured to attach a 12 in. piece of 1/16 in. O.D., 0.01 in. wall, 316 stainless steel tubing which connected to the UV detector (Rainin UV-1). Phenol was selected as the first tracer because of its high extinction coefficient (i.e., high sensitivity) with absorbance measured at a wavelength of 254 nm. Unfortunately, the tests with phenol had poor results for reasons not completely understood. Acetone, with measurements at 290 nm, was then chosen as the tracer primarily because of its complete miscibility in water, but unfortunately it has reduced sensitivity for UV absorbance (extinction coefficient two orders of magnitude less than that of phenol).

An example of the test results is shown in Figure 2.4. This figure compares the absorbance of the acetone-water mixture over time versus the absorbance of an acetone-

Figure 2.4 UV Absorbance Traces for Continuous Monitoring Tests of Direct Organic Feed Mixing Assembly. UV absorbance measured at 290 nm. UV tracer was acetone.



water solution flowing only from the syringe pump. If the water and organic streams were mixed completely uniformly, the two absorbance traces for the same concentrations should look the same. As seen from the figure, the absorbance of the mixture from the mixing cross is more erratic, particularly at higher organic flow rates. Nevertheless, the estimated average absorbance of each trace is approximately equal to the absorbance expected for the target concentration (exact averages were difficult to obtain). Varying the location of the end of the cooled nozzle within the cross did not significantly affect the results. One cause of the erratic results may be pulsations from the HPLC pump. Mixing of the pulsating water stream with the pulse-less organic stream probably caused the effluent stream composition to fluctuate from high concentrations during the refill stroke of the HPLC pump to low concentrations during the dispense stroke of the HPLC pump.

The point sampling test consisted of flowing methanol and water through the mixing cross, collecting approximately 1 mL effluent point samples and analyzing them by GC/FID. The flow rates of methanol were varied between 1 and 5 $\mu\text{L}/\text{min}$ and the water flow remained constant at 8 mL/min. The concentrations of the effluent were consistently 10 to 20% higher than the expected calculated values and showed variations similar to those observed in the continuous monitoring tests.

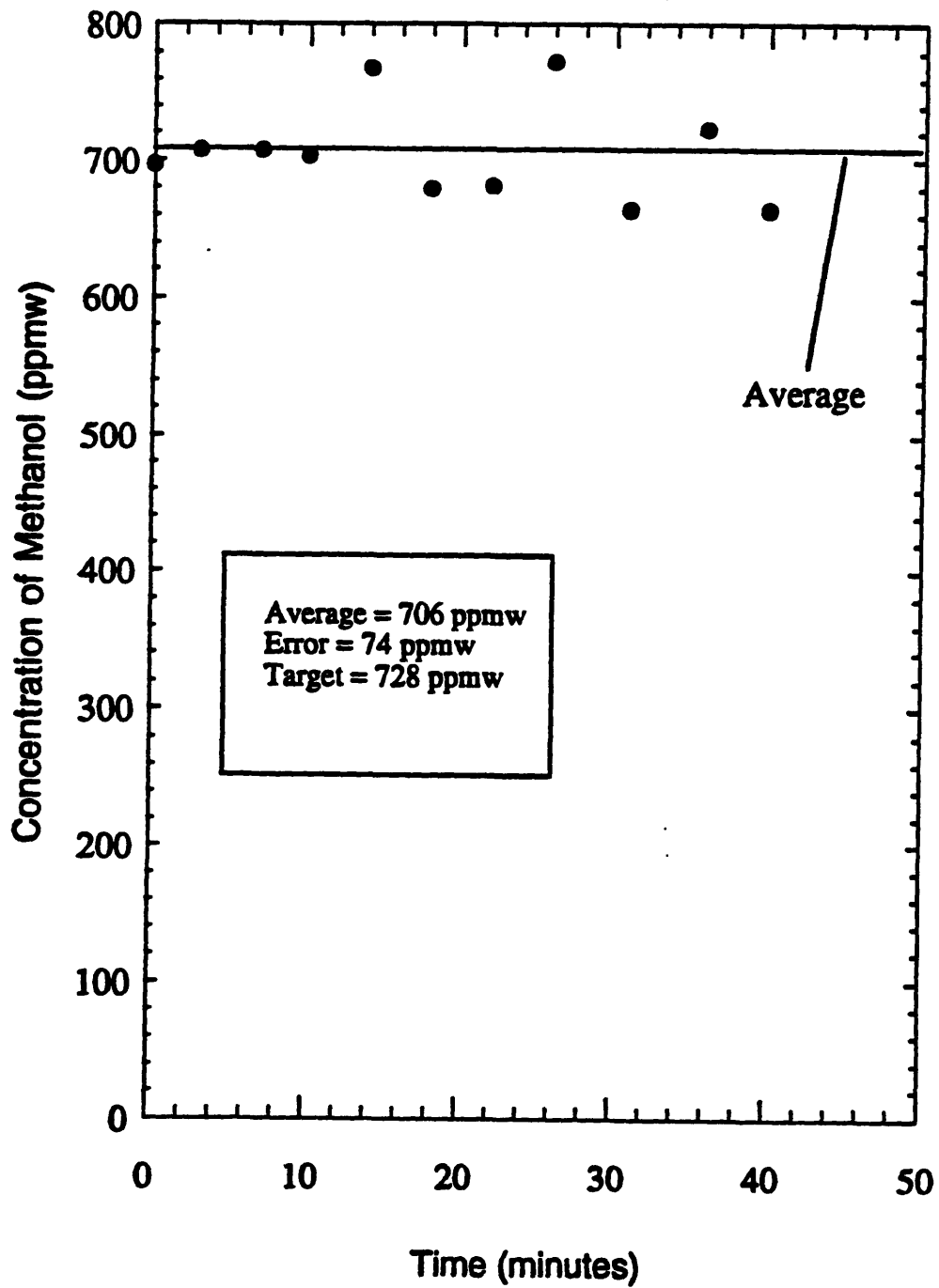
Overall, the results of these tests were discouraging for the application of this design to the PFR apparatus. However, there are several important issues to consider. Reynolds numbers corresponding to the flow conditions for these cold tests in the cross and connecting lines were well within the laminar region (the Reynolds number in the tubing was approximately 140). Thorough mixing under laminar conditions, with possible parabolic velocity and concentration profiles, is typically more difficult than under turbulent conditions and may require a much greater mixing length to become fully developed. The disappointing results of these preliminary tests may be due in part

to this poor mixing fluid dynamics regime. Flow conditions for the PFR apparatus, operating with water in the supercritical region, are much more turbulent (Reynolds numbers at least 20 times greater) and the fluid is more gas-like with reduced viscosities and increased diffusivities. Also, the zirconia beads mentioned in Section 2.1.2 were added after these tests and should drastically increase the local turbulence of streams in the mixing cross.

The mixing cross with the cooled nozzle was attached to the PFR system for the third series of tests. Methanol was chosen as the test organic because of its negligible hydrolysis degradation in supercritical water (SCW) and accurate existing analytical methods for its quantification. The system was operated at 250 bar and temperature was varied from ambient to 500 °C. Approximately 1 mL point samples of the effluent were taken after the gas-liquid separator over a period of time and concentrations of those samples were recorded. Naturally, sampling at a point so far away from the reactor gives results not representative of mixing in the cross or the reactor, but we are not at present equipped for in-situ analysis. An example of the results of this test is provided in Figure 2.5. Regardless of temperature, the average of the measured methanol concentration was generally within 5% of the target concentration and all samples fell within $\sim\pm 10\%$ of the average. As in the UV tests, the variability of the results may be attributed to the pulsed water flow. The system pump had much greater pulsations than the HPLC pump ($\pm 3-7$ bar versus ± 1 bar). Also, the increased pulsations probably had a greater effect on the more compressible SCW medium.

An oxidation experiment with methanol was performed as an initial evaluation of kinetics with the direct organic feed system. Twelve effluent point samples were taken over the course of one hour and their average concentration gave a conversion that roughly agreed with the results from an organic solution feed into the same reactor at the same conditions (67% here versus 64% before). However, the compositions of

Figure 2.5 Test of Direct Organic Feed System in PFR Apparatus. Conditions for test: water flow = 12.43 mL/min, methanol flow = 686 μ L/hr, T=500 °C, P=246 bar.



the effluent samples were very erratic with some samples varying as much as 25% from the average. It was the results of this specific test which convinced us to add the zirconia beads to the cross to improve mixing.

The series of tests performed on the direct organic feed design proved that the syringe pump is accurate but the method of mixing the organic and water streams may need improvement. It also proved that there is a need for further, more accurate testing. Additional difficulties with the direct organic feed system were discovered during the thiodiglycol experiments and are described in Section 4.4.2.

2.7 Evaluation of Plug-Flow Criteria

The analysis of kinetic data from the reactor system assumes isothermal, isobaric, plug-flow conditions. The reliability of the experimental results thus depends on how well these assumptions are satisfied. Earlier studies in our group (Helling, 1986; Webley, 1989; and Holgate 1993) evaluated the reactor under typical, supercritical conditions and found that these assumptions were satisfied under most operating conditions. A similar analysis is presented here for operations at supercritical pressures but subcritical temperatures which correspond to some of the conditions of the TDG study.

Similar to the analysis for supercritical experiments, the isothermal and isobaric assumptions for these subcritical experiments were confirmed by the temperature and pressure measurements taken in the system. The assumption of plug-flow, however, requires some knowledge of the fluid dynamics for these conditions. One can compare the flow characteristics between the supercritical and subcritical fluid through the use of Reynolds numbers, defined as:

$$Re = \frac{v\rho d}{\mu} = \frac{\dot{m}d}{A\mu} = \frac{\dot{m}d}{\frac{\pi d^2}{4}\mu} = \frac{4\dot{m}}{\pi d\mu} \quad (2.3)$$

where v is the axial velocity, ρ is the fluid density, d is the tube inner diameter, μ is the fluid viscosity, A is the tube cross sectional area and \dot{m} is the mass flow rate of the fluid. For supercritical experiments, Reynolds numbers typically ranged from 2200 to 5000 which corresponded to transition or turbulent flow, but for TDG subcritical experiments, Reynolds numbers dropped below the critical value for laminar flow with values between 400 and 1900. In the laminar flow regime, one would expect a deviation from plug-flow conditions which must be evaluated through basic transport equations.

At steady-state, the axial component of the continuity equation of species i for flow through a tube, in cylindrical coordinates assuming constant fluid density and species diffusivity and neglecting all angular (azimuthal) dependencies is (this equation is an adaptation of Eqn 18.1-17 in Bird et al., 1960):

$$-v_r \frac{dC_i}{dr} - v_z \frac{dC_i}{dz} + D_i \left(\frac{\partial^2 C_i}{\partial r^2} + \frac{1}{r} \frac{\partial C_i}{\partial r} + \frac{\partial^2 C_i}{\partial z^2} \right) - R_i = 0 \quad (2.4)$$

where C_i is the concentration of species i , D_i is the diffusivity of species i in the reactor fluid, v_r is the radial velocity of fluid in the tube, v_z is the axial component of velocity, and r and z are the radial and axial coordinates, respectively. Formation or loss of species i is included in the source/sink reaction term, R_i . For systems of multiple species, there is an equation similar to Equation (2.4) for each species. Also, for multiple reactions (e.g., an elementary reaction mechanism), there will be additional reaction terms in each species continuity equation for those reactions in which the

species participates. Under plug-flow conditions ($v \neq v(r)$, $\partial v / \partial r = 0$, $C_i \neq C_i(r)$, $\partial^2 C_i / \partial z^2 \approx 0$), Equation (2.4) reduces to

$$-v_z \frac{dC_i}{dz} - R_i = 0 \quad (2.5)$$

The first term in Equation (2.5) is essentially the temporal variation of C_i since $z/v = t$. Equation (2.5) is thus equivalent to the purely kinetic equation

$$\frac{dC_i}{dt} = -R_i = -k^* C_i \quad (2.6)$$

assuming a first order rate law with k^* equal to the rate constant.

Identifying the conditions that allow Equation (2.4) to be replaced by Equation (2.6) has been the topic of numerous studies. Cutler et al. (1988) have recently summarized the “plug-flow criteria” resulting from those studies. The primary requirements for plug-flow are:

(1) Radial (transverse) diffusion must occur rapidly enough to ensure the fluid is compositionally homogeneous or well-mixed radially.

(2) Axial (longitudinal) diffusion is slow relative to convection.

The first requirement can be evaluated by the criterion (Cleland and Wilhelm, 1956)

$$\frac{\text{time for radial diffusion}}{\text{time for axial convection}} = \frac{vr^2}{DL} = Pe \left(\frac{r}{L} \right) < 1 \quad (2.7)$$

where D is the diffusivity, v is the characteristic velocity and L and r are the reactor length and radius, respectively. Radial concentration profiles are also affected by

reaction occurring on time scales faster than those of radial diffusion, such that diffusion cannot eliminate gradients prior to reaction taking place. The criterion for insuring rapid radial diffusion relative to reaction is (Walker, 1961; Poirier and Carr, 1971)

$$\frac{\text{time for radial diffusion}}{\text{time for reaction}} = Da = \frac{k^* r^2}{D} < 1 \quad (2.8)$$

where k^* is the first order rate constant for the reaction. The dimensionless quantity in Equation (2.8) is one of the traditional Damköhler numbers, Da .

The value of D in Equations (2.7) and (2.8) depends on the flow regime. In the case of TDG subcritical experiments, we can assume we have fully developed laminar flow conditions where molecular diffusion dominates and the total diffusivity D can be approximated by the molecular diffusivity, D_m . For the criteria of Equations (2.7) and (2.8), choosing the molecular diffusivity, which is typically smaller than the total diffusivity, is a worst case approximation. Experimental values for D_m are not readily available for the systems studied here, but it can be approximated by the self-diffusivity of pure water. Lamb et al. (1981) provide the following semiempirical expression for the self-diffusion coefficient of water applicable to our conditions:

$$\rho D_m = 2.24 \times 10^{-6} T^{0.763} \quad (2.9)$$

The second criterion for plug flow, negligible axial diffusion relative to bulk convection, can be expressed by the equivalent conditions (Azatyan, 1972; Norton, 1990)

$$\frac{-D \frac{dC_i}{dz}}{C_i v} = -\frac{1}{C_i} \frac{dC_i}{dt} \frac{D}{v^2} = \frac{Da}{Pe^2} = \frac{k * D}{v^2} < 1 \quad (2.10)$$

The first and second expressions represent a characteristic-velocity analysis of axial diffusion and convection (Norton, 1990): the numerator in the first expression is the axial diffusive flux of species i , and the denominator is the convective flux. The second expression is the same as the first but with distance (z) converted to time (t). The third and fourth expressions from Azatyan (1972) results from a dimensional scaling analysis of Equation (2.5), but can also be derived from the second expression using the definition of k^* .

Table 2.1 displays the conditions for the TDG subcritical experiments and evaluates each experiment against the criteria established in Equations (2.6), (2.7) and (2.10). Equation (2.6) is satisfied for all our experimental conditions; the dimensionless quantity ranges approximately from 0.087 to 0.409 over the range of temperatures and flow rates used in the present study. Similarly, Equation (2.8) is satisfied with $Da < 0.2$. Furthermore, the reactor is coiled which introduces a secondary flow (with radial components), thereby enhancing radial mixing and reducing radial gradients (Kramers and Westerterp, 1963). Radial concentration and velocity gradients in the tubular reactor are therefore probably negligible. The third criterion of Equation (2.10) is the one most easily satisfied with all the calculated dimensionless quantities being at least six orders of magnitude below 1.

In conclusion, the tubular reactor operates within the plug-flow regime for the supercritical and subcritical conditions explored in this study and the corresponding data may be treated using the plug-flow assumption.

Table 2.1 Plug-Flow Evaluation Criteria**Conditions:**

P=255 bar

 $k^*=4.47 \times 10^{-3} \text{ s}^{-1}$ This k^* corresponds to the highest value observed in subcritical experiments.**Reactor Geometry:**

L=471 cm

r=.0855 cm

Criteria Results:

T (°C)	m (g/min)	D_T (cm ² /s) ($\times 10^4$)	μ (Pa-sec) ($\times 10^4$)	ρ (g/mL)	Re	Pe	Pe(r/L)	Da	Da/Pe ($\times 10^5$)	Da/Pe' ($\times 10^5$)
200	5.83	2.79	1.40	0.881	517	1472	0.267	0.125	8.49	5.77
250	5.49	3.24	1.12	0.821	608	1281	0.233	0.108	8.40	6.56
276	5.24	3.51	1.01	0.785	644	1180	0.214	0.099	8.42	7.13
301	4.93	3.84	0.916	0.743	668	1072	0.195	0.091	8.47	7.90
326	4.54	4.26	0.825	0.692	683	956	0.174	0.082	8.56	8.96
351	11.03	4.87	0.725	0.624	1888	2253	0.409	0.072	3.18	1.41
351	5.79	4.87	0.725	0.624	991	1182	0.215	0.072	6.06	5.12
351	3.99	4.87	0.725	0.624	683	815	0.148	0.072	8.79	10.8
351	3.07	4.87	0.725	0.624	526	627	0.114	0.072	11.4	18.2
351	2.35	4.87	0.725	0.624	402	480	0.087	0.072	14.9	31.1

CHAPTER 3

Experimental Studies of Methylene Chloride Hydrolysis and Oxidation in Supercritical Water

3.1 Introduction

This study of methylene chloride hydrolysis and oxidation in supercritical water was a collaborative effort of several members of our research group. Philip Marrone served as the primary investigator overseeing and participating in the entire operation and personally interpreting the results, while this researcher was responsible for conducting several experimental runs and portions of the analytical work. A paper recently accepted for publication describes the details of all experiments and gives a complete analysis of our results for methylene chloride (Marrone et al., 1995). Material in this chapter has been extracted from that paper in order to provide the most thorough and accurate description of the entire methylene chloride study.

Chlorinated organics represent an important class of highly stable, toxic hazardous waste. Incineration of these compounds has been used in the past as a means of remediation but this process can result in equally toxic byproducts such as dioxins (Hoke et al., 1992). The SCWO process, however, has been shown to have great success with chlorinated organics resulting in high destruction efficiencies and no formation of toxic byproducts under appropriate operating conditions. For example, MODAR, Inc. has demonstrated greater than 99.99% destruction of several chlorinated aromatics and hydrocarbons such as polychlorinated biphenyls (PCBs), DDT, chlorinated dioxins, chlorobenzenes, trichloroethylene, and chlorinated methanes, to name a few, under temperatures of 550-650°C and residence times of 1 minute or less (Staszak et al., 1987; Thomason et al., 1990). Destruction studies such as these are

useful to outline the capabilities of SCWO, but more information, such as detailed kinetic experiments, is needed for design optimization of commercial SCWO processes.

Published kinetic studies on the supercritical water oxidation of chlorinated organics have focused on a limited number of chlorinated aromatics. Yang and Eckert (1988) studied oxidation kinetics of p-chlorophenol in a flow reactor under conditions of 310–400°C and 5–60 seconds residence time. Jin et al. (1990) studied catalytic oxidation of 1,4-dichlorobenzene with a V₂O₅ catalyst in a batch reactor under conditions of 343–412°C and up to 60 minute residence times. Lee et al. (1990) used both O₂ and H₂O₂ as oxidants in reactions with 2,4-dichlorophenol. Li et al. (1993) determined the global kinetics of 2-chlorophenol oxidation in a plug-flow reactor at temperatures of 300–420°C and residence times of 4–70 seconds.

A detailed investigation of methylene chloride hydrolysis and oxidation in supercritical water was undertaken to characterize the kinetics and reaction pathways for this model chlorinated organic compound. The specific objectives for these experiments were to determine global kinetic parameters and mechanisms and identify and quantify the reaction product spectrum. The early work on SCWO of methylene chloride in our lab was conducted by Meyer (1993). The experimental and analytical challenges of that early work have resulted in improved operational and analytical techniques. These developments have in turn led to an enhanced overall understanding of methylene chloride reactions in supercritical water as presented here and in Marrone et al. (1995).

3.2 Literature Review

Reported kinetic studies of methylene chloride in supercritical water are scarce. Several investigators have performed destruction efficiency tests with CH₂Cl₂ including

Rice et al. (1993), but these tests only focused on reactions run to completion and not the collection of kinetic data under well-defined conditions. However, there have been several kinetic studies of catalytic combustion reactions and moderate temperature but subcritical hydrolysis reactions of CH_2Cl_2 . The catalytic combustion studies of methylene chloride by Young (1982), Liepa (1988), Hung and Pfefferle (1989), Shaw et al. (1993) used a variety of catalysts that includes chromium oxide, platinum, palladium oxide, manganese oxide, and cobalt oxide. These studies compared conversions and product distributions resulting from the different catalysts tested.

However, the study most relevant to the work here is the hydrolysis investigation of Fells and Moelwyn-Hughes (1958). This research explored the homogeneous kinetics of CH_2Cl_2 hydrolysis under acidic and basic conditions in temperatures of 80 - 150°C. Under acidic conditions, they found the CH_2Cl_2 -water reaction followed first order kinetics with the formation of formaldehyde and hydrochloric acid. Under caustic conditions, CH_2Cl_2 reacted not only with water but also with hydroxide ion which resulted in several additional reactions. The reaction with OH^- was found to be first order in each reactant and second order overall. Similar hydrolysis studies include Chuang and Bozzelli (1986) who investigated the vapor phase hydrolysis of chloroform at 611 to 1050°C and 1 atm, Gaisinovich and Ketov (1969) who investigated carbon tetrachloride hydrolysis at 350-500°C, and Jeffers et al. (1989) who studied the hydrolysis of a number of chlorinated methanes, ethanes, ethenes, and propanes over temperatures ranging from 0 to 180°C and pHs from 3 to 14.

3.3 Experiments Performed

This study was composed of a total of 66 experiments with 23 being under hydrolysis (no added oxygen) conditions. All experiments were carried out in the plug-flow

apparatus described in Section 2.1.1 at a fixed pressure of approximately 246 bar. The two categories of experiments were: temperature variation runs and reactor residence time and concentration variation runs. For the temperature variation runs, experiments were conducted by varying temperature from 450 to 600°C (each one isothermal) at a fixed reactor residence time of approximately 6 seconds and fixed organic feed concentration between $0.7\text{-}1.0 \times 10^{-3}$ mol/L (under reactor conditions) for both hydrolysis and oxidation conditions. CH_2Cl_2 feed concentrations varied only because of the difficulty in preparing the feed. For oxidation runs, feed ratios ($\text{O}_2/\text{CH}_2\text{Cl}_2$) were just above stoichiometric (based on complete oxidation of CH_2Cl_2 to CO_2) ranging from 1.1 to 1.5. Feed ratios for hydrolysis runs were two orders of magnitude less at values of 0.02-0.04 based on calculated oxygen concentrations in high purity water assumed to be in equilibrium with air at STP. The reactor bypass described in Section 2.1.1 was used in two separate hydrolysis runs at 450 and 575°C. With the exception of reactor residence time, all other run operating conditions were kept the same as that for the corresponding run with the reactor in place. These reactor bypass experiments were used as a method of determining the degree of CH_2Cl_2 breakdown in the organic feed preheater coil.

Concentration variation and reactor residence time runs were performed under oxidation conditions only. For both groups of runs, reactor residence times varied from 4.0 to 9.0 seconds at a fixed temperature of 550°C. Concentrations of each reactant were varied both together and independently so as to explore reaction rate dependence on relative and absolute amounts of reactants. These runs are best categorized in five separate groups based on the values of individual reactant feed concentrations and their ratios, as shown in Table 3.1. Feed ratios for these runs ranged from substoichiometric to superstoichiometric with O_2 concentrations ranging from $0.5\text{-}2.1 \times 10^{-3}$ mol/L and CH_2Cl_2 concentrations ranging from $0.24\text{-}0.9 \times 10^{-3}$ mol/L under reactor conditions.

TABLE 3.1 Groupings of Oxidation Runs for Residence Time and Concentration Variations.
($T=550^{\circ}\text{C}$, $P\sim 246$ bar)

Group #	Experimental Runs in Group	$[\text{O}_2]_0^{\text{a}}$ (10^{-3} mol/L)	$[\text{CH}_2\text{Cl}_2]_0^{\text{b}}$ (10^{-3} mol/L)	Feed Ratio ^c	Feed conditions	Residence Time Range (s)
1	6	1.08	0.84	1.3	stoichiometric	4 - 9
2	6	0.58	0.49	1.2	stoichiometric	4 - 9
3	3	2.08	0.80	2.6	superstoichiometric	4,6,8
4	3	0.56	0.24	2.3	superstoichiometric	4,6,8
5	6	0.56	0.84	0.7	substoichiometric	4 - 9

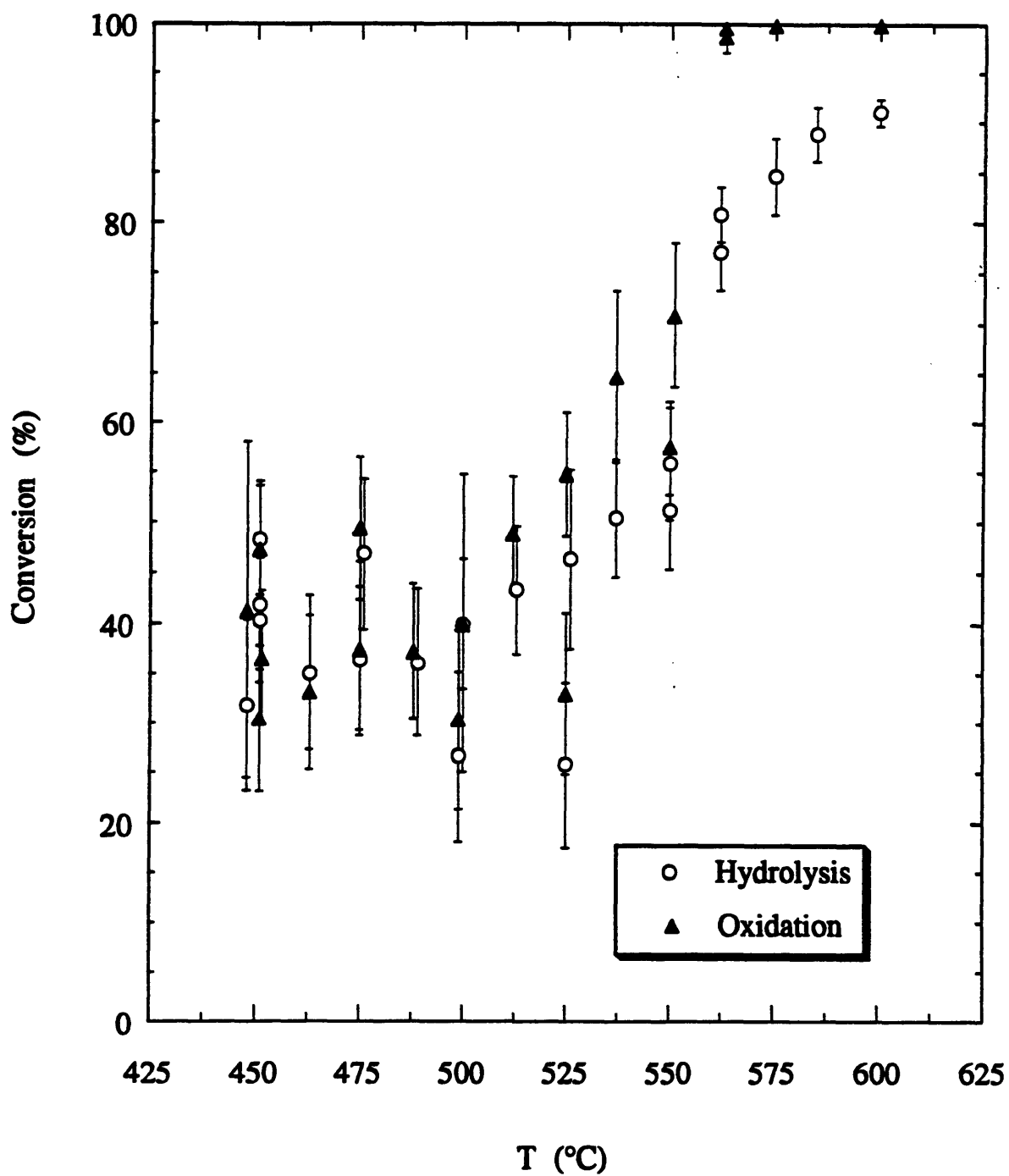
^a Average inlet O_2 concentration; ^b Average inlet CH_2Cl_2 concentration; ^c Feed ratio = $[\text{O}_2]_0/[\text{CH}_2\text{Cl}_2]_0$

3.4 Kinetic Results

3.4.1 Effects of Temperature Variation

As a result of temperature variation, methylene chloride conversions ranged between $26\pm 9\%$ and $91\pm 1\%$ under hydrolysis conditions and between $30\pm 9\%$ and $99.9\pm 0.1\%$ (complete conversion, occurring at 563°C) under oxidation conditions (see Figure 3.1). One of the most striking trends observed is the similarity between hydrolysis and oxidation conversions. With only one exception, hydrolysis and oxidation conversions between $450\text{-}550^{\circ}\text{C}$ are within experimental error of each other. This phenomenon of similar incomplete conversions with and without oxidant is unique compared to that observed for the other model compounds we have studied. In previous work in our laboratory, the typical observation, such as in the case of CO , CH_3OH and CH_3COOH , was much greater conversion in oxidation versus hydrolysis conditions (Holgate et al., 1992; Webley et al., 1990; Meyer, 1993). In the limited cases where hydrolysis and oxidation rates were comparable, it was usually for relatively labile, more complex compounds, such as glucose, that underwent complete conversion, rather than incomplete conversion, under all conditions in SCW (Holgate et al., 1995).

Figure 3.1 Hydrolysis and Oxidation Conversion of CH_2Cl_2 as a Function of Temperature. $[\text{CH}_2\text{Cl}_2]_0 \sim 1 \times 10^{-3}$ mol/L for hydrolysis and oxidation; $[\text{O}_2]_0 \sim 1 \times 10^{-3}$ mol/L for oxidation. Error bars represent estimated 95% confidence intervals. From Marrone et al. (1995).



The relative agreement of hydrolysis and oxidation conversions suggests that oxygen does not play a significant role in methylene chloride breakdown in supercritical water, and thus should be zero order in a global rate expression for CH_2Cl_2 destruction. This result is actually consistent with the observed behavior of the oxidation of other model compounds in supercritical water although for apparently different reasons. In those cases, oxygen is zero order because it is assumed not to participate in any rate limiting steps of the elementary reaction network, even though it must be present for the reaction to occur. In the case of methylene chloride, a zero order dependence on O_2 could result because oxygen may not be involved in the primary breakdown of CH_2Cl_2 .

If oxygen is not needed for significant methylene chloride degradation to occur, then the initial conversion of CH_2Cl_2 in solution may actually begin in the preheater coil even before entering the reactor. Two sources of experimental evidence corroborate this theory. First, significant corrosion was observed in the organic feed preheater coil, presumably from the presence of HCl formed from the breakdown of CH_2Cl_2 (see section 3.6). Second, results from the two reactor bypass hydrolysis experiments show the same conversion within experimental error with and without the reactor present. For 450°C , the reactor bypass conversion was $36 \pm 10\%$ while the reactor conversion was $41 \pm 13\%$ (average of four separate 450°C runs). For 575°C , the reactor bypass conversion was $82 \pm 2\%$ while the reactor conversion was $85 \pm 4\%$. Although the results are only based on two reactor bypass experiments, they do imply that most, if not all, CH_2Cl_2 conversion occurs before reaching the reactor.

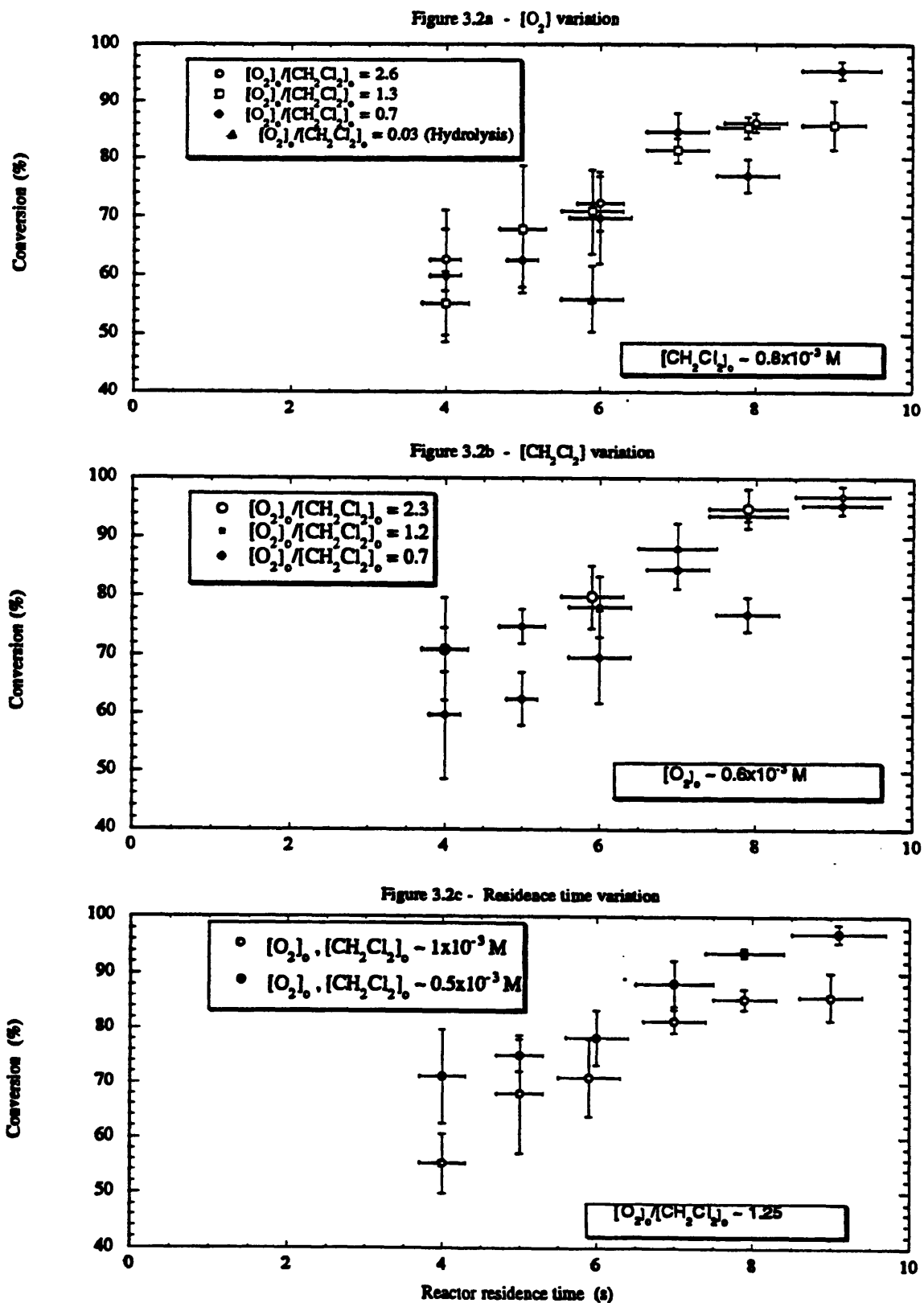
For a fixed flow rate, the time that feeds spend in our fixed geometry preheater coil is a function of density which changes considerably as the solutions heat from ambient temperatures up to $450\text{-}600^\circ\text{C}$. The preheater coil residence times are estimated to range from 9 to 20 seconds depending on flow rates and sandbath

temperatures. Therefore, the total time for reaction under high-temperature hydrolysis conditions is probably much greater than just the six seconds spent in the isothermal reactor. In fact, the apparent low-temperature plateau in the temperature - conversion graph (Figure 3.1), may be the result of different total residence times for the temperature variation runs. For example, a longer time in the preheater coil at temperatures below 500°C and/or a shift in mechanisms from ionic to free radical in nature may explain why conversion appears to level off rather than decrease with decreasing temperature. In any event, the point should be clear that any correlation of kinetic data must account for the nonisothermal, variable residence time in the preheater coil in addition to the isothermal, fixed residence time reactor. The determination of the time-temperature history of the organic feed in the preheater and its subsequent use in determining kinetic parameters for CH₂Cl₂ breakdown in the complete reactor system are under investigation by Philip Marrone.

3.4.2 Effects of Residence Time and Concentration Variation

The experimental conditions listed in Table 3.1 resulted in conversions from 55 ± 5% to 97 ± 2%. For run groups 1, 3, and 5, the methylene chloride feed concentration was fixed while the oxygen feed concentration was varied from substoichiometric to superstoichiometric conditions. Figure 3.2a is a plot of conversion versus reactor residence time for these groups of runs. Also included for comparison is one hydrolysis data point which had the same CH₂Cl₂ feed concentration as the other points and can be considered the limiting example of substoichiometric conditions. As one might expect, conversion increases with increasing time in all cases. Not as intuitive is the fact that most data points with the same reactor residence time fall well within experimental error of each other, indicating again that conversion is the same regardless of the relative amount of O₂ initially present.

Figure 3.2 CH_2Cl_2 Conversion vs. Reactor Residence Time. $T=550^\circ\text{C}$. P-246 bar. a) constant CH_2Cl_2 feed concentration; b) constant O_2 feed concentration; c) constant feed ratio. From Marrone et al. (1995).



For experimental run groups 2, 4, and 5, the oxygen feed concentration was held constant while the organic feed concentration was varied from substoichiometric to superstoichiometric conditions. Figure 3.2b is a similar graph of conversion versus time for these groups of runs. Here there appears to be a greater difference between the 2.3 and 1.2 feed ratio data points which are practically on top of each other, and the 0.7 feed ratio data points (higher relative CH_2Cl_2 feed concentration) which are at consistently lower values. Comparison to Figure 3.2a reveals that the values achieved by lowering the CH_2Cl_2 feed concentration (feed ratios of 2.3 and 1.2 in Figure 3.2b) are higher than those achieved by raising the O_2 feed concentration (feed ratios of 2.6 and 1.3 in Figure 3.2a runs).

Figure 3.2c is a plot of data from experimental run groups 1 and 2, both at stoichiometric conditions but at different concentrations of both CH_2Cl_2 and O_2 . As in Figure 3.2b, this graph shows consistently higher conversions at the same reactor residence time for conditions with lower CH_2Cl_2 feed concentrations. Since Figures 3.2a and 3.1 show that changing the O_2 concentration has little effect on conversion, the results in Figures 3.2b and 3.2c must be due to the magnitude of the CH_2Cl_2 feed concentration. Thus, it appears that lower CH_2Cl_2 feed concentrations result in higher conversions.

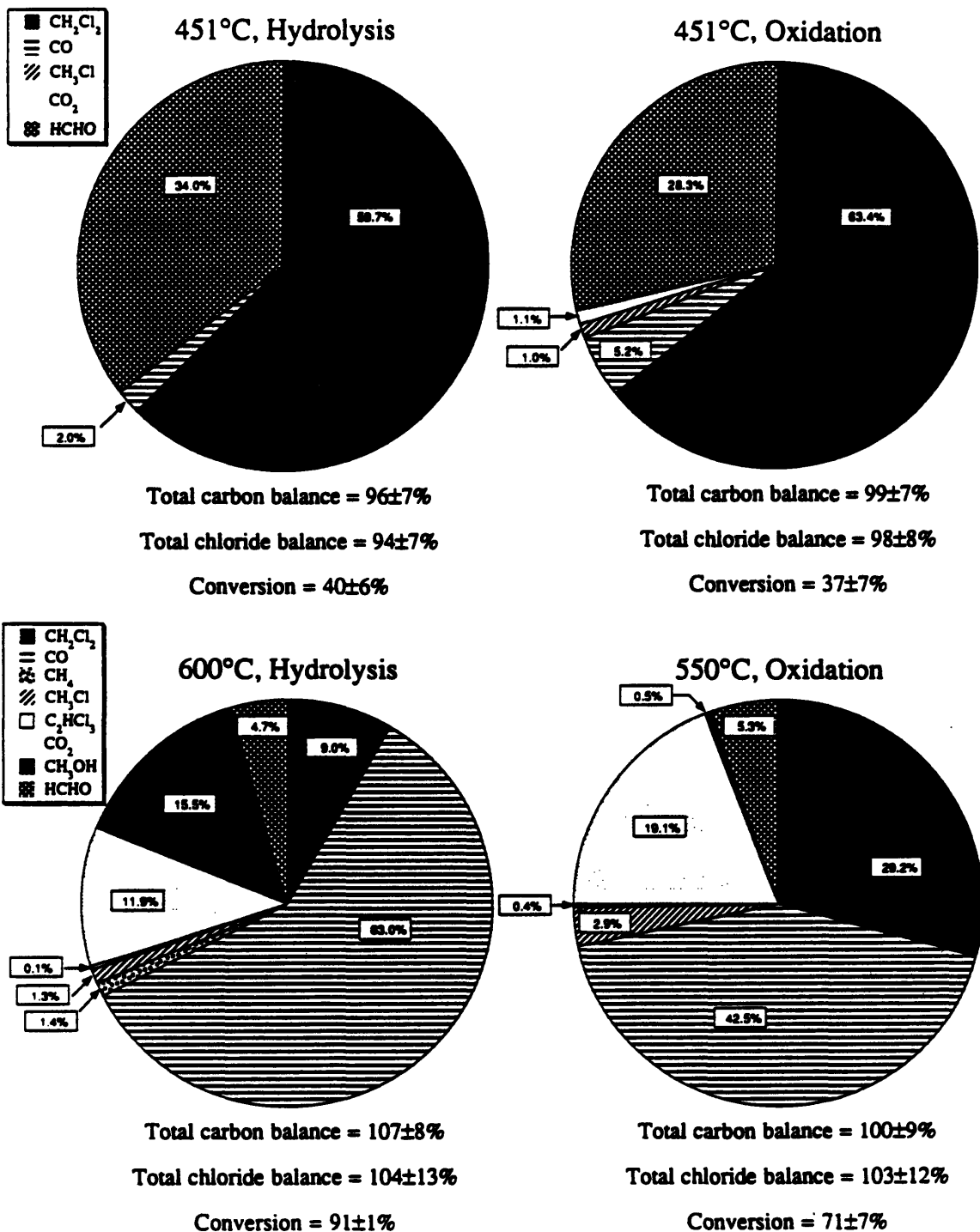
3.5 Product Distribution

The following major products were detected following both hydrolysis and oxidation of CH_2Cl_2 in supercritical water: CO , CO_2 , HCHO , CH_3OH , H_2 , and HCl . The methods of detection and quantification are described in Section 2.2. CH_4 was also detected in small amounts (< 1.5% of total carbon fed) but only at 562°C and above at 6 seconds reactor residence time and at 7 to 9 seconds reactor residence time at 550°C . Also,

there were trace amounts of the following chlorinated hydrocarbons detected in the vapor phase: chloromethane (CH_3Cl), chloroform (CHCl_3), 1,1-dichloroethylene ($\text{C}_2\text{H}_2\text{Cl}_2$), cis-1,2-dichloroethylene, trans-dichloroethylene, and trichloroethylene (C_2HCl_3). Of the total carbon mass balance, CH_3Cl accounted for <3%, C_2HCl_3 accounted for <0.7%, and the remaining chlorinated hydrocarbons accounted for <0.1% together. The presence of Cl_2 , C_2H_4 , C_2H_6 and C_2H_2 was not detected despite performing tests sensitive to these species. Atomic absorption tests were performed on liquid samples indicating the presence of nickel ions in the effluent at concentrations on the order of ppmw levels. Probably corrosion of the Hastelloy C-276 preheater tubing was the source of nickel. Based on equilibrium calculations, the formation of NiCl_x soluble complexes was unlikely at the concentrations of soluble nickel observed in the effluent samples. Good closure of carbon and chlorine balances ensured the identification all major products. Carbon and chlorine balances $\geq 87\%$ closure was observed for all experiments, with all but three out of the 66 runs having $\geq 90\%$ closure.

Although hydrolysis and oxidation resulted in the same types of products, the relative amounts of each product differed depending on temperature as well as the presence of oxygen. Figure 3.3 illustrates the relative amounts of carbon-based products found at two temperature extremes for hydrolysis and oxidation at fixed pressure, feed concentration and reactor residence time. The percentages for each product shown represent the fraction of total carbon feed recovered in that product. Thus, the percentages for all products shown add up to the total carbon mass balance for that run. A similar illustration for chlorine-based species would consistently show HCl as the only major product and is therefore not included. At 451°C , formaldehyde is easily the dominant product for both hydrolysis and oxidation. For hydrolysis at 600°C , the product spectrum is more diverse. In this case, the product CO dominates followed by significant amounts of CO_2 and CH_3OH but much less HCHO. For

Figure 3.3 Distribution of Carbon-containing Products. Units: percent of total amount of carbon fed in CH_2Cl_2 . $P \sim 246$ bar; $\tau \sim 6$ seconds. $[\text{CH}_2\text{Cl}_2]_0 \sim 1 \times 10^{-3}$ mol/L for hydrolysis and oxidation; $[\text{O}_2]_0 \sim 1 \times 10^{-3}$ mol/L for oxidation. From Marrone et al. (1995).



oxidation at 600°C, complete conversion was achieved and practically all the carbon was in the form of CO₂. Thus, 550°C was chosen for this illustration as a more interesting spectrum to represent high temperature SCWO. At this temperature, CO is the dominant product with a significant amount of CO₂ but little HCHO and hardly any CH₃OH. As one can see from this complete illustration, the percentage of gaseous products and the variety of total products increases with increasing temperature.

Figures 3.4 and 3.5 show the molar yield of major products versus temperature for hydrolysis and oxidation respectively. In this case, molar yield is defined as the moles of product formed divided by the moles of CH₂Cl₂ feed *that reacted*. Thus, the total of all molar yield values for the major carbon products at any given temperature should add up to 1 while the molar yield for chlorinated products should equal 2. CO, CO₂, and HCHO are shown in Figures 3.4a and 3.5a while H₂, CH₃OH, and HCl are shown in Figures 3.4b and 3.5b. The trends from these figures indicate that the molar yield of HCHO always decreases with increasing temperature for both hydrolysis and oxidation while the molar yield of all other products (except HCl) increases with increasing temperature under hydrolysis conditions. For oxidation, however, CO₂ is the only product that continually increases with increasing temperature. As the major chlorinated species, the molar yield of HCl remains near 2 for conditions with and without oxidant.

A comparison of Figures 3.4a and 3.5a shows that that amount of HCHO present under oxidation conditions is always less than that under hydrolysis conditions at any given temperature. The amount of CO (up to 550°C) and CO₂ under oxidation conditions, however, is always more than that under hydrolysis conditions. The molar yield of CO exhibits a maximum under oxidation conditions at 550°C, above which its value decreases essentially to zero by 600°C. Comparing Figures 3.4b and 3.5b shows that the amount of H₂ and CH₃OH increases with temperature for hydrolysis

Figure 3.4 Molar Yield of Products vs. Temperature: CH₂Cl₂ Hydrolysis. P~246 bar; τ~6 seconds. [CH₂Cl₂]₀~1x10⁻³ mol/L. a) for CO, CO₂, HCHO; b) for H₂, CH₃OH, and HCl. From Marrone et al. (1995).

Figure 3.4a - CO, CO₂, HCHO

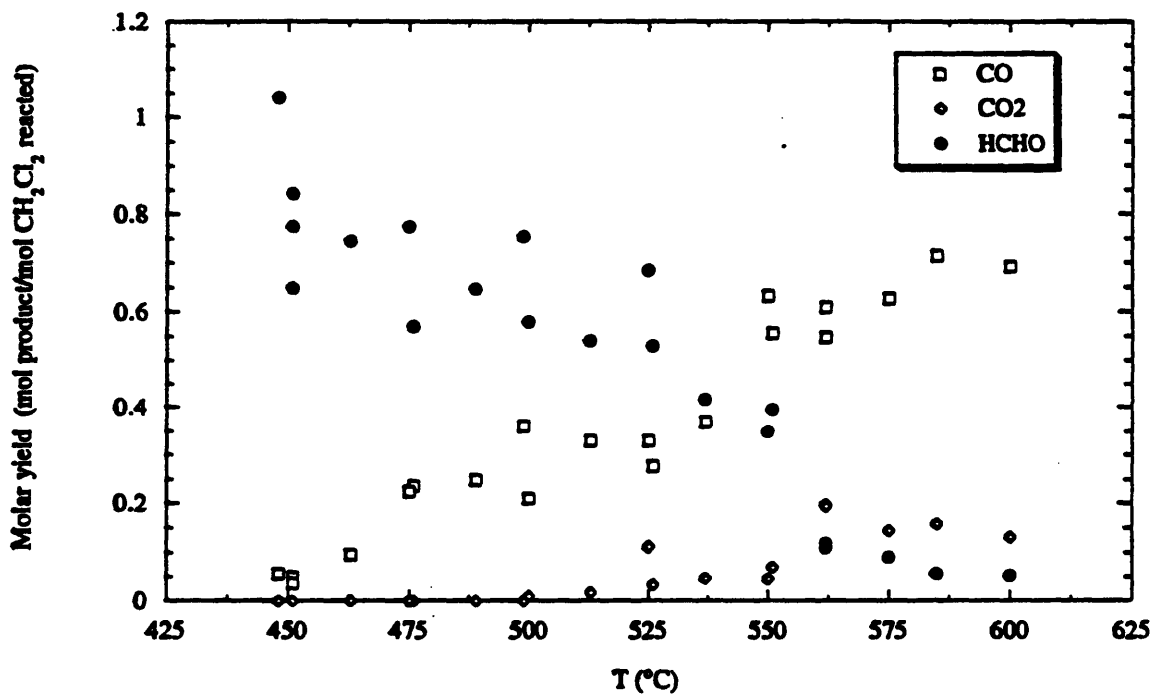


Figure 3.4b - H₂, CH₃OH, HCl

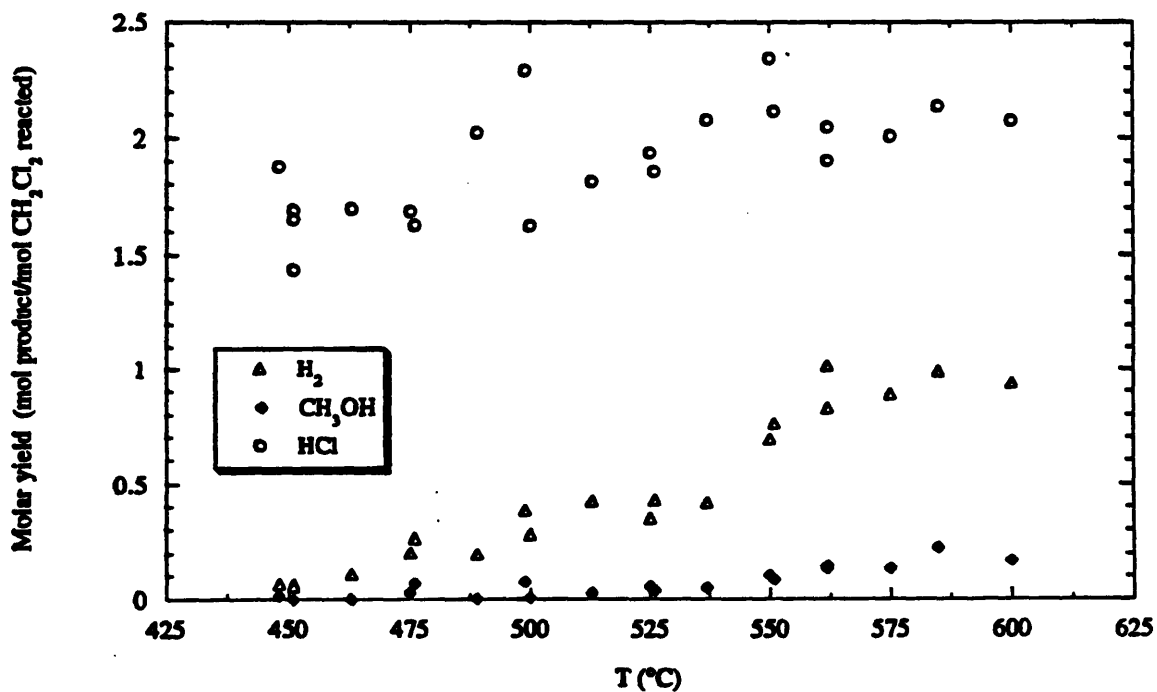


Figure 3.5 Molar Yield of Products vs. Temperature: CH_2Cl_2 Oxidation. P~246 bar; τ ~6 seconds. $[\text{CH}_2\text{Cl}_2]_0 \sim 1 \times 10^{-3}$ mol/L. $[\text{O}_2]_0 \sim 1 \times 10^{-3}$ mol/L. a) for CO, CO_2 , HCHO; b) for H_2 , CH_3OH , HCl. From Marrone et al. (1995).

Figure 3.5a - CO, CO_2 , HCHO

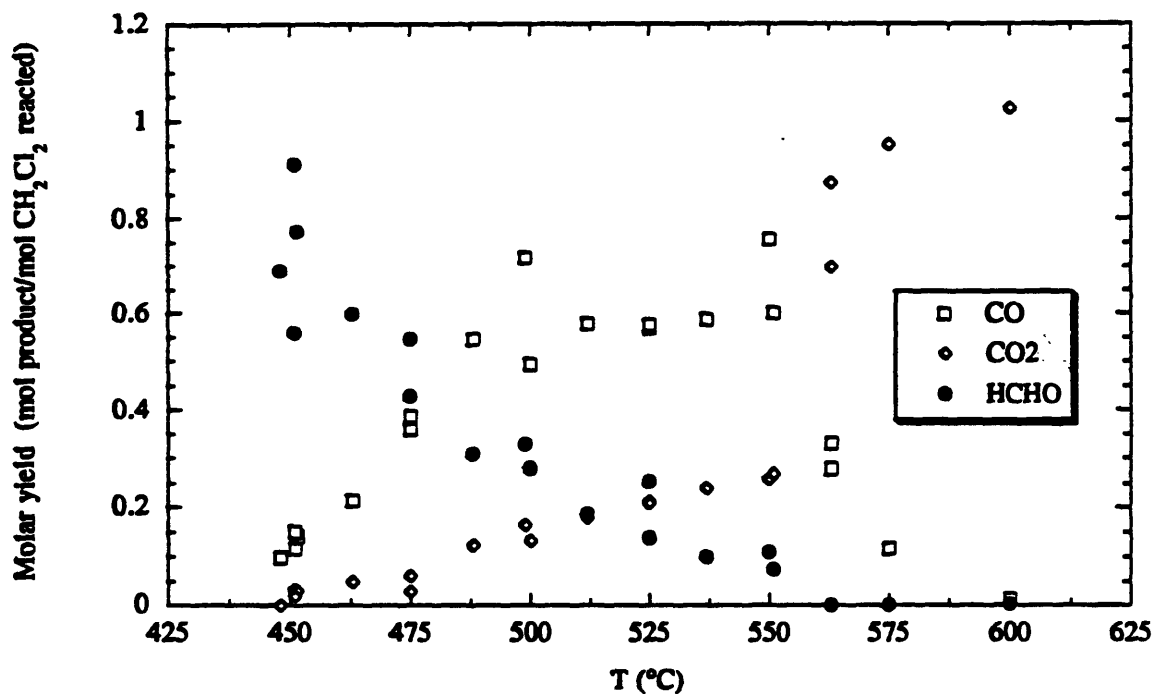
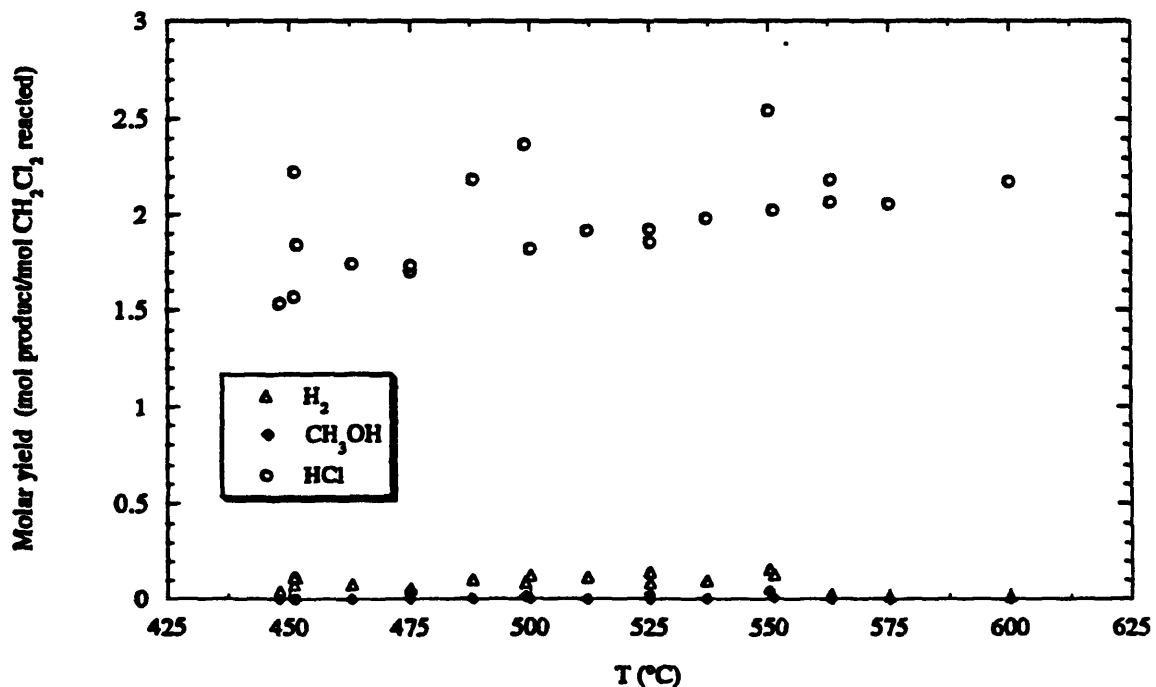


Figure 3.5b - H_2 , CH_3OH , HCl



conditions, but remains close to or at zero for all temperatures under oxidation conditions. The fact that very little CH_3OH remains under oxidation conditions compared to hydrolysis conditions is consistent with an earlier study of CH_3OH oxidation (Webley et al., 1990; Tester et al., 1992), which found less than 3% conversion under hydrolysis conditions but more than 98% conversion under oxidation conditions by 550°C at reactor residence times longer than 6 seconds. Similar trends of no significant hydrolysis conversion but $> 98\%$ oxidation conversion were also observed in an early study of H_2 at 600°C and 5 seconds reactor residence times (Holgate and Tester, 1993). In summary, the presence of oxygen increases the amount of CO (up to 550°C) and CO_2 formed while reducing the yield of HCHO and also hindering the buildup of CH_3OH and H_2 .

One further point from Figure 3.4b is that under hydrolysis conditions above 560°C , the yield of hydrogen atoms per mole of CH_2Cl_2 reacted for HCl and H_2 sums to about 3. This clearly exceeds the number of H atoms that can possibly be generated from CH_2Cl_2 and is strongly indicative of solvent (H_2O) participation in the reaction.

Under hydrolysis conditions, the concentration of trace chlorinated hydrocarbons in the vapor phase increased with increasing temperature. Higher amounts were observed under oxidation conditions up to a maximum at 550°C , above which concentrations quickly dropped to $< 0.2\%$ of the total carbon mass fed by 600°C . Highest concentrations were observed at 550°C for the runs with the highest O_2 feed concentrations (superstoichiometric conditions). Although these chlorinated hydrocarbons, in general, accounted for only a very small amount of the products, their presence and increase or decrease with temperature do provide insights into possible mechanisms and side reactions that may be important.

Varying reactor residence time under oxidation conditions did not significantly affect overall product distributions. The only effects were a relatively greater amount of CO₂ and HCl and a smaller amount of CO as residence time increased; observations which normally accompany increased conversion of CH₂Cl₂ and CO with increasing residence time.

3.6 Corrosion

Corrosion was observed in the Hastelloy C-276 organic preheater coil. Several pieces of evidence corroborate this observation. After pressure letdown following most experiments, the effluents were discolored and contained visible particulates consisting mostly of nickel (confirmed by elemental x-ray analysis of the filtrates). Four separate preheater coils failed after about 104, 44, 54, and 65 hours of operation with CH₂Cl₂ feed. Post-failure microscopic analysis of the failed sections of preheater tubing showed signs of enhanced corrosion at grain boundaries (Mitton et al., 1994). The preheater coils all ruptured within a zone from 150 to 450 cm downstream of where the preheater coil enters the sandbath. Although the exact temperature of the fluid in this region is unknown, it is likely that the temperature was high but subcritical (probably less than 300°C) - giving exactly the conditions (a moderately hot but subcritical, ionic environment) where corrosion is predicted to be particularly aggressive (Huang et al., 1989).

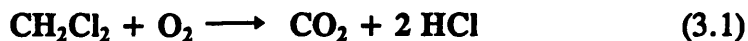
Consistent with this theory, post-failure analysis performed at MIT has found that corrosion appears to be confined to the region around the rupture point of the preheater coils (Mitton et al., 1994). Negligible corrosion has been detected at both the entrances (cold) and exits (supercritical temperatures) of the preheater coils. Although the exact type of corrosion has yet to be confirmed, there appears to be a

selective dissolution of nickel in corroded region of the preheater tubing. Atomic absorption tests performed on liquid effluent samples support these conclusions. Concentrations of soluble nickel in the samples tested were on the order of 3 to 16 ppmw, with higher concentrations found for experiments performed just before the time of failure of a preheater coil. Similar atomic absorption tests to determine the concentrations of chromium in the effluent indicated levels near the detection limit (≤ 0.6 ppmw). Rice et al., (1993) report similar corrosion results with SCWO of CH_2Cl_2 and other chlorinated organics. Concentrations of nickel and chromium in their effluent were comparable to those found in this study at values of 30.7 ppmw and 0.02 ppmw respectively.

The evidence of aggressive corrosion strongly suggests that there was significant and early breakdown of methylene chloride to HCl in the organic preheater coil - enough to result in the failure of the tube in a relatively short amount of exposure time. In addition, it is also possible that the corroding metal surface of the preheater coil and/or the presence of HCl may have influenced the rate of CH_2Cl_2 destruction in a catalytic manner. Houser and Liu (1994a) present evidence that the reactivity of chlorinated hydrocarbons in supercritical water, and the resulting product spectra, can be affected significantly by the metal walls of the reactor. However, no specific attempts were made in our work to determine the extent, if any, of catalytic effects due to the above mentioned sources.

3.7 Mechanistic Insights from Experimental Results

The complete oxidation of methylene chloride to carbon dioxide and hydrochloric acid can be written as:

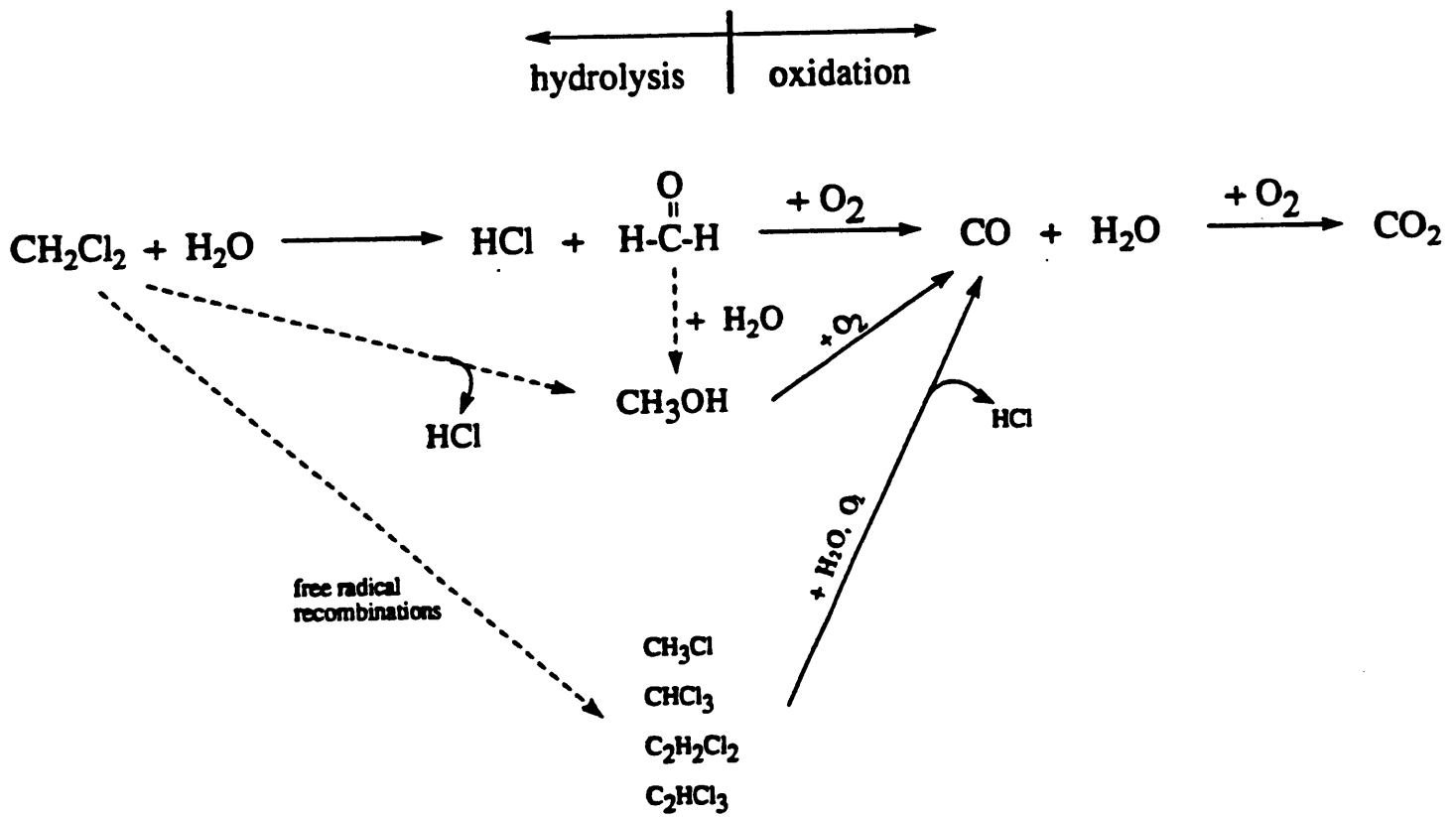


The kinetics, product spectrum and distribution, and corrosion evidence gathered in this study, however, suggest that the supercritical water oxidation of CH_2Cl_2 in this particular apparatus does not proceed directly as written in Equation (3.1). Based on the experimental data, a network of possible reaction pathways is plausible. The following important facts bare restating: 1) conversions were similar under hydrolysis and oxidation conditions, 2) conversion already occurs early in the preheater coil, and 3) the presence of O_2 only shifts the product spectrum to more CO and CO_2 and less HCHO . These facts collectively suggest that most of the breakdown of CH_2Cl_2 itself probably occurs by early reaction with water at low subcritical temperatures, not by oxidation. The main products of this initial reaction appear to be HCl and HCHO :



Formaldehyde is essentially the only carbon product at 450°C . The same two products were reported by Fells and Moelwyn-Hughes (1958) for CH_2Cl_2 hydrolysis under acidic conditions at subcritical temperatures between $80\text{-}150^\circ\text{C}$. For temperatures above 450°C , another pathway for CH_2Cl_2 breakdown (or possibly HCHO reduction under hydrolysis conditions) to form CH_3OH seems to become significant. Side reactions involving the production of chlorinated hydrocarbons seem to also increase with increasing temperature, with their formation probably resulting from recombination of free radical fragments derived from CH_2Cl_2 , since only trace amounts of these compounds are produced. Once formed, the first intermediate compounds of HCHO and CH_3OH can then be further oxidized to CO , which in turn is oxidized to CO_2 . Figure 3.6 shows a diagram of this proposed reaction network.

Figure 3.6 Plausible Reaction Network for CH₂Cl₂ Oxidation in SCW. From Marrone et al. (1995).



Note that the individual reactions in this network can add up to the net reaction in Equation (3.2). The important distinction, however, is that O_2 is not involved in the initial breakdown of CH_2Cl_2 itself, which proceeds by a hydrolysis pathway. This network is consistent, then, with the observation that O_2 had little affect on the kinetics of CH_2Cl_2 destruction in our supercritical water experiments.

CHAPTER 4

Experimental Studies of Thiodiglycol Hydrolysis and Oxidation in Supercritical Water

4.1 Introduction

Sulfur is one of several heteroatoms prevalent in hazardous organic wastes around the world. One example of a particularly dangerous class of sulfur-containing waste is the stockpiled and non-stockpiled chemical munitions housing the agent HD mustard, $(\text{ClC}_2\text{H}_4)_2\text{S}$. Incineration is the present U.S. method of choice for destruction of all chemical munitions. However, public resistance has forced the Army to investigate alternate destruction methods which may be more acceptable (Ember, 1990).

Supercritical water oxidation (SCWO) is one of the alternate technologies being examined with initial tests on actual chemical warfare agents already performed by General Atomics (Downey et al., 1994).

A fundamental understanding of C-S chemistry in supercritical water (SCW) hydrolysis/pyrolysis and oxidation reactions is important to the development of a SCWO process which can effectively destroy organosulfur wastes. Published studies of reactions of sulfur compounds in SCW are limited. Destruction efficiency measurements under SCWO conditions have been reported by Thomason et al. (1990) for dimethylsulfoxide (DMSO), and by Rice et al. (1994) for several sulfur-containing military dyes. Studies of organosulfur compounds under hydrolysis/pyrolysis conditions in SCW include the work of Houser and Liu (1994b) with benzylsulfide and thianaphthene, and a dibenzothiophene study by Townsend et al. (1988). In addition, Turner (1993) used thiodiglycol as a model compound in a kinetic analysis of C-S chemistry in SCW reactions. A detailed study of thiodiglycol hydrolysis and oxidation in SCW was undertaken here to build on the initial understanding of organosulfur

compounds in this environment gathered from these previous studies as well as to investigate the behavior of an important chemical agent simulant under well-defined experimental conditions.

4.2 Literature Review

Thiodiglycol (TDG), $(\text{HOC}_2\text{H}_4)_2\text{S}$, is a colorless, viscous liquid with a distinctive odor at ambient conditions. It is formed by reacting ethylene oxide and hydrogen sulfide with alkali as the catalyst; one by-product of this reaction being 2-mercaptoethanol $(\text{HSC}_2\text{H}_4\text{OH})$. TDG has many commercial uses in such items as elastomers, lubricants, inks, dyes, and antioxidants (Lundin, 1991). Perhaps its most famous use is that of a primary ingredient in the production of the chemical agent, HD or sulfur mustard, $(\text{ClC}_2\text{H}_4)_2\text{S}$, according to the following chlorination reaction.



For this reason, TDG is a compound of international interest and its production and end-use will be monitored throughout the world for compliance with the Chemical Weapons Convention (CWC) (Lundin, 1991). Noteworthy is that the reverse of reaction (4.1) is the major hydrolysis degradation pathway of HD mustard.

In this study, TDG is also used as a simulant for HD mustard agent. Select properties of each compound are listed in Table 4.1. TDG has the same C-S bond arrangement as mustard with a similar density but it is relatively non-toxic. TDG is much more soluble in ambient water than mustard, which is unfortunately a property of interest in simulating feed preparation for reactions in SCW. TDG is more stable than HD mustard in hydrolysis, pyrolysis and oxidation reactions, but they share some of the same products from these reactions as described below.

Table 4.1 Physical Properties of TDG and HD (from Lide, 1993).

Property	TDG	HD Mustard
Structure	HO-C ₂ H ₄ -S-C ₂ H ₄ -OH	Cl-C ₂ H ₄ -S-C ₂ H ₄ -Cl
Molecular Weight	122.19	159.07
Boiling/Melting Point (°C)	165/-10	217/14.5
Density @ 25°C	1.221	1.2741
Solubility in Distilled Water (g/100 g) @ 25°C	completely miscible	0.092

A literature search revealed the results of several thiodiglycol (TDG) reactions which are of interest to this study. Neat thiodiglycol is stable at 180°C for many hours, but it reacts to form dithiane (S(C₂H₄)₂S) and thioxane (O(C₂H₄)₂S) when passed over alumina at 200 to 275°C. Esters and ethers of TDG can be formed under various conditions of alkalinity and acidity and in the presence of organic acids or alcohols (Reid, 1960). Three oxidation studies using hydrogen peroxide under ambient conditions were identified. Ross (1946) and Ogata and Sawaki (1963) reported the oxidation rate of TDG to be second order overall, with and without catalyst, producing thiodiglycol sulfoxide as shown:



Both studies conclude that the reaction proceeds through ionic mechanisms which are pH dependent. Gilbert et al. (1973) performed a third oxidation study of TDG in a titanium (III) - hydrogen peroxide system. Their investigation of radical formations suggested the following primary reaction pathway:



Mohan and Mittal (1991) also investigated the role of hydroxyl radicals in the oxidation of TDG via a pulse radiolysis study of ambient aqueous solutions.

The study most relevant to our work is the single, detailed investigation of thiodiglycol hydrolysis and oxidation in supercritical water conducted at the University of Texas by Turner (1993). As a first step in his study, hydrolysis and oxidation reactions were conducted in a stainless steel U-tube batch reactor. Table 4.2 lists the range of conditions for the batch study. The batch tests were performed as

Table 4.2 Previous Batch Test Operating Conditions for TDG from Turner (1993).

Initial Concentration (ambient)	1 % by volume
Temperature	425 to 500°C
Pressure	352 to 552 bar
Density (fixed)	0.3 g/cm ³
Retention Time	1 to 8 minutes
Oxygen (% of Stoichiometric Demand)	200% and 0%

screening tests to determine parent compound conversion trends and provide preliminary identification and analysis of partial degradation products. Detailed kinetic experiments were performed on a laboratory-scale, continuous-flow apparatus with a coiled, stainless steel tubular reactor in order to develop global kinetic models and

identify major reaction mechanisms. The ranges of conditions for the continuous-flow study are listed in Table 4.3.

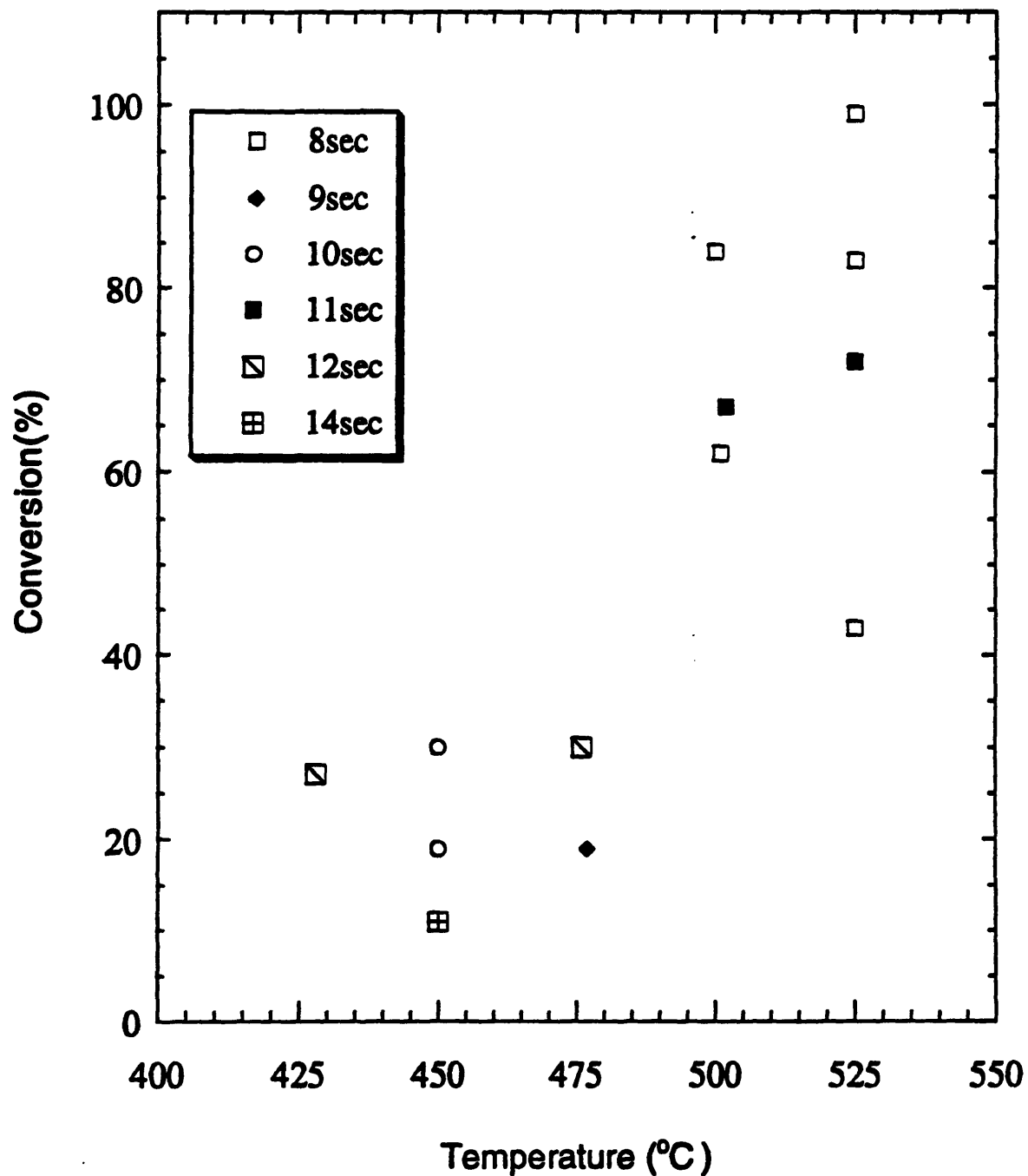
Table 4.3 Previous Continuous-flow Operating Conditions for TDG from Turner (1993).

Initial Concentration (ambient)	500 mg/L, 1000 mg/L
Temperature	425 to 525°C
Pressure	276 bar
Mass Flow Rate	25 g/min
Retention Time	5 to 16 seconds
Reactor Lengths	10 and 20 ft
Oxygen (% of Stoichiometric Demand)	0% and 100 to 325%

Turner (1993) reports essentially complete conversion under oxidation conditions and significant conversion without oxidant over the range of conditions explored. Figure 4.1 is a plot of his hydrolysis data. Corrosion was believed to be significant throughout this study, occurring mostly during hydrolysis/pyrolysis and to a lesser degree during oxidation experiments. The apparent corrosion resulted in equipment failures, leaks, and pressure and flow control problems due to plugging by particulates. Most of the liquid effluents had a “milky” appearance that gradually cleared, forming a white precipitate. As a result of these operational problems, kinetic measurements were limited to identification of degradation products and pathways.

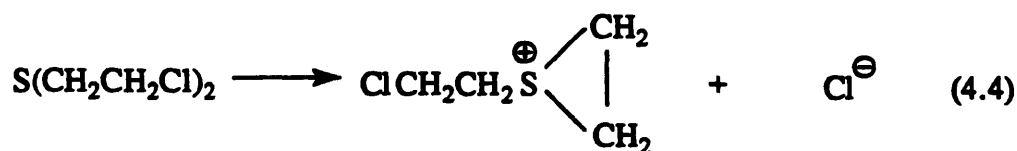
For hydrolysis, gas phase effluents were composed of CO, CH₄, H₂S, C₂H₄ and C₂H₆. Liquid phase products consisted of hydrogen sulfide, acetate, and ethanol

Figure 4.1 TDG Hydrolysis Conversion versus Temperature Reported by Turner (1993). $C_0 = 970\text{-}1000$ ppm; $P = 276$ bar; Reynolds number (Re) = $5400\text{-}8100$.



with sulfite and sulfate also present in trace amounts. Upon quantification, CO and CH₄ accounted for approximately 50% of the carbon-containing by-products found and ethanol and C₂H₄ accounted for the remaining 50%. H₂S was the dominate sulfur product. For oxidation, CO, CO₂, CH₄, C₂H₆, and H₂S were identified in the gas phase and ethanol, acetic acid, hydrogen sulfide, sulfite and sulfate were found in the liquid phase. Quantification revealed that CO, CO₂, and CH₄ accounted for most of the reacted carbon and sulfate accounted for most of the reacted sulfur.

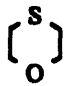
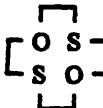

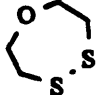


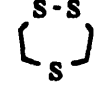
Several reactions of HD mustard are also of interest to this study. Many investigators have studied HD mustard hydrolysis at ambient pressure for various conditions of temperature, degree of agitation, pH and with co-solvents present (Yang et al., 1986; Rohrbaugh et al, 1989; Harris and McManus, 1985; and several authors listed in a review report by MacNaughton and Brewer, 1994). In general, hydrolysis of HD is mass-transfer limited due to its limited solubility in water. Typically, at temperatures greater than 70°C and residence times of 3 minutes or more, hydrolysis is complete. The reaction is thought to proceed first to a sulfonium ion intermediate as diagrammed below.



Depending on several conditions, the sulfonium ion can then react to form TDG or a variety of more complex molecules including higher molecular weight ions, polymers,

and ether and alcohol compounds. The most recent work on the ambient-pressure caustic hydrolysis of mustard is that of Harvey et al. (1994). They studied a variety of conditions including temperatures ranging from 30 to 90°C, reaction times of minutes to several hours, NaOH concentrations of 25% to 15,530% molar excess and HD mustard concentrations up to 40% by volume. They also performed an extremely detailed analysis to identify all products of the reaction resulting in three phases; a solid phase, an organic liquid phase and an aqueous liquid phase. Table 4.4 is an example of the wide variety of products identified in these reactions. In this case, area percent values listed do not reflect concentrations but merely detector responses to these extracted compounds in this chloroform phase.

Table 4.4 CHCl_3 -soluble Products Identified by GC/MS from 40% by volume HD Hydrolysis Reaction. (reproduced from Harvey et al, 1994).

Compound	Area %	Compound	Area %
$\text{CH}_2 = \text{CH S CH}_2 \text{CH}_2 \text{OH}$	26.4	$\text{CH}_2 = \text{CH S CH}_2 \text{CH}_2 \text{S CH} = \text{CH}_2$	1.2
$\text{HO CH}_2 \text{CH}_2 \text{S CH}_2 \text{CH}_2 \text{S CH} = \text{CH}_2$	13.3	$\text{CH}_2 = \text{CH S CH}_2 \text{CH}_2 \text{S CH}_2 \text{CH}_2 \text{OCH}_2 \text{CH}_2 \text{OH}$	0.9
$\text{HO CH}_2 \text{CH}_2 \text{S CH}_2 \text{CH}_2 \text{OH}$	10.8	$\text{HO CH}_2 \text{CH}_2 \text{S CH}_2 \text{CH}_2 \text{S CH} = \text{CH}_2$	0.7
	8.7	 Isomers	0.3
$\text{CH}_2 = \text{CH S CH}_2 \text{CH}_2 \text{O CH}_2 \text{CH}_2 \text{OH}$	6.9		0.2
$\text{HO CH}_2 \text{CH}_2 \text{S CH}_2 \text{CH}_2 \text{S CH}_2 \text{CH}_2 \text{OH}$	5.9	Unknown	0.1
$\text{CH}_2 = \text{CH S CH}_2 \text{CH}_2 \text{O CH}_2 \text{CH}_2 \text{S CH}_2 \text{CH}_2 \text{OH}$	5.1		0.1
	4.0	Unknown	0.1
$\text{HO CH}_2 \text{CH}_2 \text{S CH}_2 \text{CH}_2 \text{O CH}_2 \text{CH}_2 \text{OH}$	3.9	Unknown	0.1
Higher MW Hydrolysis/Elimination products	3.6	$\text{HO CH}_2 \text{CH}_2 \text{OH}$	0.07
 and  ~3:1	2.7		
$\text{CH}_2 = \text{CH S CH}_2 \text{CH}_2 \text{O CH}_2 \text{CH}_2 \text{S CH} = \text{CH}_2$	2.5		
$\text{CH}_2 = \text{CH S CH}_2 \text{CH}_2 \text{S CH} = \text{CH}_2$	2.4		

Williams (1947) studied the pyrolysis of neat HD mustard at temperatures of 180°C to 450°C. Table 4.5 lists the by-products found in this pyrolysis study. Analysis of the non-volatile residue revealed a high sulfur content (> 40%). Brooks and Parker (1979) studied the pyrolysis and incineration of HD mustard and found that oxidation (incineration in air) and pyrolysis rates for HD were not significantly different from each other.

Table 4.5 Product Yields of HD Pyrolysis Reported by Williams (1947). Values in % of initial HD weight.

Product	180°C	220°C	350°C	450°C
HCl	8.0	21.2	25.8	31.5
C ₂ H ₄	4.2	11.2	7.9	10.4
1,2 Dichloroethane	6.9	11.1	0	0
H ₂ S	0	0	3.9	5.2
Vinyl Chloride	0	0	14.6	19.4
Dithiane	1.3	3.3	Trace	Trace
2,2'-Dichlorodiethyl Disulfide	5.8	8.5	2.0	0
Unreacted HD	56.0	14.2	13.0	0
Nonvolatile Residue	12.2	25.7	ca. 31	ca. 32
Carbon Disulfide	0	0	ca. 1	ca. 1

The supercritical water oxidation of HD has recently been investigated by researchers at General Atomics (Downey et al., 1994). A 1 wt% feed solution was prepared by hydrolyzing HD mustard at 80-90°C for 7 minutes creating a homogeneous mixture. All tests were performed at a pressure of 276 bar with 100% excess oxygen and residence times of 30 to 40 seconds in a tubular reactor with a titanium liner. No agent was detected in any liquid effluent, signifying a destruction removal efficiency (DRE) of 99.9999% based on the detection limit for mustard agent. Table 4.6 lists the results of product analysis for these experiments. In addition to these products, several unknown, nonagent peaks of ~50-100 ppm each were also detected. Downey et al. (1994) explain that the SO_x concentrations were due to poor mixing/mass transfer limitations resulting in incomplete conversion to sulfate.

Table 4.6 Analytical Results for Mustard Testing Reported by Downey et al. (1994).

	Component	Unit of Measure	450°C	500°C	525°C
Liquid Analysis	Acetate	ppm	597	47	<1
	Formate	ppm	211	16	<1
	Sulfate	ppm	6008	5336	3105
Gaseous Analysis	CO	mole%	14.5	1.4	0.17
	H ₂	vppm ^a	3000	BDL ^b	BDL
	C ₂ H ₄	vppm	700	BDL	BDL
	SO _x	vppm	2133	1098	2600

^a Part per million by volume

^b Below detection limit

4.3 Experiments Performed

The present thiodiglycol study consisted of a total of 50 experiments, 15 of which were oxidation experiments with a stoichiometric feed of oxygen (oxygen/organic feed ratio of 7/1 based on complete conversion to CO₂). Table 4.7 provides an outline of the TDG study listed by groups of experiments performed in chronological order.

Table 4.7 TDG Experiments Performed in This Study.

Group	# of Runs	Temperature (°C)	Hydrolysis or Oxidation	Period	Comments
A	5	425,500,600	Hyd(3),Oxd(2)	Jul 94	Scoping
B	7	200,300,425-525	Hyd	Jan 95	Reactor Bypass
C	15	425-525	Hyd,Oxd	Feb-Mar 95	Direct Org Feed (DOF)
D	1	100-425	Hyd	10 Mar 95	Scoping, DOF
E	12	400-525	Hyd,Oxd	Mar 95	Soluble Organic Feed
F	6	200-350	Hyd	Mar 95	Soluble Organic Feed
G	4	350	Hyd (τ varied)	Mar 95	Soluble Org Feed, Residence Time Varied

The variety of experimental conditions explored was specifically chosen to examine reaction regimes of partial as well as complete conversion.

All experiments were performed using the two configurations of the plug-flow apparatus described in Section 2.1 at a fixed pressure of approximately 250 bar. With the exception of Group G, all experiments were designed to hold concentrations, reactor residence time and pressure constant while only varying temperature. The

experiments in Group G, however, were designed to study the effect of residence time with feed concentrations, pressure and temperature held constant while varying flow rates to change residence time in the reactor. For all supercritical experiments (groups A-E), the initial organic concentration under reactor conditions was approximately 5×10^{-4} mol/L. For subcritical experiments, the initial concentration was changed to approximately 2.5×10^{-3} mol/L which allowed for the use of similar ambient feed concentrations for both sub- and supercritical runs. The operating conditions for the reactor bypass runs (Group B) were kept the same as those for the corresponding run with the reactor in place.

Most TDG experiments were plagued by problems similar to those encountered by Turner (1993). For example, hydrolysis experiments at supercritical temperatures produced liquid effluents with a very “milky” appearance which gradually cleared, forming a pale-colored precipitate. Usually after each hydrolysis experiment, oxygen was added to the system to begin the oxidation experiment. With added oxygen, the cloudy liquid effluent generally cleared to its normal transparent appearance within 20 to 30 minutes. Several samples of the hydrolysis effluent were filtered and the solids were analyzed for elemental composition using a scanning electron microscope (SEM) with an x-ray detector. The results showed that this solid phase was mostly sulfur, leading us to believe that we were forming solid, elemental sulfur under hydrolysis/pyrolysis conditions (see Section 4.5 for a description of solids collected).

This solid phase frequently plugged filters and the back-pressure regulator (BPR). All filter elements had to be replaced and the filter manifold dismantled and cleaned usually after every second hydrolysis experiment. The seals in the BPR had to be replaced generally after every other run. The BPR itself was eventually replaced with a different model which performed better in this environment. During actual experiments, the solids would apparently accumulate in the system and then

periodically dislodge, causing pressure fluctuations as high as ± 21 bar. These fluctuations also made gas flow rates extremely difficult to measure, but the impact on liquid flow rates was generally small. In some cases the solid phase would gradually build-up on the filters with no significant release. Usually under these circumstances, pressure could not be controlled with small adjustments to the BPR, and the experiments were aborted when pressures approached the rated burst pressure of system rupture disks (~ 310 bar).

Several attempts were made to flush the system between experiments with an appropriate solvent to help dissolve the solids. We avoided using carbon disulfide (CS_2), which is an ideal solvent for some forms of elemental sulfur, because of its toxic nature and adverse effect it may have on reaction effluents which may contain trace amounts of CS_2 . Acetone, which does reasonably well at dissolving solid sulfur, was used on a few occasions with limited success. It seemed to be successful at flushing away some solids, but it was an additional struggle to flush residual acetone from the system.

In summary, the solid phase production typical of hydrolysis experiments presented a severe obstacle to our supercritical water experiments with thiodiglycol. Similar problems were not encountered in subcritical runs, although elemental sulfur may have been present at much smaller concentrations. Each supercritical hydrolysis/pyrolysis experiment usually had large pressure fluctuations and large variations in gas flow rates. Also, the solid phase may have accumulated on the walls of system tubing, presenting an inconsistent environment from experiment to experiment.

4.4 Kinetic Results

4.4.1 Scoping and Reactor Bypass Experiments

Five scoping experiments, 3 hydrolysis and 2 oxidation, were performed to take a first look at thiodiglycol (TDG) conversion over a range of conditions and begin work on identifying and quantifying the product spectra. A third oxidation experiment at 600°C was attempted but aborted due to extremely poor pressure control. The results are captured in a conversion versus temperature plot in Figure 4.2. All but the first experiment, hydrolysis at 425°C, resulted in high conversions, with and without oxidant. TDG concentrations for this initial work were determined by GC/FID analysis of the liquid phase. As described in Section 2.2, this technique may have resulted in higher than actual concentrations due to the inconsistent elution of TDG. With actual concentrations being lower, conversions for these runs may even be higher. However, the same samples were analyzed by HPLC four months later and concentrations were essentially the same. The results of this initial work are also in reasonable agreement with Turner's results (see Figure 4.1).

Since we found considerable conversion of TDG without oxidant, it is highly likely that initial degradation may be happening during preheating, even before reaching the reactor. Using the same reactor bypass tubing as in the methylene chloride work (see Section 2.1 for a description), experiments were performed at seven different temperatures to investigate conversion in the preheater coil. The results are plotted in Figure 4.3. For subcritical temperatures, conversion is essentially zero. At supercritical temperatures, conversion in the preheater coil is significant with complete

Figure 4.2 Results from Scoping Runs: TDG Hydrolysis and Oxidation in SCW. Estimated 95% confidence intervals are shown and the line is drawn to indicate trends.

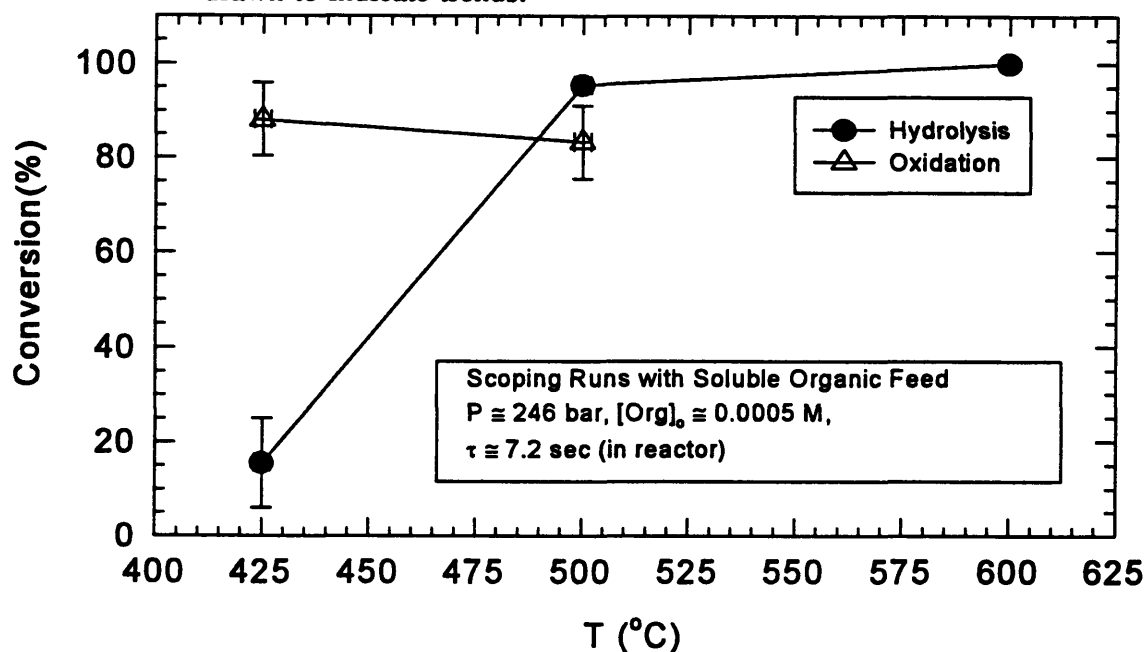
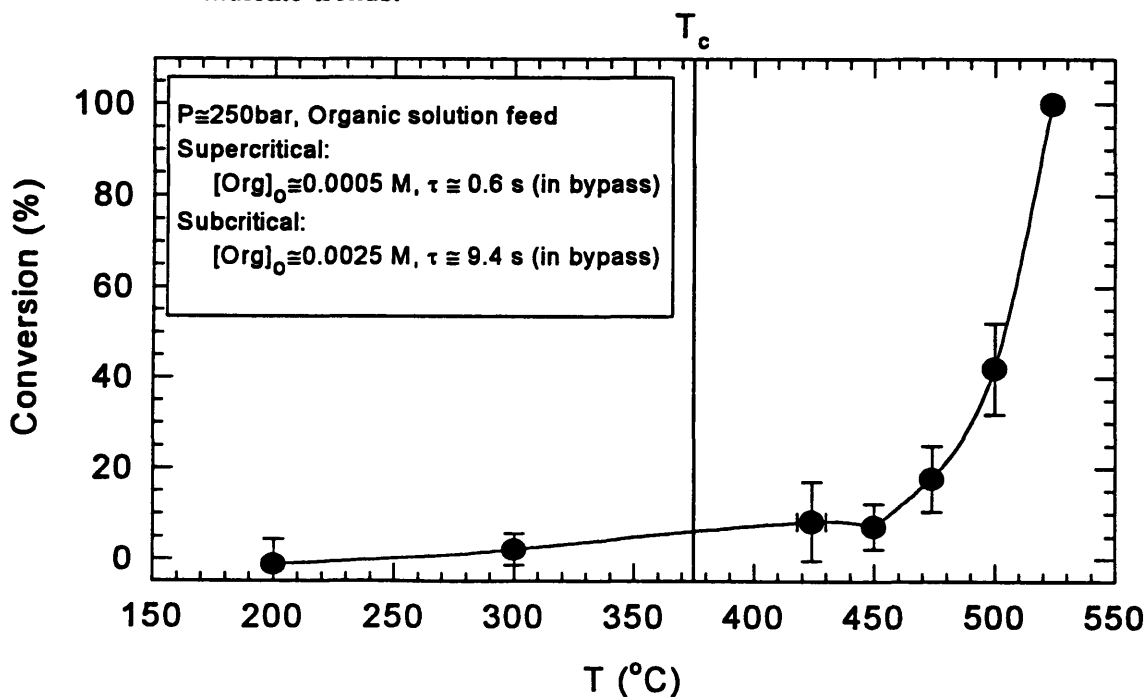


Figure 4.3 Results from Reactor Bypass Runs: TDG Hydrolysis in SCW. Estimated 95% confidence intervals are shown and the line is drawn to indicate trends.



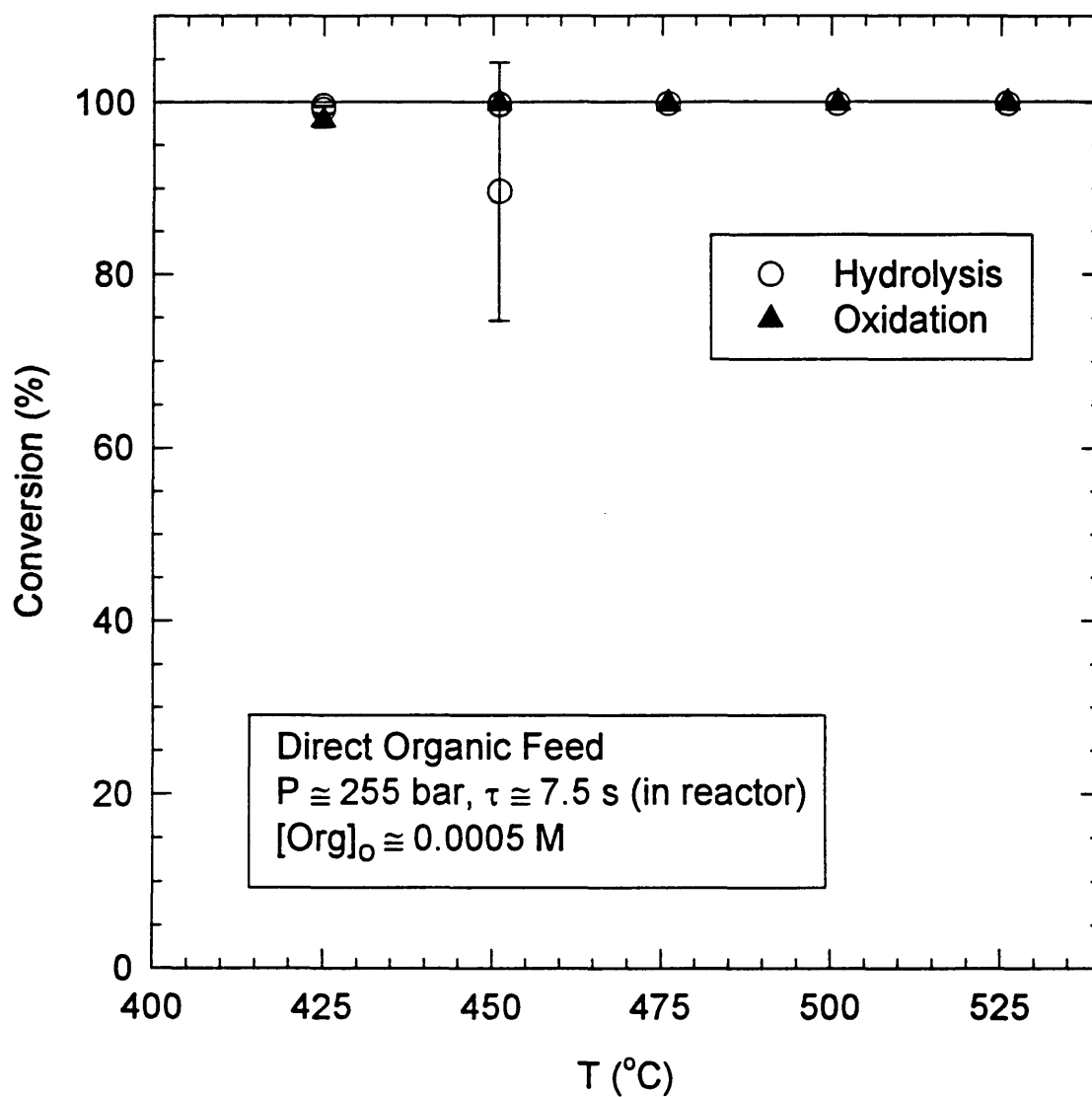
conversion occurring by 525°C. Unlike methylene chloride, which saw similar conversions with and without the reactor present, the results from these few TDG reactor bypass experiments seem to imply that degradation starts in the preheater and continues in the reactor. For example, conversion at 500°C without the reactor present was $42 \pm 10\%$ (Figure 4.3), and conversion with the reactor present was $95 \pm 2\%$ (Figure 4.2).

4.4.2 Direct Organic Feed Experiments

To avoid the observed degradation of TDG in the preheater coil, an alternate organic feed system was designed and tested as described in Chapter 2. The conversion versus temperature results are presented in Figure 4.4. With the exception of the very first hydrolysis experiment performed at 450°C, all conditions resulted in essentially complete conversion. The results for hydrolysis, particularly at 425°C, do not agree with the results from earlier scoping runs or those reported by Turner (1993). This disagreement led us to believe that TDG may be degrading at some point in the cooled injection nozzle. In an effort to reduce the temperature of TDG in the nozzle, two hydrolysis experiments were performed in which the cooling water flow rate was increased one order of magnitude from approximately 3 to 30 mL/min. Despite this higher cooling water flow, conversions were still essentially 100%.

At this point, one scoping experiment was performed (Group D in Table 4.7) using the direct organic feed technique to explore a range of conditions that may result in only partial degradation of TDG. Measurements were taken isothermally from 100-350°C every 50 °C with a reactor residence time of approximately 120 s and a pressure of approximately 246 bar. One liquid and one gas sample were taken at each temperature and immediately analyzed. TDG decomposition was clearly in evidence at

Figure 4.4 Results from Direct Organic Feed Runs: TDG Hydrolysis and Oxidation in SCW. Estimated 95% confidence intervals are shown for the data at 450°C. For all other data, 95% confidence was within the point symbol.



temperatures as low as approximately 300°C with a calculated conversion of approximately 18%. Also, at this temperature, a noticeable increase in the gaseous effluent concentration of C₂H₄, as measured by the sensitive GC/FID analysis, seemed to corroborate the observed conversion. The conversion increased at 350 °C to approximately 32% with slightly more C₂H₄ in the gas phase. At 425°C, the TDG flow rate was increased by one order of magnitude from 345 to 3450 μL/min which significantly reduced the residence time in the cooled nozzle but also increased the initial TDG feed concentration by an order of magnitude. In this case, two liquid samples and three gas samples were taken and the calculated conversion was approximately 47%; significantly less than the previously observed conversion of 100% for two earlier experiments at the same temperature but a slower TDG flow rate.

Additional problems hampered these experiments with the direct organic feed system. As described in Section 2.6, all effluent concentrations had relatively large fluctuations perhaps due to the pulse-less feed of organic going into the pulsed-fed water medium and possibly due to poor mixing in the large volume mixing cross. Also, the cooling water in the nozzle made the inlet temperature typically 10 to 15 °C lower than the exit temperature. This observation may be due in part to the proximity of the inlet thermocouple to the cooled nozzle. Nevertheless, the exit thermocouple was always in good agreement with the three thermocouples in the fluidized sand, and this particular non-isothermal problem may not have been significant.

In conclusion, the direct organic feed results may be tainted by the partial degradation of the slowly-moving organic in the cooled nozzle. Increasing the cooling water flow rate did not seem to have an effect, but increasing the organic flow rate, thereby reducing the organic residence time in the cooled nozzle, seemed to decrease the premature decomposition of TDG as evidenced by a significant overall decrease in measured conversion. More detailed tests of the effects of higher cooling water flow

rates and higher pure organic flow rates must be performed to verify these results. The performance of the direct organic feed system may be easily improved by reducing the residence time in the cooled nozzle, taking temperature measurements in the nozzle to better characterize the conditions of the pure organic before reaching the reactor, and converting to a pulse-less water feed pump to reduce concentration variations. Also, the internal volume of the mixing cross should be reduced and its design improved to provide for better mixing in less space.

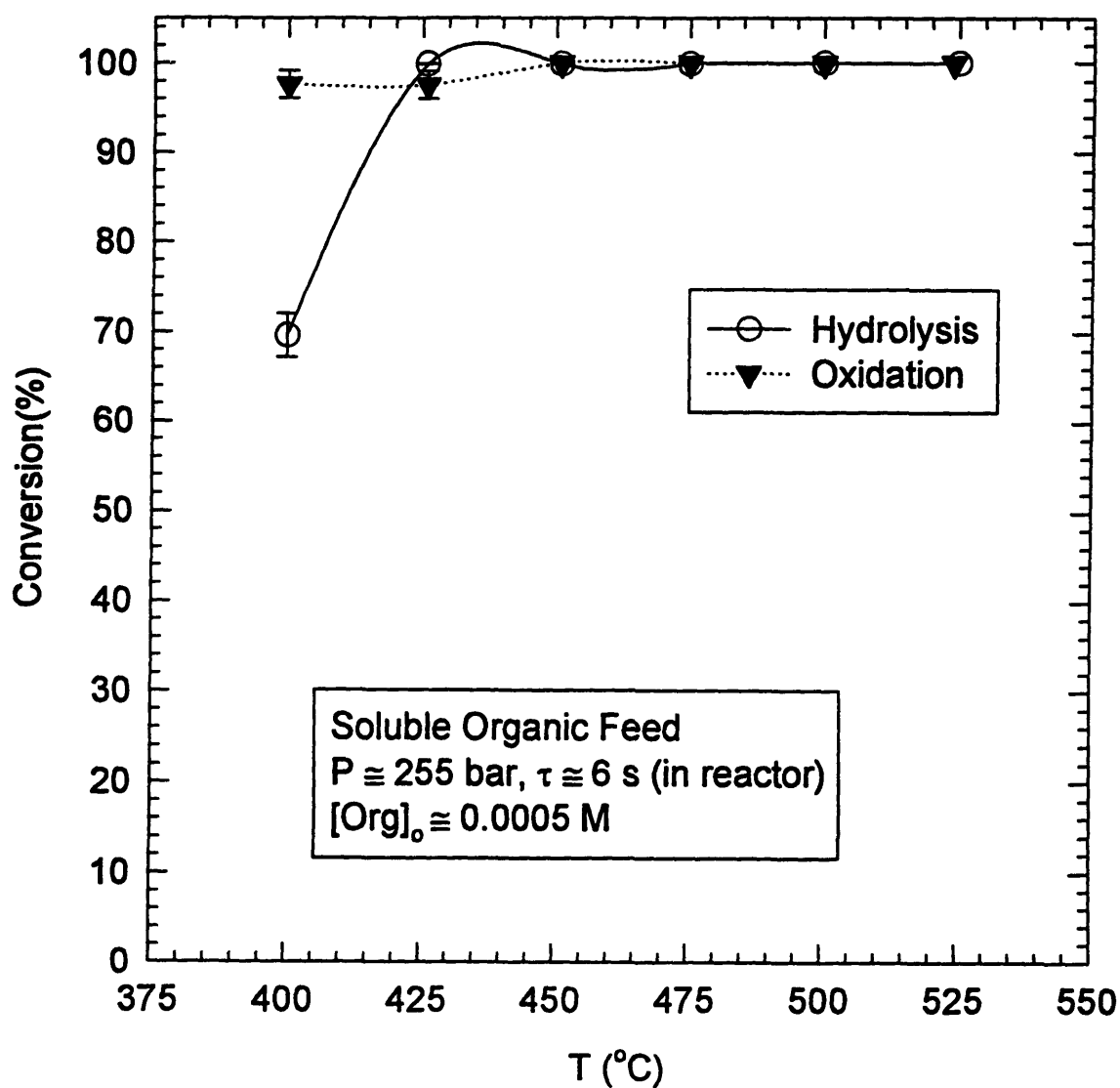
4.4.3 Soluble Organic Feed Experiments

At this point we returned to the soluble organic feed technique because conditions throughout this system were better understood based on several years of experience. Hydrolysis and oxidation experiments were conducted in supercritical water (Group E in Table 4.7), and additional hydrolysis experiments were conducted in subcritical water (Groups F and G in Table 4.7).

4.4.3.1 Results in Supercritical Water

Conversion versus temperature results are plotted in Figure 4.5. As you can see, the hydrolysis results from 425-525°C show essentially complete conversion and generally agree with the direct organic feed experiments but not necessarily with the initial scoping experiments or similar experiments conducted at the University of Texas. The experiments at 400°C were the last in this group in an attempt to find a condition in supercritical water that would give only partial conversion. Hydrolysis at 400°C resulted in $70 \pm 2\%$ conversion, and this particular run had no obvious problems which would make this result suspect.

Figure 4.5 Results from Soluble Organic Feed Runs: TDG Hydrolysis and Oxidation in SCW. Estimated 95% confidence intervals are shown and line is drawn to indicate trends.

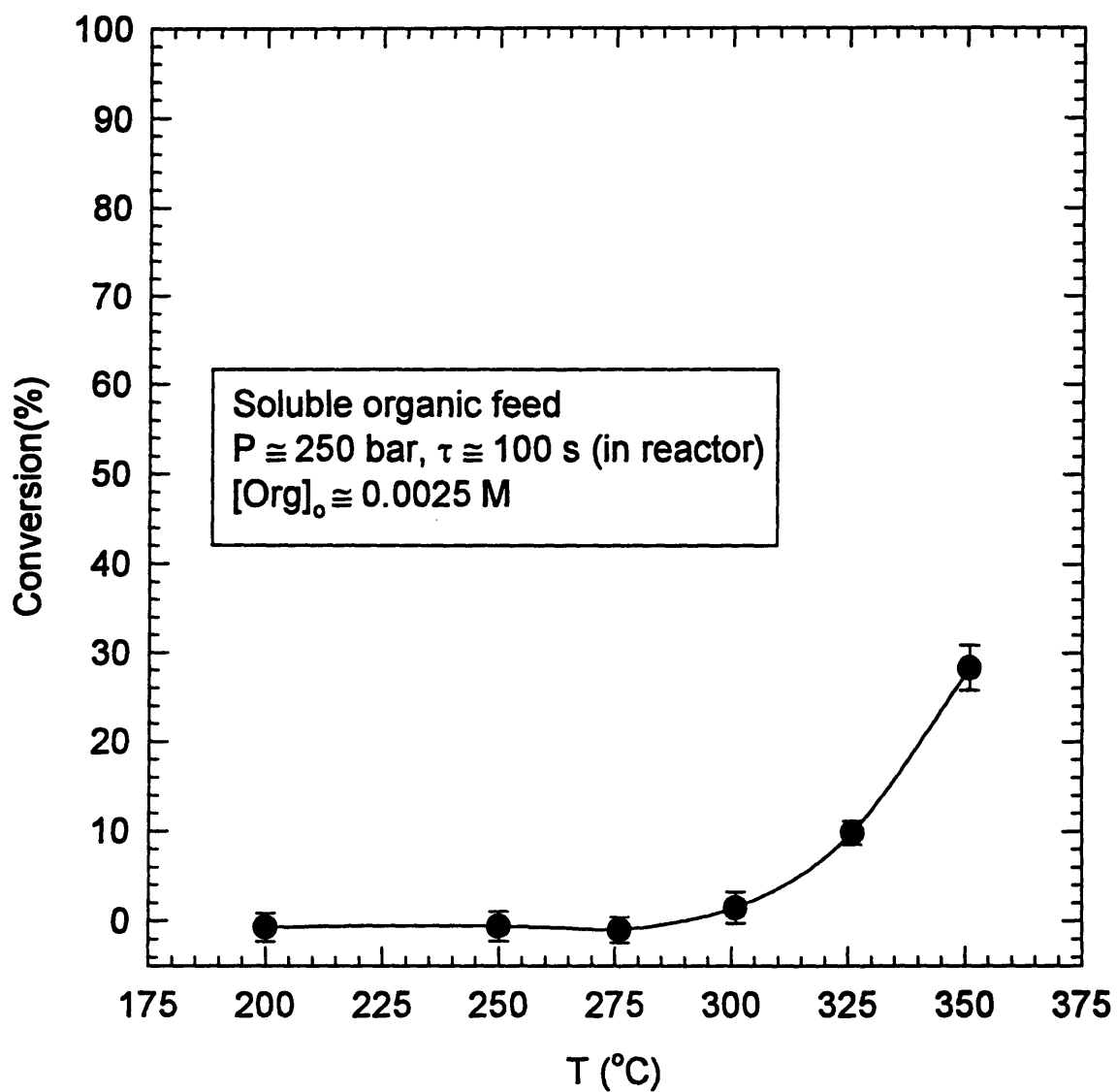


Among the many possible explanations for the inconsistent results between similar experiments is the potentially inconsistent condition of the system tubing. Although we did not specifically examine tubing surfaces in this study, it is possible that the solid phase produced during hydrolysis runs may be adhering to and “conditioning” the walls of the system tubing, including the reactor, which may then influence future reactions. Evidence to support this theory was found in the initial scoping runs and the direct organic feed runs. In both cases, the very first experiment performed, which happened to be a hydrolysis experiment producing a solid phase, resulted in a conversion less than 100%. Prior to the scoping experiments, the system had never been exposed to sulfur compounds, and prior to the direct organic feed runs, the system had been used for several methanol experiments which may have returned the tubing to its original surface composition. In fact, the first direct organic feed experiment was repeated twice approximately one week later, but the results this time were essentially 100% conversion. A similar phenomenon of changing reaction results has been observed in pyrolysis reactors where metal coils are purposely exposed to sulfur-containing compounds to reduce coke formation and increase ethylene yields (Albright et al., 1983). Nevertheless, in our case, experiments specifically designed to study surface effects and sulfur effects must be performed to verify this theory.

4.4.3.2 Results in Subcritical Water

Subcritical experiments were performed to gain a better understanding of initial TDG breakdown in this aqueous environment. Conversion versus temperature results are plotted in Figure 4.6. In full agreement with subcritical reactor bypass experiments (see Figure 4.3) and the subcritical direct organic feed scoping experiment, measurable decomposition did not appear to begin until 300 °C and approximately 100 seconds reactor residence time. Even though the calculated conversion under these conditions was only $1.5 \pm 1.7\%$ (statistically no different than zero conversion), evidence of some

Figure 4.6 Results from Soluble Organic Feed: TDG Hydrolysis in Subcritical Water. Estimated 95% confidence intervals are shown and the line is drawn to indicate trends.

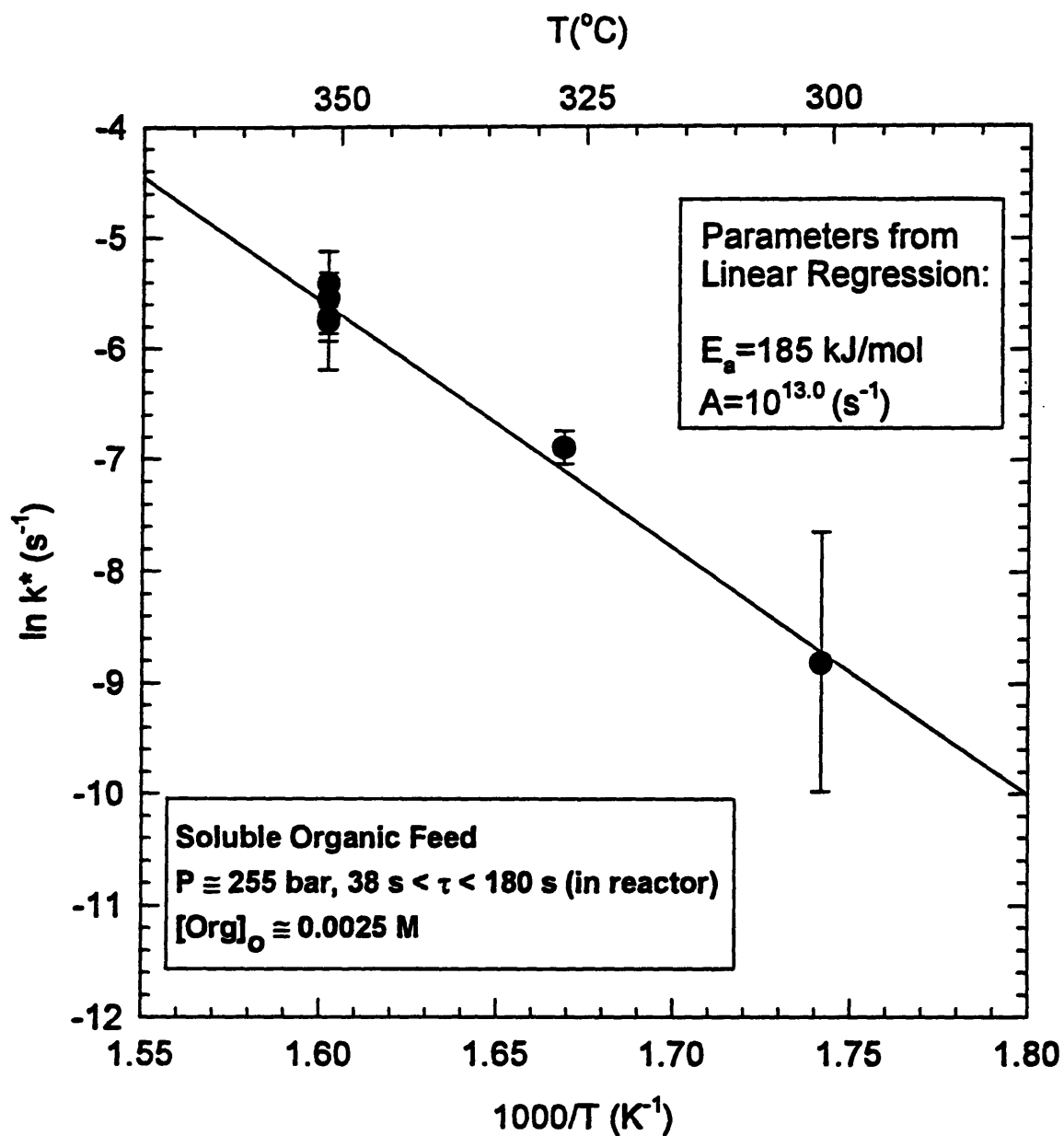


degradation was supported by the slowly increasing C_2H_4 concentrations in the gas phase. After 300°C, conversion gradually increased to $28 \pm 3\%$ at 350°C and the same reactor residence time of approximately 100 seconds.

Unlike supercritical hydrolysis experiments, subcritical hydrolysis effluents were never cloudy although some were clear with a slight yellow tinge. This observation may be the result of reduced conversions possibly making elemental solid sulfur in reduced concentrations. The resulting amount of sulfur may be so small that it dissolves in water or forms a smaller amount of particles that are invisible to the human eye.

Figure 4.7 shows an assumed first order Arrhenius plot of the subcritical hydrolysis experiments that resulted in measurable conversions. The straight line through the data represents a linear regression fit - the behavior expected if the rate was strictly first order with respect to thiodiglycol. The activation energy and pre-exponential factor shown are parameters derived from the slope and intercept of this linear fit. The five data points at 350°C represent five isothermal, residence time variation runs. The stacking of these points may be due to experimental error or possible non-first order effects. The large error bars associated with the value at 300°C is typical of relatively large errors in small conversions leading to much larger propagated errors in k^* . Although this plot is based on only seven experiments, the linear fit to the data is relatively good (r-squared value of 0.984).

Figure 4.7 Assumed First Order Arrhenius Plot for TDG Hydrolysis at Subcritical Temperatures. Estimated 95% confidence intervals are shown and the line drawn is a linear regression of the data.



A nonlinear, multivariable regression program employing a modified Marquardt method (Press et al., 1986) was also used to obtain best-fit values of the rate parameters A , E_a , and a for the following rate expression:

$$R_{TDG} = \{A \exp(-E_a / RT)\} [TDG]^a \quad (4.5)$$

Because water is present in such excess, its concentration was assumed constant and thus was not included as a separate reactant in this rate form. Holgate (1993) and Meyer (1993) describe this calculational approach in more detail. The method was used exactly as described in those two sources for hydrolysis experiments. The best fit global rate expression was

$$R_{TDG} = 10^{10.0 \pm 4.6} \exp(-(178 \pm 22) / RT) [TDG]^{0.1 \pm 1.3} \quad (4.6)$$

Units for the rate is mol/Ls^{-1} , concentration is in mol/L , and activation energy is in kJ/mol . All parameter uncertainties are at the 95% confidence interval and were determined by an ANOVA routine (Press et al., 1986). Although this nonlinear regression appears to be a good representation of the data with an r-squared value of 0.987, unfortunately, the result for the order with respect to TDG is highly suspect (0.1 ± 1.3) and not statistically different than unity. The large estimated error for the TDG order is most likely due to the fact that we did not deliberately explore different feed concentrations in any experiments on which this regression is based. A further discussion of the TDG reaction order is provided in the paragraphs that follow.

Residence time was varied isothermally at 350°C to obtain data at five different reactor residence times ranging from 38 to 180 seconds. Figure 4.8 captures the results in a TDG decay profile as a function of reactor residence time. TDG concentration has

been normalized by the initial TDG concentration ($[\text{TDG}]_0$). The line in the plot is a linear regression fit of the data and the dotted lines indicate the 95% confidence interval of that fit. The intercept of this line with the y-axis is essentially 1.0, which is the value expected if negligible conversion occurred before entering the reactor. Also, a good linear fit here indicates a zero order dependence with respect to TDG. Without further analysis, one could easily conclude from Figure 4.8 that this reaction is globally zero order with respect to TDG.

A plot of the same data on a logarithmic basis is presented in Figure 4.9. If the hydrolysis reaction were truly first order in TDG, then the data should show an exponential decay by decreasing linearly with increasing time on this plot. The solid line is a regressed linear fit of the data and the dotted lines indicate the 95% confidence interval of that fit. This linear regression seems to do a good job of representing the data within its 95% confidence, including a trace through the anticipated y-intercept of zero. However, there does seem to be a slight curvature to the data which may indicate a non-first order dependence.

At this point, we have three global models based on different orders with respect to TDG that do a good job of representing the limited data; a 0.1 model from a non-linear regression approach, a zero order model from the normalized decay profile and a first order model from the exponential decay profile. The performance of these models is displayed in Figure 4.10. Clearly all three models do a great job at predicting the experimental conversion from different residence time runs. Certainly more data including replicates over a wider range of residence times and concentrations are required to gain a better understanding of the reaction rate order with respect to thiodiglycol.

Figure 4.8 Normalized Decay Profile: TDG Hydrolysis in Subcritical Water.
 Estimated 95% confidence intervals are shown.

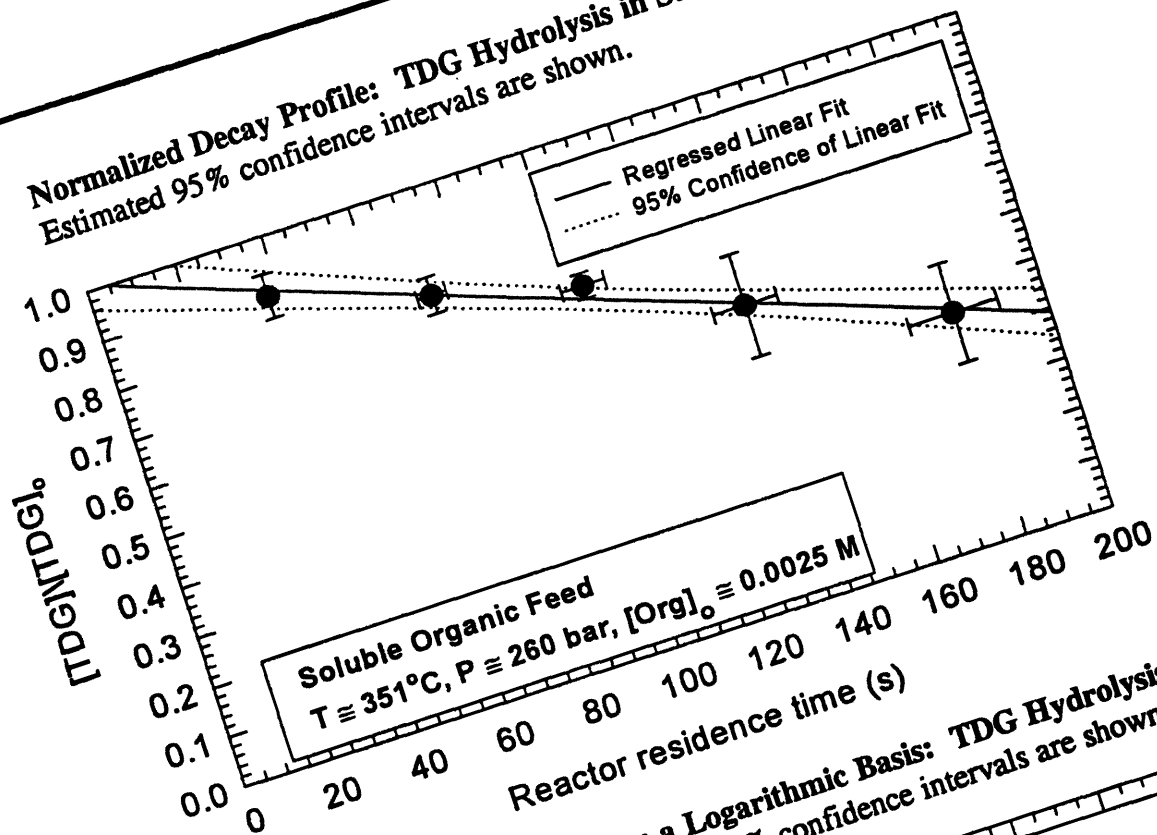


Figure 4.9 Normalized Decay Profile on a Logarithmic Basis: TDG Hydrolysis in Subcritical Water. Estimated 95% confidence intervals are shown.

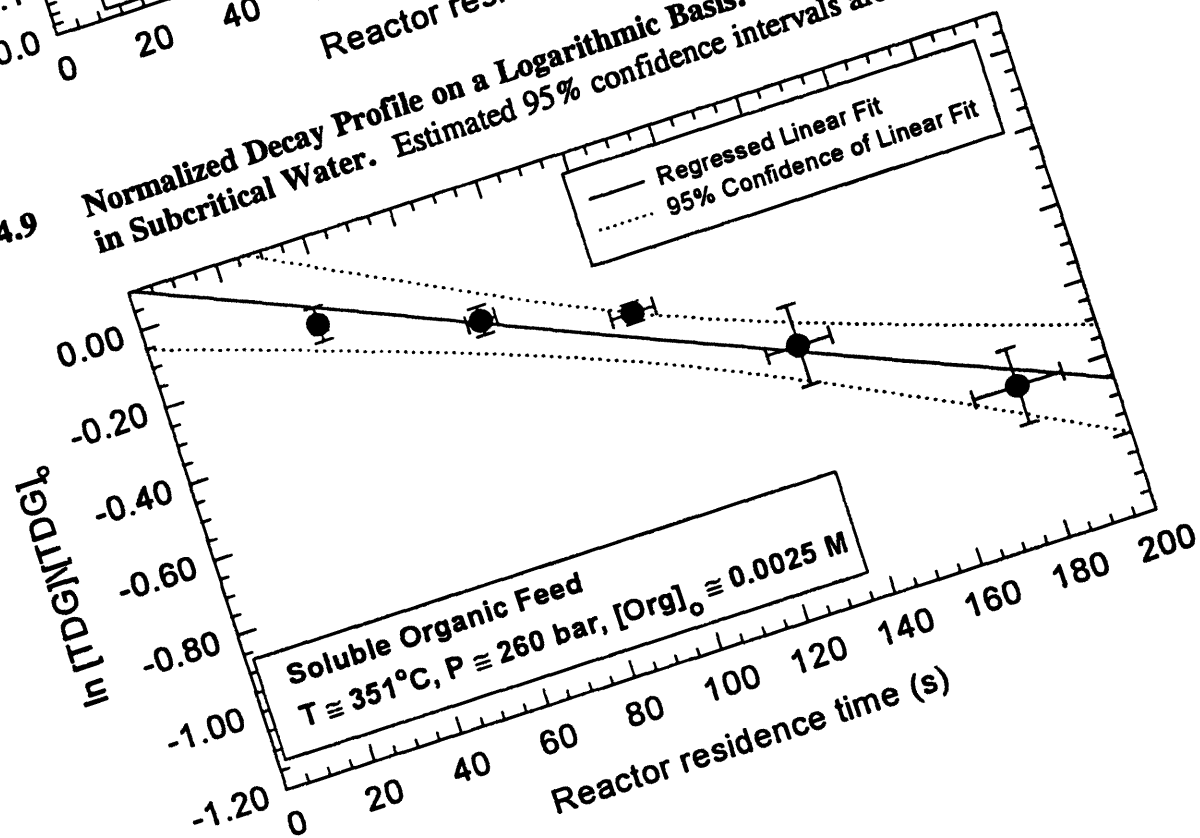
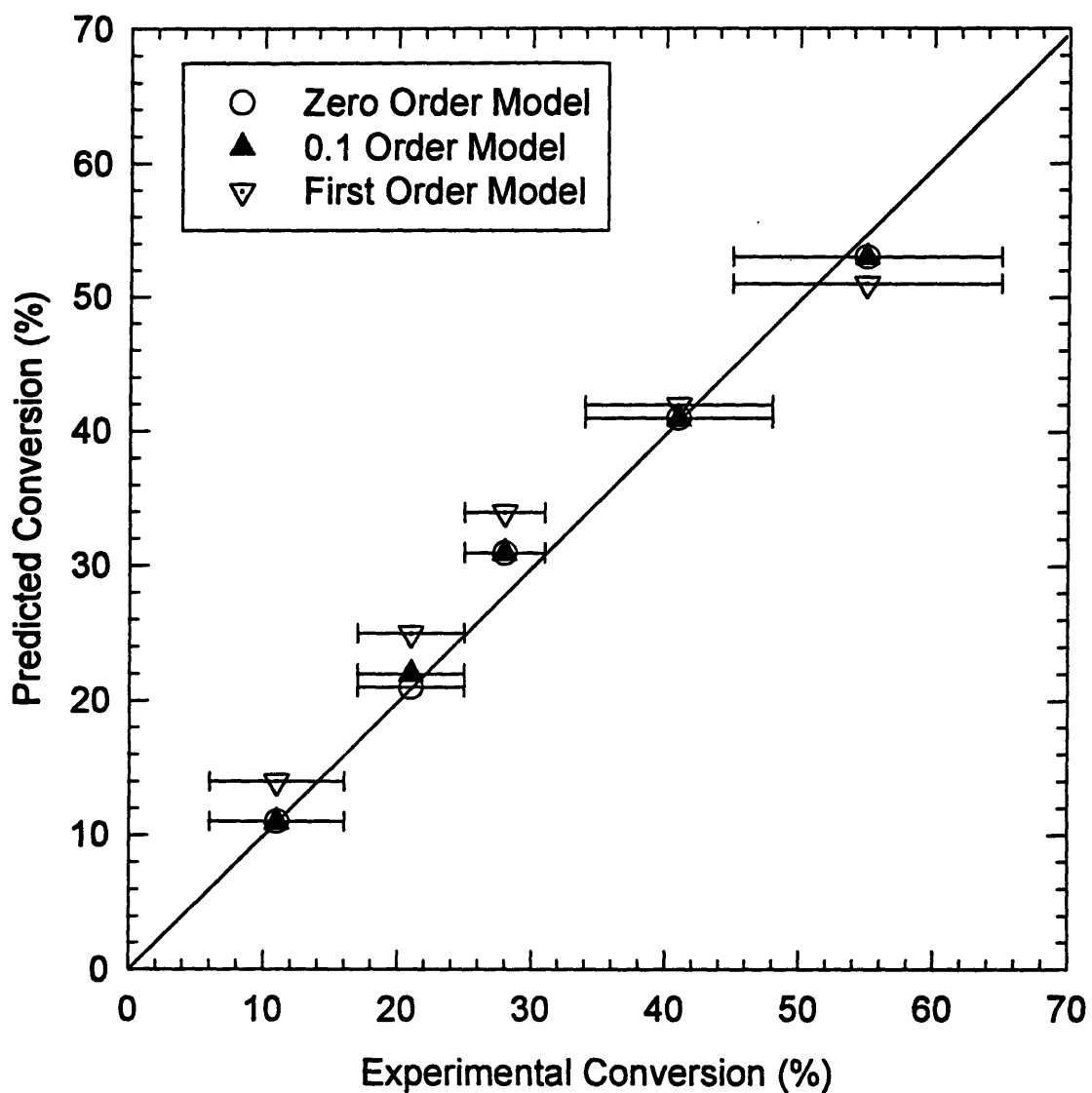


Figure 4.10 Predicted Conversion of Three Different Models vs. Experimental Conversion: TDG Hydrolysis in Subcritical Water. Estimated 95% confidence intervals are shown.



4.4.4 Summary of Kinetic Results

In general, thiodiglycol (TDG) reacts rapidly and completely in supercritical water, with and without oxidant. On those few occasions when conversion due to hydrolysis was not complete, adding oxygen usually decomposed the remaining TDG rapidly. The very first hydrolysis experiments in different groups of runs were not reproducible, with much higher conversions being observed during subsequent experiments at apparently the same conditions. One possible explanation of this non-reproducibility between the initial and later experiments is changes in system conditions (e.g., contamination of tubing walls from formation of solid sulfur).

Thiodiglycol begins to decompose in hot, pressurized, subcritical water at approximately 300°C and a residence time of 100 seconds. A conversion as high as 55±10% was achieved at 350°C and 180 seconds reactor residence time. Non-linear regression of the limited subcritical data resulted in an activation energy of 178±22 kJ/mol and a pre-exponential factor of $10^{10.0\pm4.6}$. More data are needed to verify these values and establish the appropriate concentration dependence in the global rate law for TDG.

4.5 Product Identification

Analysis of all reactor effluents was performed following procedures described in Section 2.2. For chromatography analysis, products were identified by matching their peak retention times to retention times given by known standards. In some cases, redundant detection methods were able to corroborate peak identification. Following positive identification of specific compounds, quantification was performed through calibration over a range of concentrations. For the chemical analysis of liquid effluents (sulfate, formaldehyde, and sulfide tests), identification was confirmed or denied by observing the appropriate response to the specific test. For each analytical technique used, feed solutions and PFR system blanks were analyzed to differentiate between responses associated with TDG in solution and water from the PFR apparatus versus responses due to actual reaction products.

The majority of effort on this project went towards product identification and quantification. This work is described in the paragraphs that follow; broken down by gas, liquid and solid phase components and ending with a discussion of carbon and sulfur balances and unidentified peaks.

4.5.1 Gas Phase Products

Table 4.8 shows the standard gas phase compounds tested, the specific GC detectors used and a qualitative assignment of their general presence in hydrolysis and oxidation effluents from experiments in both supercritical and subcritical regimes. Details of the quantitative analysis of the gas and liquid phases are presented in Section 4.6.

Table 4.8 Summary of Compounds Tested as Possible Gas Phase Products.

Compound	TCD ^a	FID ^a	ECD ^a	Hyd ^b	Oxd ^b
H ₂	*			2	3
He	*			2	3
O ₂	*		*	3	1
N ₂	*			2	3
CO	*			2	1
CO ₂	*			2	1
CH ₄	*	*		2	2
C ₂ H ₄	*	*		1	2
C ₂ H ₆	*	*		3	3
C ₂ H ₂	*	*		ND	ND
C ₃ H ₈		*		?	ND
C ₃ H ₆		*		?	ND
C ₃ H ₄		*		ND	ND
C ₄ H ₈		*		?	ND
H ₂ S	*		*	2	3
SO ₂	*		*	ND	ND
HSCH ₂ CH ₃		*	*	?	ND
(CH ₃) ₂ S		*	*	?	ND
CS ₂		*	*	ND	3

a * - Method of detection sensitive to compound

b 1 - Present in significant amounts

2 - Present in different amounts

3 - Present in trace quantities

ND - Not detected

? - Possibly matches retention time of peak in sample

The specific TCD methods employed have been used by several previous investigators at MIT (see Section 2.2) for identification of H₂, He, O₂, N₂, CO, CO₂, CH₄, C₂H₄, C₂H₆, and C₂H₂. One of these methods was also found to be sensitive to H₂S and SO₂. This study marks the first time that our research group has made extensive use of an FID in gas phase analysis which provided for a more sensitive means of detecting hydrocarbon gases. This FID technique also served as a redundant means of detection for CH₄, C₂H₄, C₂H₆, and C₂H₂. The ECD was used to detect the presence of sulfur gases. Most gases were identified and calibrated by making 5 to 150 μL syringe injections of the respective pure gases into the appropriate GC. C₃ and higher gases were part of a standard gas mixture. Ethyl mercaptan (HSCH₂CH₃), dimethyl sulfide ((CH₃)₂S) and carbon disulfide (CS₂) were identified, but not calibrated, by taking multiple syringe samples of the head space of a vial containing pure liquid samples of these compounds.

In general, the major product in the gas phase of hydrolysis reactions was identified as C₂H₄, which usually had the largest volume fraction, with varying amounts of H₂, CO, CO₂, CH₄, C₂H₆, H₂S, He, and N₂. Helium was present since it was used in feed preparation, and nitrogen was present probably as a result of air entrained in feeds and residual nitrogen still in gas sampling lines due to incomplete purging. Some hydrolysis experiments, particularly at lower temperatures, resulted in very low gas flow rates (some < 0.10 mL/min) which made it difficult to purge the gas sampling lines; this was further complicated by the pressure fluctuations which accompanied solids production during hydrolysis experiments. As a result, gas phase concentrations changed over the course of an experiment and were difficult to resolve. The major products typically found in the gas phase of oxidation experiments were O₂, CO and CO₂ with lesser amounts of CH₄, C₂H₄, and trace amounts of H₂, He, N₂, H₂S, He, and C₂H₆.

Sample gas chromatograms from the TCD, FID and ECD are included in Figures 4.11, 4.12, and 4.13, respectively. These particular chromatograms are from experiments at 525°C and were chosen because they contained a variety of peaks. Hydrogen and helium are not found on the TCD chromatograms because they were identified and quantified using a second TCD (see Section 2.2). The oxygen and nitrogen peaks in the hydrolysis chromatogram are examples of incomplete purging of gas sampling lines, but they correspond to only trace amounts, representing mole fractions of less than 0.005. SO₂ corresponds to a TCD retention time of 14.322 minutes and an ECD retention time of 1.071 minutes. As one can see, an SO₂ peak is not found in these or any other chromatograms in this study and therefore must be below the detection limit (approximately < 500 ppmv - part per million on a volume of gas sample basis). In general, we do not know peak retention times to three decimal places, but the retention times cited here are merely provided as a detailed means of identifying peaks in the chromatograms shown.

The FID chromatograms in Figure 4.12 are an excellent illustration of the sensitivity of the FID over the TCD. In fact, all injections for the FID had to be made one order of magnitude less than those for the TCD (20 µL versus 200 µL) in order to reduce the size of the C₂H₄ peak and resolve the surrounding smaller peaks. For the hydrolysis samples, the FID and TCD both indicate the presence of CH₄, C₂H₄, and C₂H₆ but the FID also detects additional peaks (retention times > 8 minutes) that the TCD does not identify, either in this chromatogram or as late eluting peaks in subsequent chromatograms. In fact, the FID still detects the presence of C₂H₆ in the oxidation sample, but the TCD oxidation sample does not indicate a peak at the normal retention time for C₂H₆ of 8.358 minutes. Unfortunately, the FID was not calibrated for any compounds, but a rough calculation of a response factor indicates that the C₂H₆ peak in the FID oxidation sample corresponds to approximately 200 ppmv. Indeed, this concentration would not contribute significantly to the carbon balance, but it is not

Figure 4.11 TCD Gas Chromatograms for TDG Hydrolysis and Oxidation at 525°C, 260 bar, and Reactor Residence Time of 6.5 seconds. [TDG]₀ = 5 × 10⁻⁴ mol/L, [O₂]₀ = 3.5 × 10⁻³ mol/L.

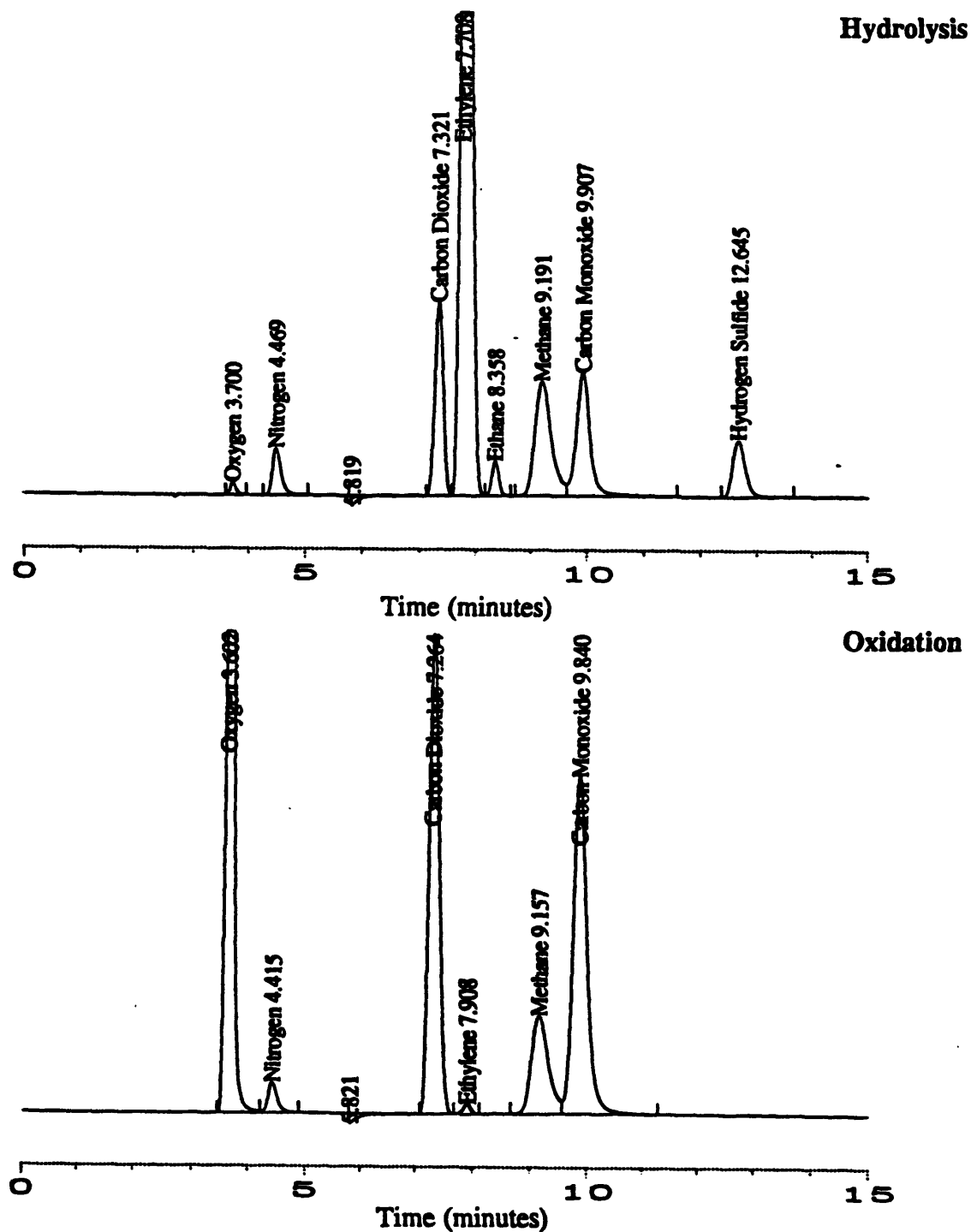


Figure 4.12 FID Gas Chromatograms for TDG Hydrolysis and Oxidation at 525°C, 260 bar, and Reactor Residence Time of 6.5 seconds. $[TDG]_0 = 5 \times 10^{-4}$ mol/L, $[O_2]_0 = 3.5 \times 10^{-3}$ mol/L.

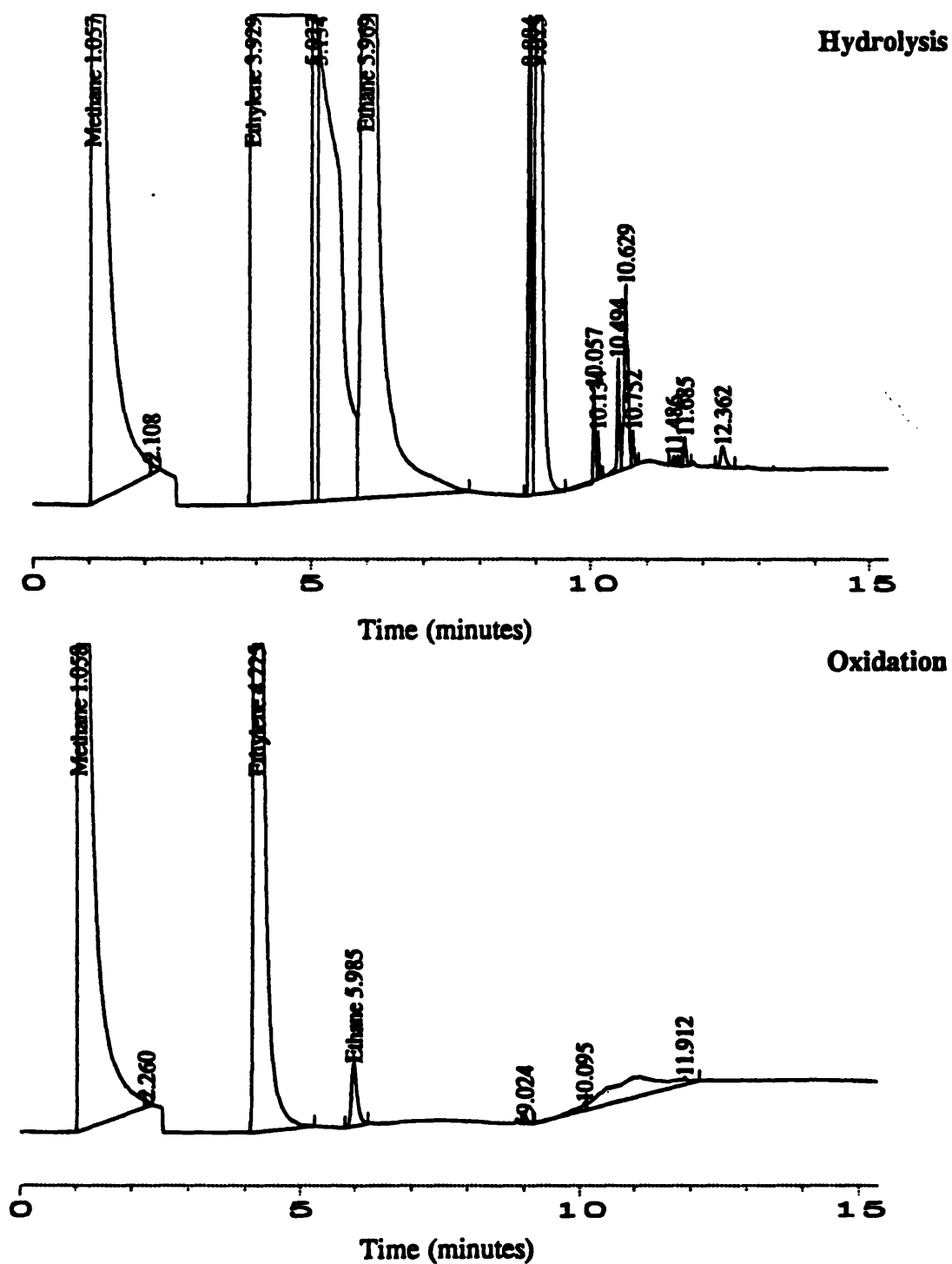
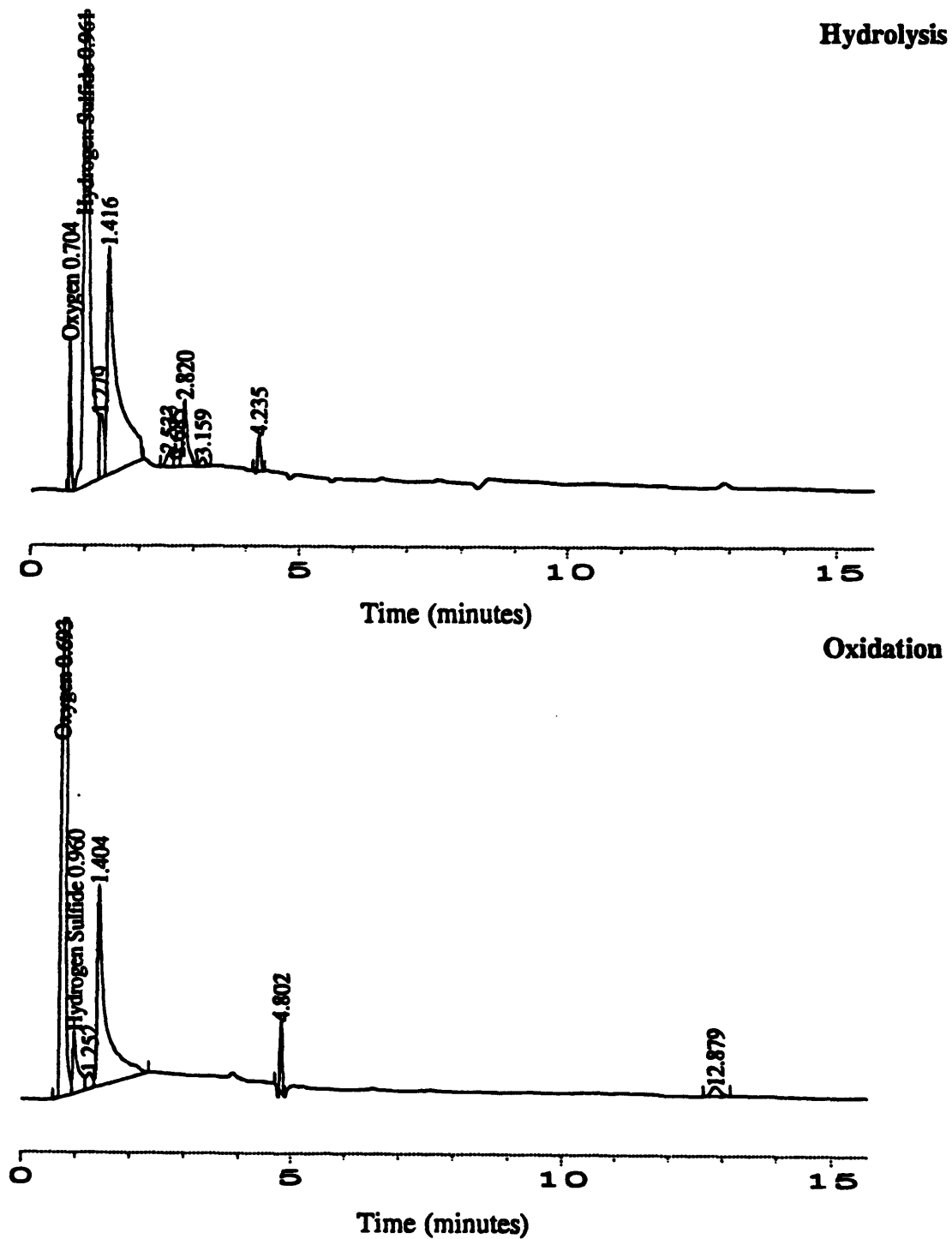


Figure 4.13 ECD Gas Chromatograms for TDG Hydrolysis and Oxidation at 525°C, 260 bar, and Reactor Residence Time of 6.5 seconds. $[TDG]_0 = 5 \times 10^{-4}$ mol/L, $[O_2]_0 = 3.5 \times 10^{-3}$ mol/L.



rigorously correct to say that a “clean” TCD chromatogram means there are no other gases present.

Along those same lines, the FID peaks in the hydrolysis sample at retention times greater than 8 minutes are probably not significant contributors to carbon mass balance closure. Nevertheless, they are present and characteristic of some hydrolysis samples; they are not found in blank injections, which are run before every experiment, nor are they typically found in oxidation samples. Some of these peaks have retention times that are close to those of some tested standards; the 8.884 min peak agrees with that for C_3H_6 (8.962 min), the 9.023 min peak agrees with that of C_3H_8 (9.102), the 10.629 min peak agrees with that of C_4H_8 (10.716), and the 11.685 peak agrees with that of $HSCH_2CH_3$ (11.613).

The ECD chromatograms of Figure 4.13 may tell a significant story in what they do not show. As stated earlier, the ECD is sensitive to sulfur gases. The absence of significant peaks in both the hydrolysis and oxidation samples indicates that there may not be any sulfur gases in substantial quantities. In both samples, the first peak corresponds to oxygen, the peak at 0.96 min is H_2S , and the peaks at 1.4 and 12.8 minutes are unknown but also found in blank injections of air. The peak at 4.232 minutes in the hydrolysis sample agrees with the retention time for ethanethiol $HSCH_2CH_3$ (4.255), and the peak at 4.802 minutes for oxidation agrees with the retention time for CS_2 (4.805). The one remaining unknown peak that stands out is at 2.820 minutes for hydrolysis. If this peak corresponded to a compound with a response factor similar to that for H_2S , its concentration would be approximately 1000 ppmv; a value which certainly qualifies it as a trace compound.

4.5.2 Liquid Phase Products

Identification of products in the liquid phase was more difficult. Even for identification and quantification of thiodiglycol, three different methods were tested in order to find one which performed satisfactorily; (1) GC with FID exhibited ghosting of TDG peaks, (2) HPLC with perchloric acid mobile phase through an ion-exclusion column resulted in peak splitting due to improper ionic strength, and (3) HPLC with sulfuric acid mobile phase finally performed well.

Table 4.9 shows the standard liquid phase compounds tested as possible products, the specific method of detection used and a qualitative assignment of their general presence in hydrolysis and oxidation samples. As described in Section 2.2, the UV detector for the HPLC was used at two different wavelengths (208 and 290 nm) providing separate detection methods which were selective to specific organic compounds exhibiting different wavelengths of high absorbance efficiency. Where the spaces in the HPLC columns are blank, the corresponding compound was not tested using this method but was believed to not absorb at this wavelength based on UV absorption theory (Silverstein et al., 1981). However, the blank spaces in the FID column also indicate that the corresponding compound was not tested using this method, but most of the organic compounds listed here (with the possible exception of some organic acids) are probably sensitive to FID detection. As stated in Section 2.2, HPLC analysis was performed on all samples throughout the entire TDG study, but FID analysis was only performed at one time approximately three weeks after the last experiment on generally one sample per experiment. All compounds in this table were analyzed by preparing aqueous solutions of various concentrations, injecting them into the HPLC or GC, observing any response, and recording the retention time of any corresponding peak.

Table 4.9 Summary of Compounds Tested as Possible Liquid Phase Products

Compound	Structure	HPLC (208nm)	HPLC (290nm)	FID	Hyd ^c	Oxd ^c
1,2 Ethanethiol	HSC ₂ H ₄ SH	* ^a			ND	ND
2-Mercaptoethanol	HOC ₂ H ₄ SH	*		*	ND	ND
2-Mercaptoethyl Ether	(HSC ₂ H ₄) ₂ O	*			ND	ND
2-Mercaptoethyl Sulfide	(HSC ₂ H ₄) ₂ S	ND ^b			?	?
Acetaldehyde	CH ₃ CHO	ND	*	*	1	2
Acetic Acid	CH ₃ COOH	*	ND	*	2	2
Acetol	CH ₃ COCH ₂ OH	*		*	ND	ND
Acetone	CH ₃ COCH ₃		*	*	ND	ND
Dimethyl Sulfide	(CH ₃) ₂ S	*			ND	ND
Dithiane	S(C ₂ H ₄) ₂ S	*	ND		ND	ND
Ethanol	CH ₃ CH ₂ OH	ND		*	ND	ND
Ethyl Acetate	CH ₃ CO ₂ CH ₂ CH ₃	*		*	ND	ND
Ethyl Ether	(CH ₃ CH ₂) ₂ O			*	ND	ND
Ethyl Mercaptan	HSCH ₂ CH ₃	ND			?	?
Ethylene Glycol	HOC ₂ H ₄ OH			*	ND	ND
Formic Acid	HCOOH	*	ND	ND	2	2
Mercapto Acetic Acid	HSCH ₂ CO ₂ H	*			ND	ND
Methanol	CH ₃ OH	ND		*	ND	ND
Oxalic Acid	HOCCOOH	*			ND	ND
Propenal (Acrolein)	CH ₂ CHCHO	*		*	ND	ND
Thiodiglycol	(HOC ₂ H ₄) ₂ S	*	ND	*	1-3	3
Thiodiglycol Sulfone	(HOC ₂ H ₄) ₂ SO ₂	ND			?	?
Thiodiglycol Sulfoxide	(HOC ₂ H ₄) ₂ SO	*	ND		ND	3
Thiodiglycolic Acid	(HOCCCH ₂) ₂ S	*			ND	ND
Thioxane	O(C ₂ H ₄) ₂ S	*	ND	*	3	3

a * - Detector sensitive to compound

b ND - Not detected

c 1 - Present in significant amounts

2 - Present in different amounts

3 - Present in trace quantities

? - Unknown; not found in detection methods used

In addition to the compounds listed here, chemical tests were performed for sulfate, formaldehyde and sulfide as described in Section 2.2. Sulfate was found in oxidation samples but not generally in hydrolysis samples. Formaldehyde was not found in tests conducted on several initial samples. One test was performed to quantify sulfide in solution in a hydrolysis sample. The corresponding result was in general agreement with the Henry's law approximation used throughout this study.

The major product in the liquid phase of hydrolysis reactions was usually acetaldehyde with acetic acid, formic acid and thioxane appearing in trace amounts. For supercritical experiments, thiodiglycol generally appeared in trace amounts and sometimes was not detected (estimated minimum detection level with 100 μL injection = 200 ppb by weight). However, the effluents of subcritical experiments, which saw reduced conversions, naturally contained significant amounts of thiodiglycol. Even in those experiments, formic acid, acetic acid and thioxane were detected in trace amounts. In oxidation experiments, sulfuric acid was the only major liquid phase product, but it is not shown in Table 4.9. Acetaldehyde generally decreased during oxidation, but acetic acid and formic acid were still present in trace amounts. Thioxane was essentially destroyed during oxidation, and lower temperature oxidation conditions saw trace amounts of thiodiglycol sulfoxide.

Sample liquid chromatograms from the HPLC analysis at 208 nm and the FID analysis are included in Figures 4.14 and 4.15 respectively. A similar chromatogram for HPLC analysis at 290 nm would simply show acetaldehyde as the only peak and is therefore not included. These chromatograms are from hydrolysis and oxidation experiments at 400°C and were chosen, as in the gas phase presentation, because they have a variety of peaks. Focusing on the HPLC results, the first peak in both

Figure 4.14 HPLC Chromatograms from UV Detection at 208 nm for TDG Hydrolysis and Oxidation at 400°C, 260 bar, and Reactor Residence Time of 7.8 seconds. $[TDG]_0 = 5 \times 10^{-4}$ mol/L, $[O_2]_0 = 3.5 \times 10^{-3}$ mol/L.

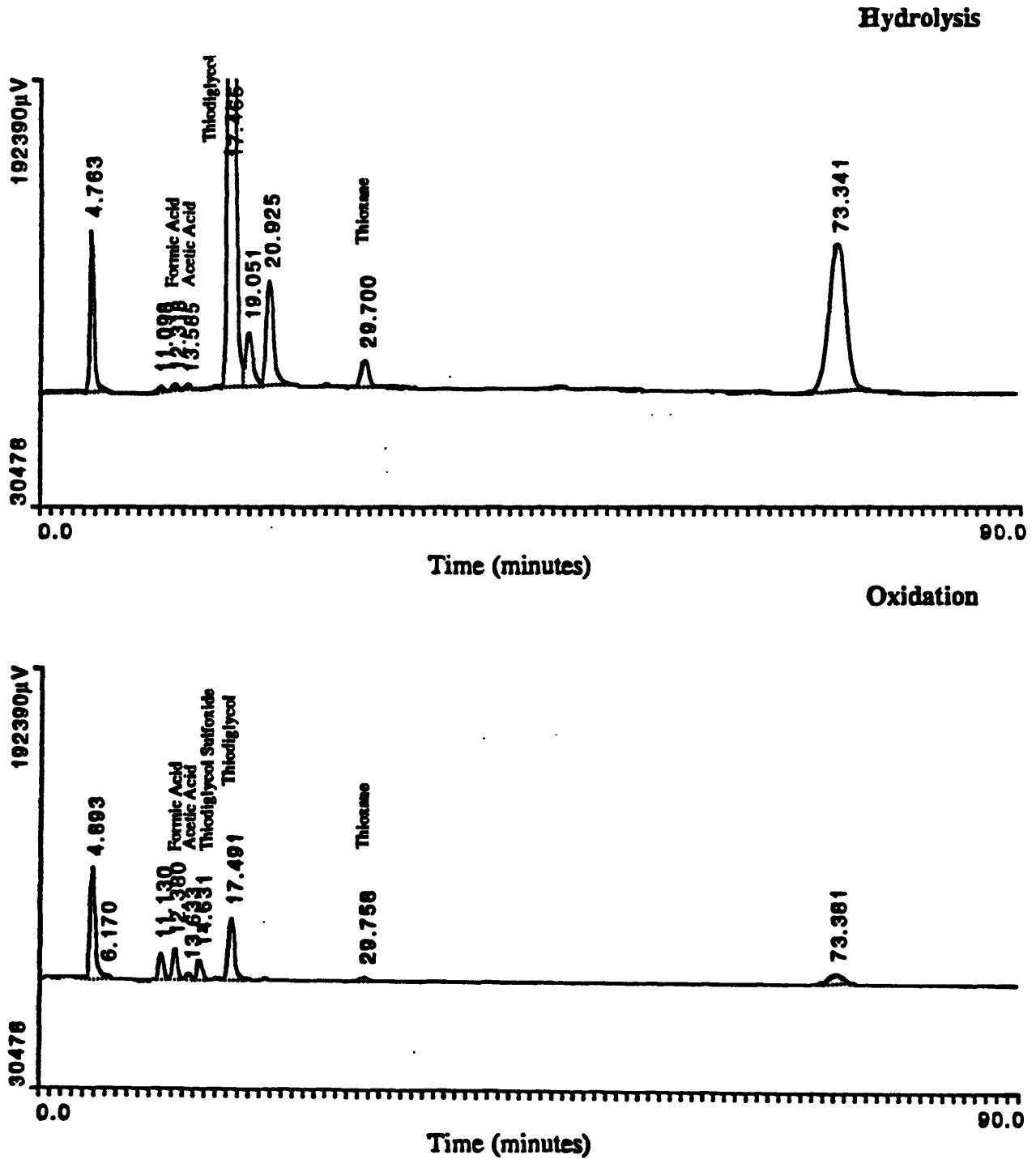
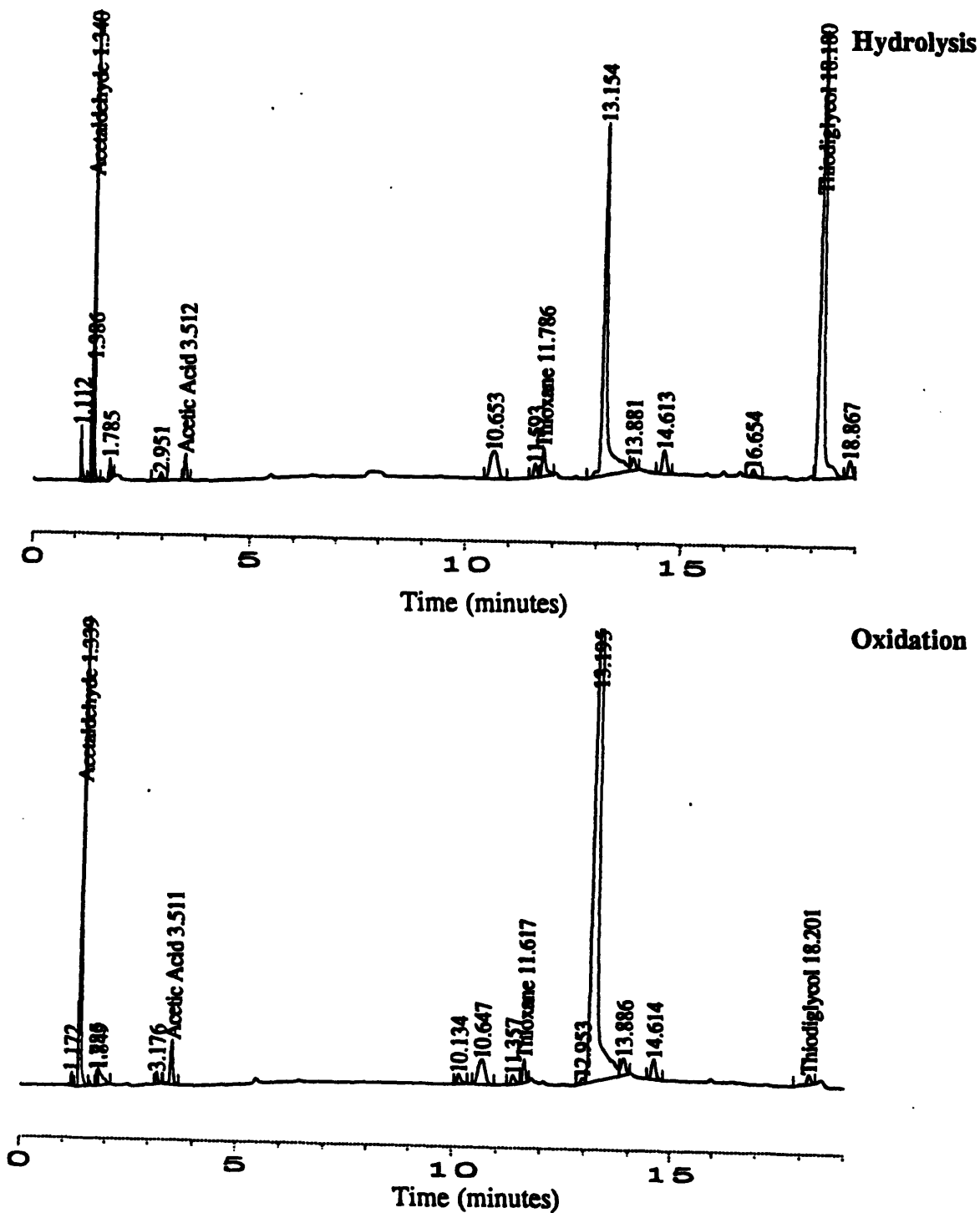


Figure 4.15 FID Chromatograms for TDG Hydrolysis and Oxidation at 400°C, 260 bar, and Reactor Residence Time of 7.8 seconds. $[TDG]_0 = 5 \times 10^{-4}$ mol/L, $[O_2]_0 = 3.5 \times 10^{-3}$ mol/L.



chromatograms at approximately 4.8 minutes corresponds to the solvent peak. This peak is present in all injections, including injections of high purity water, and is generally associated with residue that may be washed off the column and passes by the detector first. Even though this peak is also found in blank injections, it is slightly bigger for some hydrolysis and oxidation chromatograms and may contain unknown compounds not retained by the column and associated with experimental samples.

Dr. K.C. Swallow, an analytical chemist and colleague, took a great interest in the analytical work of this project and assisted with the identification of unidentified HPLC peaks found in chromatograms like Figure 4.14. The peak at 73 minutes appeared to be significant and therefore received most of our attention. Fractions of the HPLC eluent corresponding to retention times between approximately 68 and 78 minutes were collected, extracted with methylene chloride and analyzed using a GC/MS. Unfortunately, there were no significant peaks resulting from this work, possibly indicating that this mystery compound corresponding to the 73 minute peak may be a relatively large compound not amenable to GC analysis. In fact, Dr. Swallow analyzed several effluent samples using the same technique but only found inconsistent and relatively meaningless results. It is difficult to correlate peaks found in HPLC chromatograms with peaks in GC chromatograms because of different separation behavior, and, as a result, the initial interpretation of the GC/MS work did not reveal any significant information on unidentified liquid phase products.

The identification and source of the 73 minute peak may lie in our early work with methylene chloride. Meyer (1993) used HPLC analysis with the same column and mobile phase for the analysis of methylene chloride effluents and found a relatively large peak in many samples eluting at 86 minutes. This peak was never identified and we have since closed carbon and chlorine balances with compounds (e.g., formaldehyde) that could never correspond to this peak. As a result, it is believed that

this peak may be the signal associated with part of the polymeric column or guard column slowly degrading and eluting at this relatively long time. If a polymer compound is being extracted from the column, only a small amount would be required to give a large detector signal based on the potential absorbance of polymers at 208 nm. In fact, the manual for the present guard column states that the polymer found in the guard column, which is polyethyl ether ketone (PEEK), is not compatible with methylene chloride, DMSO, and concentrated nitric and sulfuric acids. By similar reasoning, the 73 minute peak found in TDG chromatograms may correspond to the gradual degradation of the guard column due to its exposure to concentrated slugs of sulfuric acid found in TDG oxidation samples. Additional evidence to support this theory lies in the fact that the size of the 73 minute peak was never consistent between multiple injections of the same sample and showed abnormal and inconsistent trends with temperature, time and the presence or absence of oxygen.

Nevertheless, both hydrolysis and oxidation samples contain other unidentified peaks, in addition to the 73 minute peak, that may correspond to actual TDG reaction products. Despite our efforts, these peaks remain unidentified as of the date of this writing (May 1995). However, the potential impact of these compounds on the carbon and sulfur balances appears to be small and is discussed in Section 4.5.4.

The FID chromatograms of Figure 4.15 generally support the hypothesis based on the HPLC data that there are few significant liquid phase products. Both hydrolysis and oxidation chromatograms show several minor peaks and one major unidentified peak at 13 minutes. If these minor peaks had response factors similar to that of TDG, the corresponding concentrations would be less than 10 ppmw and would therefore not contribute significantly to carbon and sulfur balances. However, the 13 minute peak appears to be significant, but further analysis shows that its potential contribution to elemental balances is probably small as discussed in Section 4.5.4.

4.5.3 Solid Phase Products and Corrosion Observations

Solids were observed in the liquid effluents of supercritical hydrolysis experiments in the form of a fine suspension which settled upon standing after several days. Also, after two separate oxidation runs, small dark particles were observed in the system effluent following pressure letdown. Observations similar to this were typical of methylene chloride runs and usually indicated the presence of corrosion (Meyer, 1993; Marrone et al., 1995; Section 3.6 of this thesis).

Corrosion was expected with the presence of sulfuric acid in oxidation effluents, but these two dirty effluents were the only evidence of corrosion throughout the entire thiodiglycol study. As stated in Section 3.6, corrosion will most likely occur in a moderately hot but subcritical ionic environment. The part of our plug flow apparatus that is exposed to sulfuric acid and fits this description is the tubing at the beginning of the heat exchanger. Unlike methylene chloride experiments which formed HCl even before reaching the reactor, the organic preheater coil for thiodiglycol is not exposed to any strong acids because sulfate is not produced until the organic mixes with oxygen in the mixing cross; a region which was always at supercritical conditions for oxidation experiments. No tubing was ruptured during any TDG experiment which is probably due in part to the relatively thick wall of the heat exchanger tubing (0.065 inch wall versus 0.01 inch wall of the preheater tubing).

The observations of corrosion made by Turner (1993) during his TDG study are somewhat different than the behavior we observed. He states that corrosion was more severe under hydrolysis conditions (no sulfate production) than under oxidation conditions. In addition to sulfate, sulfide in solution, from hydrogen sulfide, was another acid suspected of causing corrosion. Several factors may explain the

disagreement between the two TDG studies. Turner's entire apparatus was made of 316 stainless steel which was probably more susceptible to corrosion than our Hastelloy C276 and Inconel 625 tubing. Perhaps stainless steel is even susceptible to corrosion by weak acids like sulfide in solution. Turner did not identify the composition of a white precipitate which he observed and believed to be corrosion products. This precipitate may be similar to the precipitate observed in our study which we identified as elemental sulfur. It is possible that the pressure and flow problems observed by Turner were caused by elemental sulfur production as opposed to problems associated with corrosion.

A scanning electron microscope (SEM) with an x-ray detector was used to identify the elemental composition of solids found in effluents from the TDG studies. This method is only semi-quantitative because it merely identifies separate elements and their relative abundance as opposed to identifying and quantifying molecules. The effluents containing solids were filtered and the precipitate, still on the filter paper, was placed in the SEM chamber. Similar analysis was made of blank filter paper to differentiate between sample and paper. The suspended solid normally found in hydrolysis samples was observed as very fine particles, approximately 1 μm in diameter, and x-ray analysis revealed that it was almost entirely composed of sulfur. The dark particles observed after two oxidation runs were also analyzed. These particles were larger (approximately 5 - 10 μm in diameter) and were identified as containing mostly chromium, nickel and iron; strongly suggesting that these solids were corrosion products.

4.5.4 Carbon and Sulfur Balances

All identified major products were quantified and the resulting carbon and sulfur balances were calculated. As used here, carbon and sulfur balances are given as the percent of carbon or sulfur in the feed found as carbon or sulfur in the effluent products. Acceptable carbon or sulfur closure is considered here to be $100 \pm 10\%$. The results of carbon and sulfur balances are presented in Figures 4.16 and 4.17 respectively. These figures do not include results from scoping experiments because products from these runs were analyzed in less detail.

The carbon balances for hydrolysis and oxidation experiments are generally good. The carbon balances for hydrolysis experiments from 200 - 300°C correspond to negligible conversion and reflect our ability to recover TDG fed to the system. However, at the lower supercritical temperatures (400-450°C) for both oxidation and hydrolysis, carbon balances are slightly lower than desirable. This apparent trend is addressed below.

The sulfur balances for hydrolysis experiments are equally good at subcritical temperatures but are, in general, unacceptably low at supercritical temperatures. This is most likely due to elemental sulfur production which we could not quantify without substantial modification to our experimental techniques. Sulfur balances for oxidation runs appear to show a trend similar to carbon balances at low supercritical temperatures where values are typically less than acceptable. These trends of low balances in similar temperature regimes suggest that we are missing products which may account for roughly 10 to 40% of the carbon and sulfur in the feed.

Figure 4.16 Carbon Balances for TDG Hydrolysis and Oxidation in Sub- and Supercritical Water.

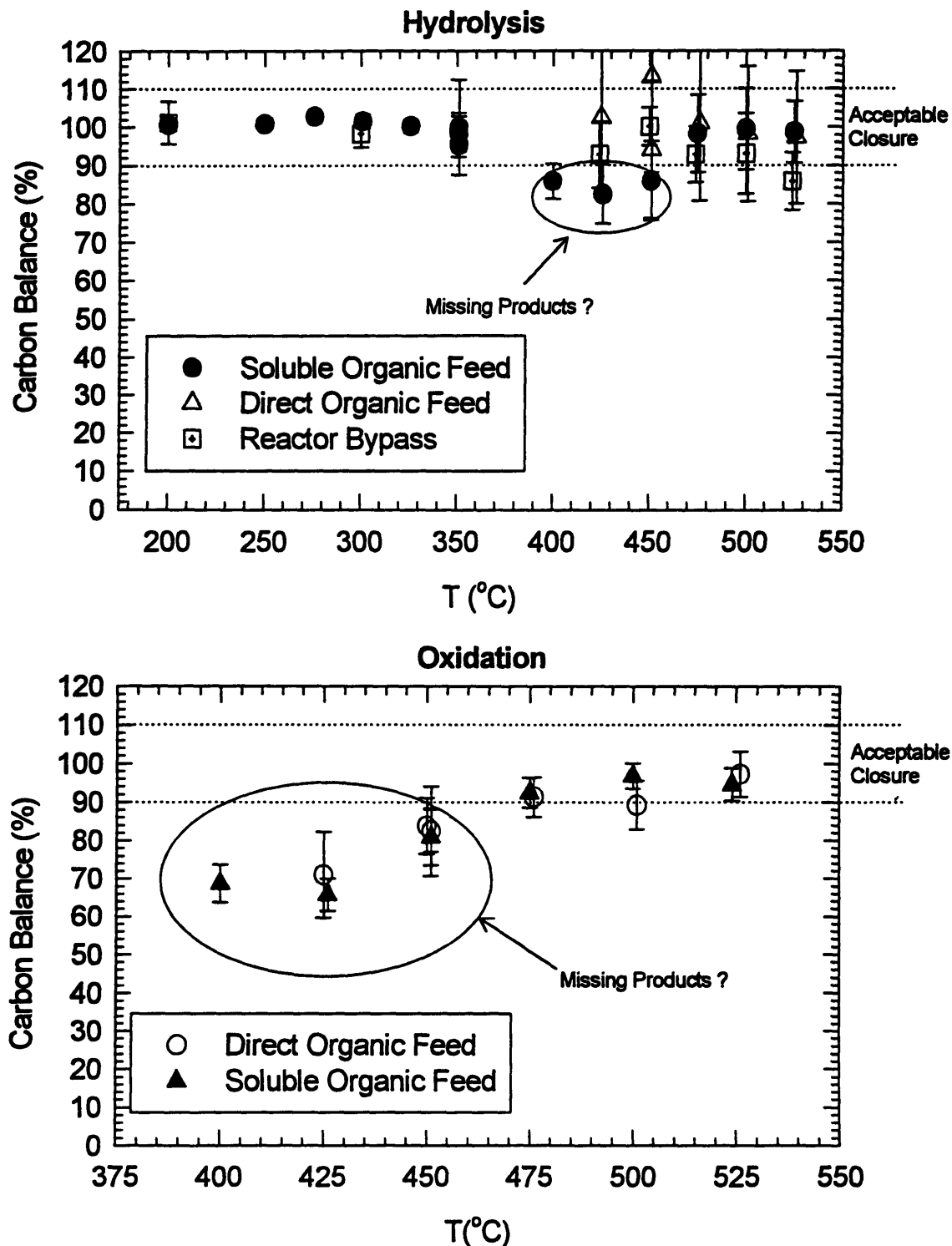
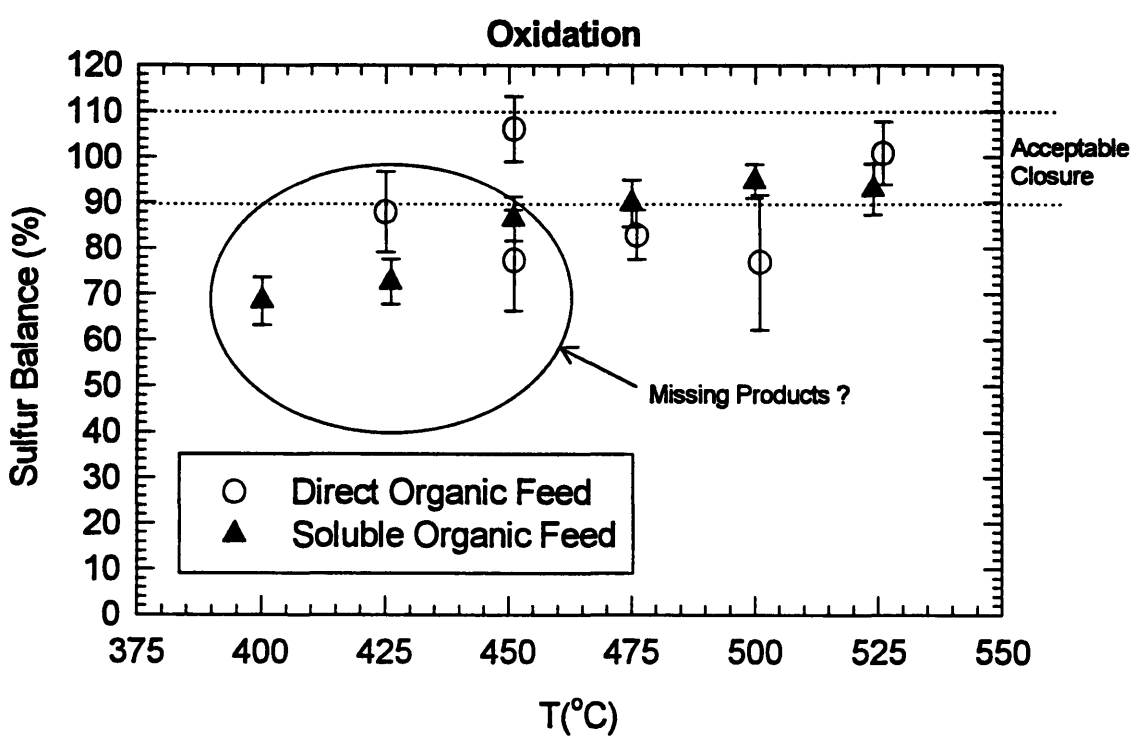
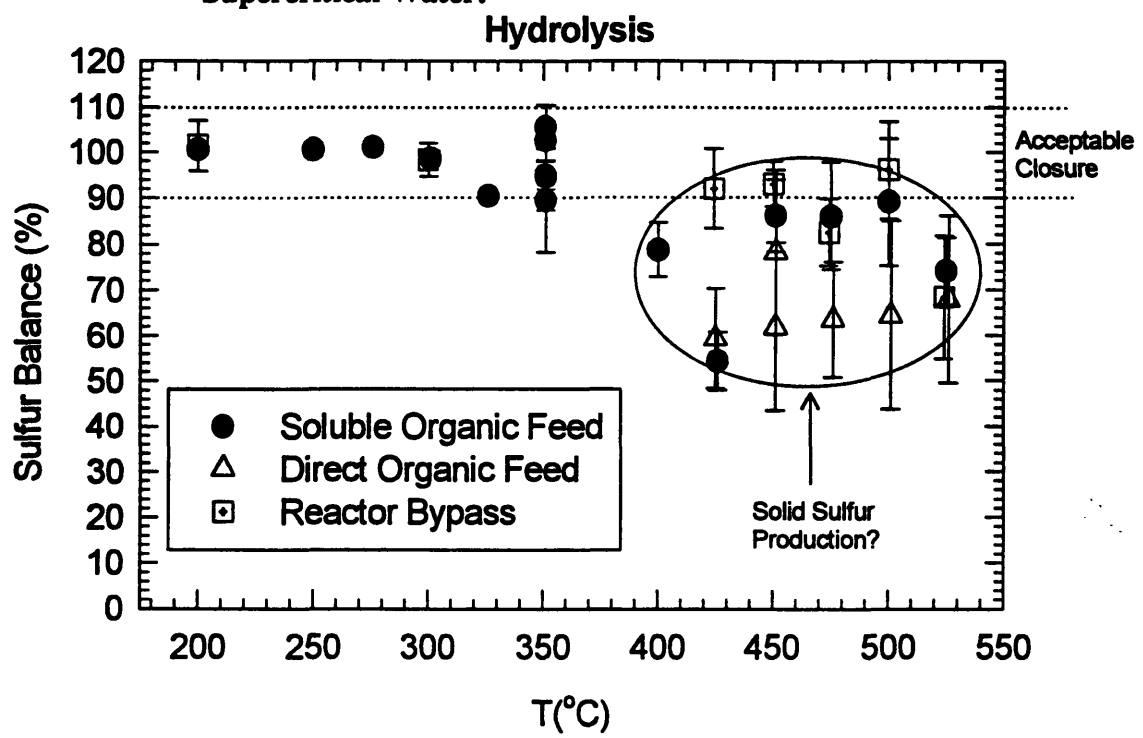


Figure 4.17 Sulfur Balances for TDG Hydrolysis and Oxidation in Sub- and Supercritical Water.



Products that we are potentially missing should satisfy the following observations:

1. These products are prevalent at 400, 425 and 450°C and virtually non-existent at higher supercritical or lower subcritical temperatures where carbon and sulfur balances presently close.
2. They should account for more carbon and sulfur in oxidation samples, which are missing approximately 20 - 40%, than in hydrolysis samples which are missing approximately 10% of the carbon. Determining the amount of sulfur missing in hydrolysis samples is difficult due to unquantified elemental sulfur present.
3. They are probably not in the gas phase based on the discussion in Section 4.5.1. There seems to be no significant unidentified peaks in the gas phase.

There are two potential candidates as major unidentified products in the liquid phase; the 13 minute peak found in FID samples (Figure 4.15) and the 20 minute peak found in HPLC samples (Figure 4.14). The 19 minute HPLC peak for hydrolysis is also a possibility, but it was only observed at 400°C and below and thus does not solve the carbon or sulfur mass balance closure shortfalls at 425 and 450°C. Other unidentified FID and HPLC peaks appear to be insignificant although collectively they could account for a reasonable amount of carbon. Unfortunately, it is extremely difficult to estimate how much carbon could be found in the remaining minor peaks with no knowledge of their structure or response to the detectors used.

Figures 4.18 and 4.19 display trends for the 13 minute and 20 minute peaks as area count versus temperature. In most cases, product concentration is linearly related to peak area count so a trend in an area count should translate to a similar trend in concentration. In the case of the 13 minute peak, the hydrolysis trend is inconsistent and it runs counter to the observation of being more prevalent at lower supercritical

Figure 4.18 Trends for Unidentified 13 Minute Peak in FID Chromatograms.

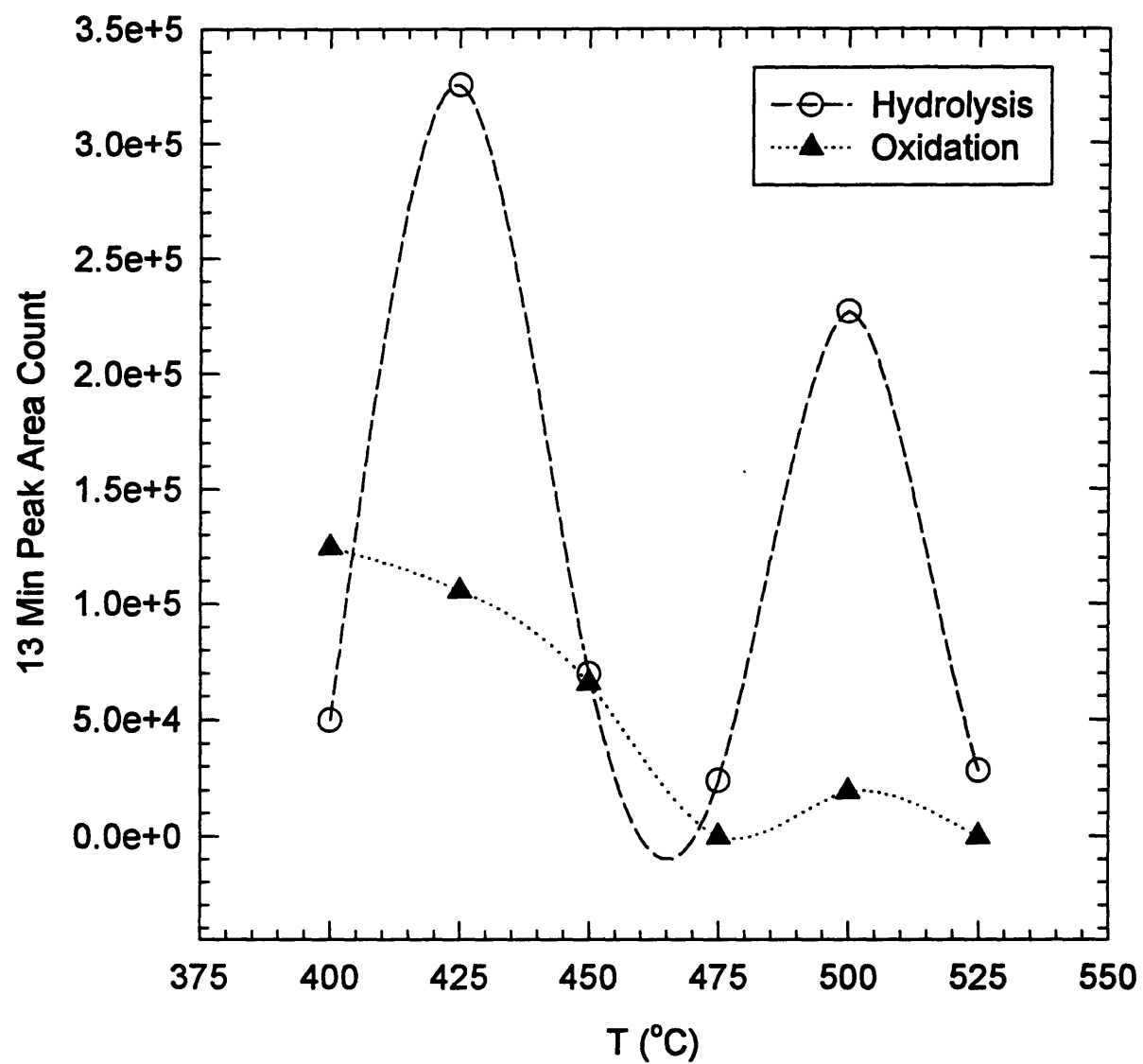
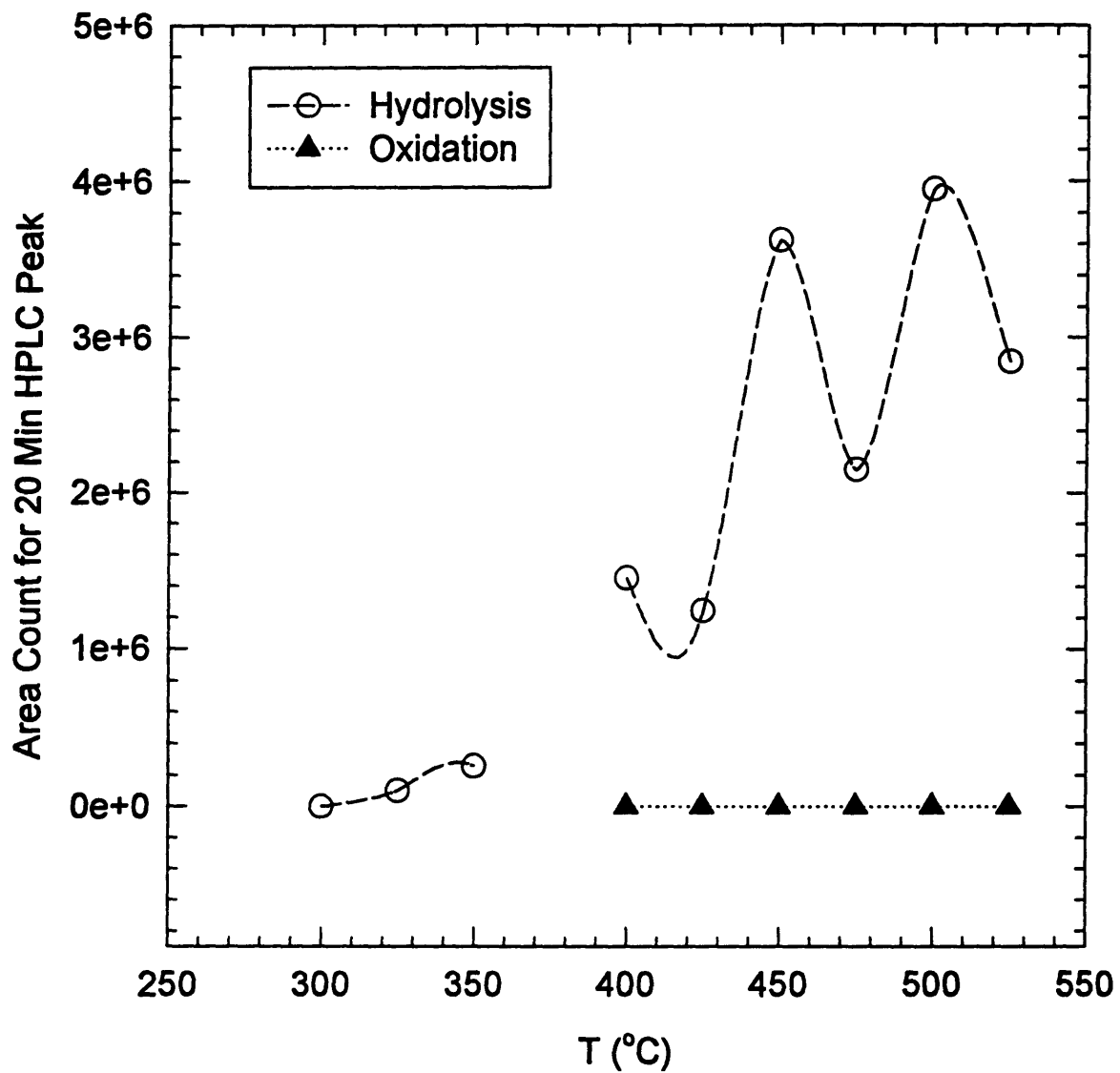


Figure 4.19 Trends for Unidentified 20 Minute Peak in HPLC Chromatograms.

temperatures. Also, this particular peak is not significant for oxidation from 400 - 450°C and does not appear to improve the carbon or sulfur balances in this regime. Unfortunately, all FID chromatograms reflect just one injection of each sample. Replicate injections of each sample may clarify the trends of this particular peak versus temperature and hence elucidate its potential contribution to carbon and sulfur accountability.

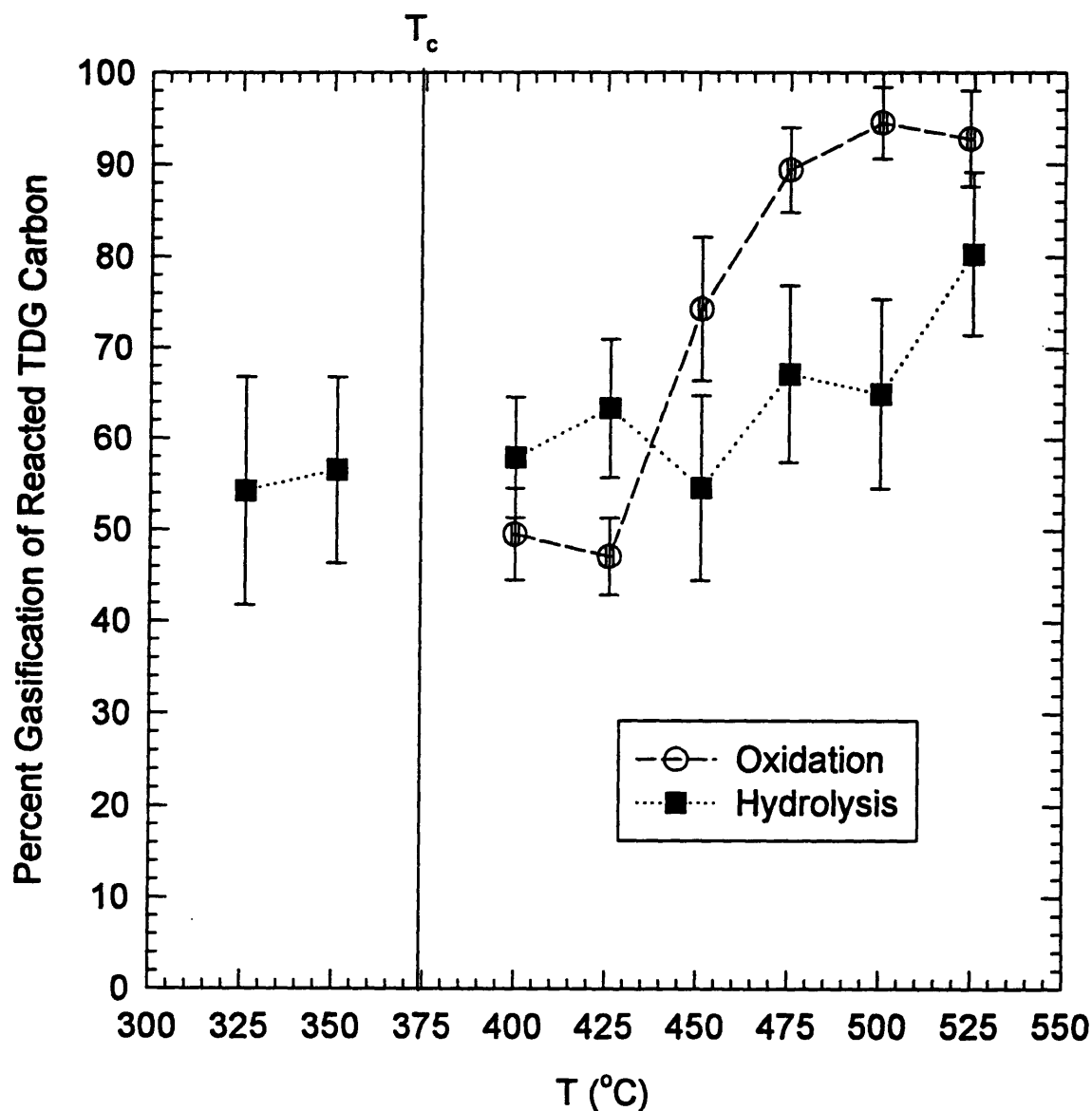
The 20 minute HPLC peak (Figure 4.19) does not appear to agree with the necessary trends either. In hydrolysis samples, this peak behaves slightly erratically and is most prevalent at higher supercritical temperatures. It is not found in oxidation samples and is therefore of no help with their carbon or sulfur closures.

In summary, carbon and sulfur balances throughout this study are generally good with the exception of supercritical hydrolysis sulfur balances due to the formation of elemental sulfur and incomplete carbon and sulfur closure at low supercritical temperatures. To resolve this issue, more experiments should be performed in this regime and replicate analysis should continue on existing and future samples.

4.6 Product Distribution

Most of the products of thiodiglycol hydrolysis and oxidation were found in the gas phase. Figure 4.20 shows the gasification of carbon as the percent of reacted carbon found in the gas phase versus temperature for hydrolysis and oxidation experiments where TDG was fed by the soluble organic method. The trends were generally the same for reactor bypass experiments and direct organic feed experiments. Even hydrolysis at 325°C produced 54±13% of the reacted carbon in the gas phase. The experiment at 300°C is not included here because its low conversion resulted in

Figure 4.20 Percent of TDG Carbon Gasification versus Temperature during Hydrolysis and Oxidation Reactions. Error bars represent estimated 95% confidence intervals.



negligible flow of gaseous products. The relatively large error bars, particularly for hydrolysis experiments, are due to the difficulties in measuring low gas flow rates and the variability of the gas flow associated with pressure fluctuations during supercritical experiments.

Figures 4.21 and 4.22 respectively show the variation of molar yields with temperature for supercritical hydrolysis and oxidation reactions. These experiments represent the trends also found in reactor bypass and direct organic feed experiments. As used here, the molar yield is defined as the moles of product divided by the moles of reacted TDG. Since TDG has four carbons, the maximum yield for single-carbon species is 4, the maximum yield for two-carbon species is 2, and the maximum yield for four-carbon species is 1. The total molar yield for sulfur products should sum to 1. As eluded to in Section 4.5, C_2H_4 , H_2S and acetaldehyde (CH_3CHO) dominate the product spectrum for hydrolysis experiments. The yields of CO_2 and H_2 as well as CO and CH_4 appear to increase with temperature although their molar yields never exceed those of the major products in the temperature range explored. The yields of acetic and formic acids as well as of thioxane and ethane are minor and do not vary dramatically from 400 to 525°C.

CO , CO_2 , and H_2SO_4 are the dominant products in oxidation experiments (Figure 4.22). As temperature increases from 500 to 525°C, the CO_2 yield increases by an amount that is essentially the same as a corresponding decrease in the CO make. However, the H_2 yield shows little net change or possibly a slight decrease from the lower temperature. Thus, direct CO oxidation seems like a more probable source of this CO_2 increase than does a water-gas shift reaction. The CH_4 yield increases with temperature even in this oxidation environment. Some of this may be methane produced under hydrolysis/pyrolysis conditions that remains in the oxidation product spectrum because of its refractory nature (Webley and Tester, 1991). However, CH_4

Figure 4.21 Variation of Product Yields with Temperature for TDG Supercritical Hydrolysis Reactions. Error bars represent estimated 95% confidence intervals.

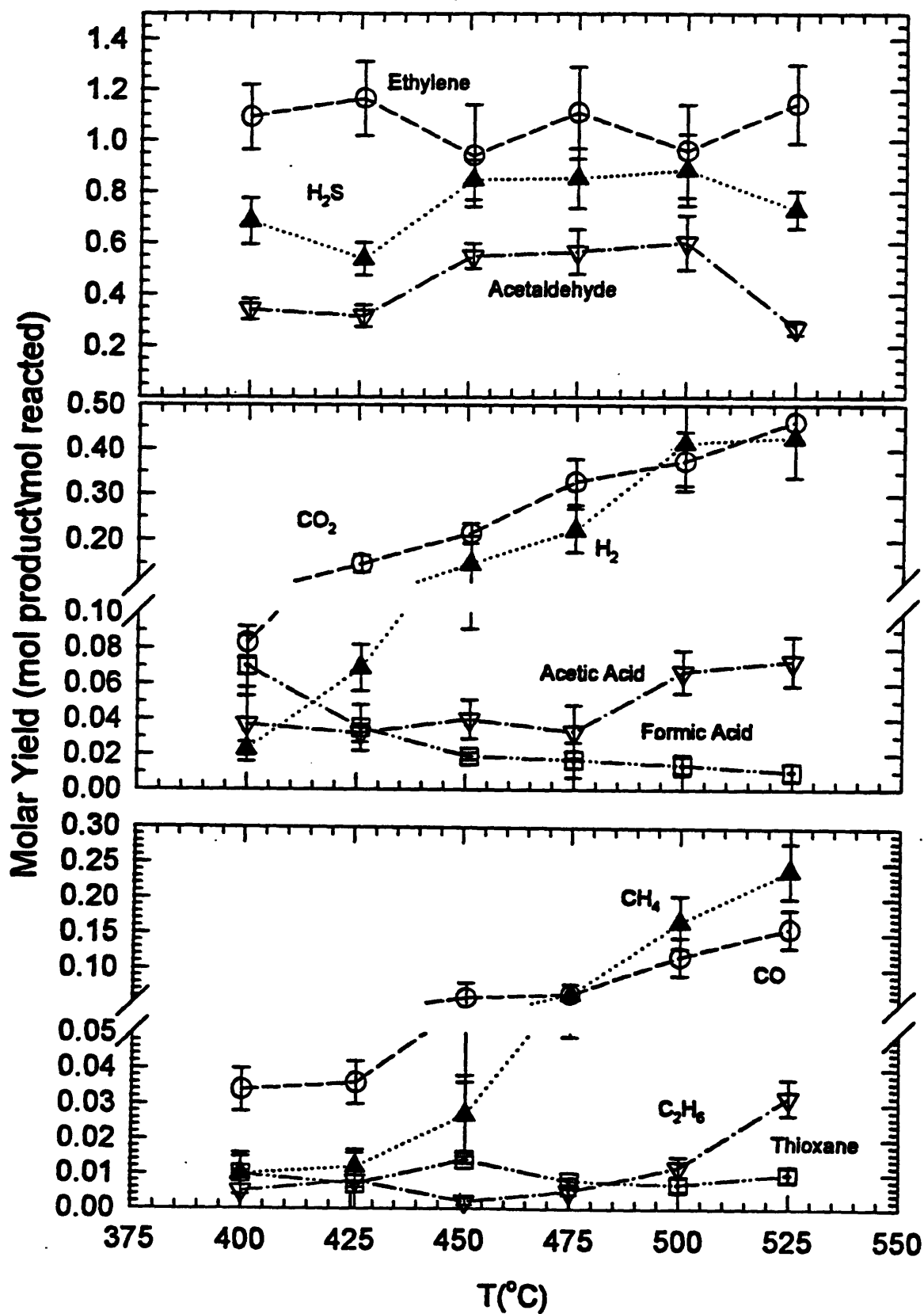
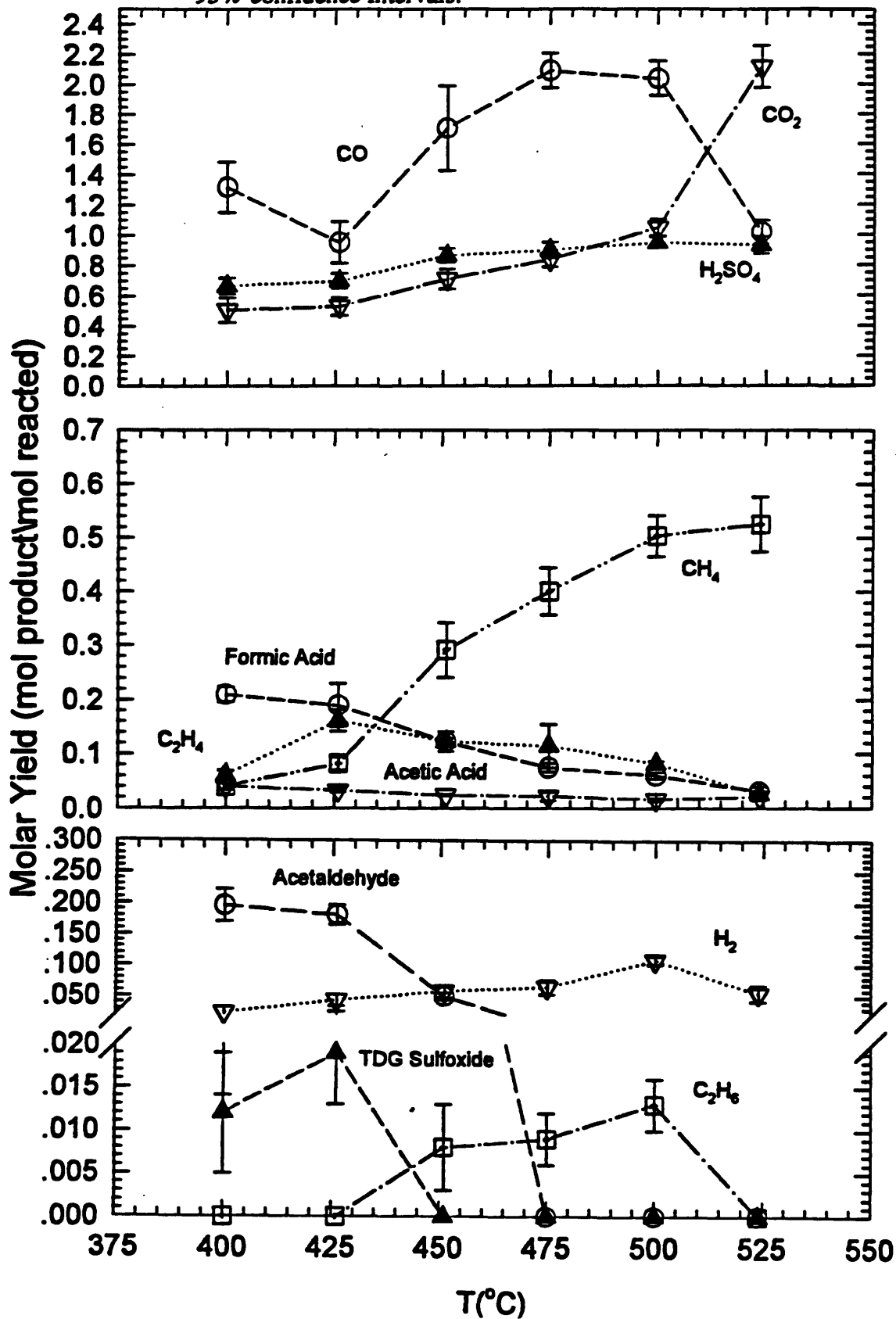


Figure 4.22 Variation of Product Yields with Temperature for TDG Supercritical Oxidation Reactions. Error bars represent estimated 95% confidence intervals.



yields for oxidation are about twice those for hydrolysis (Figure 4.22 versus Figure 4.21) and therefore an additional CH₄ production channel is indicated. There is slightly more formic acid but slightly less acetic acid produced under oxidation conditions. However, in both cases the yields remain small and decrease with increasing temperature. The hydrogen yield is significantly less during oxidation and shows little or no change with increasing temperature. The oxidation yields for acetaldehyde, thiodiglycol sulfoxide and ethane all go to zero with increasing temperature.

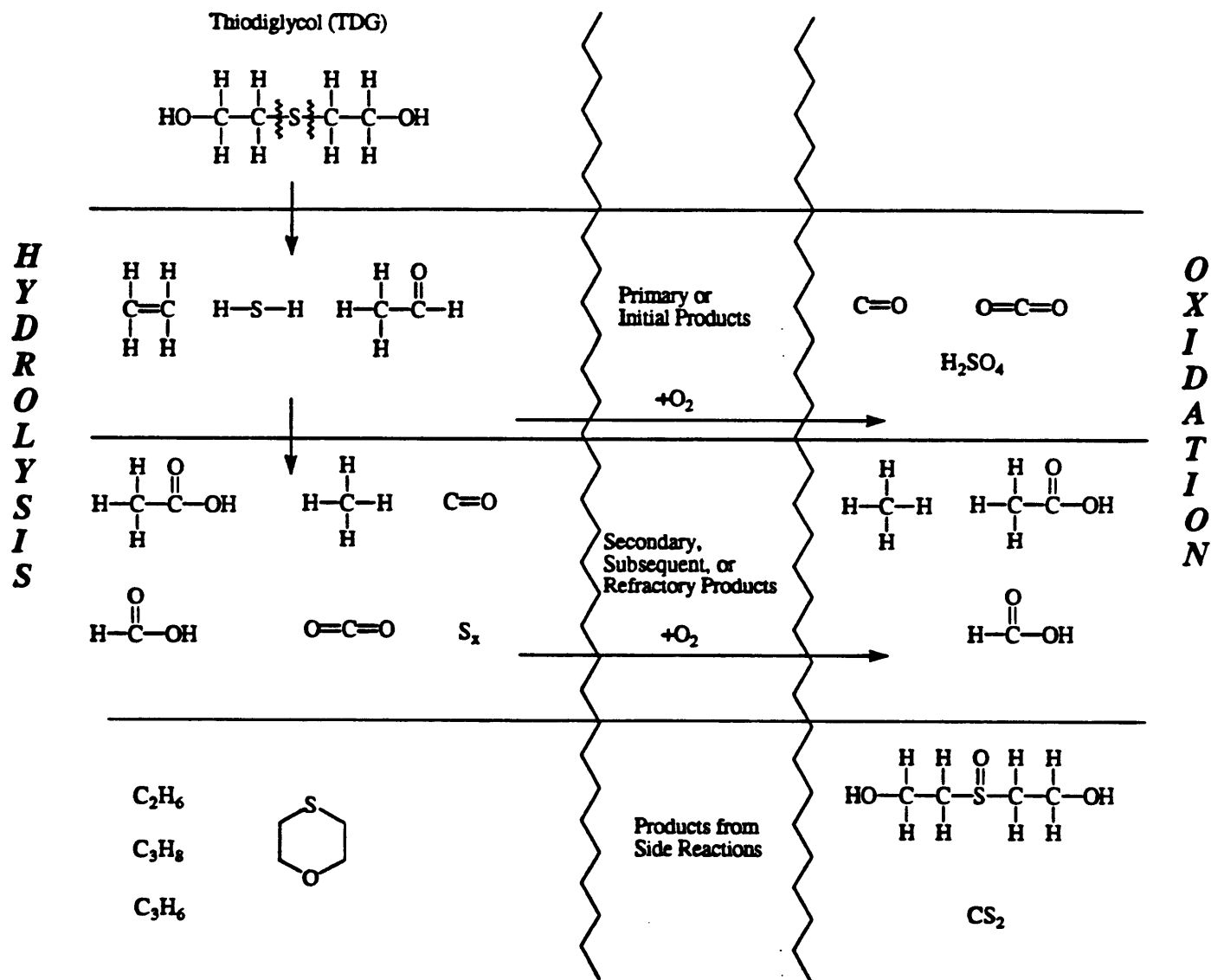
4.7 Mechanistic Insights from Experimental Results

The kinetics, product spectrum and product distribution gathered in this study suggest that thiodiglycol begins to degrade in subcritical water above 300°C and more than 100 seconds reactor residence time with rapid and complete degradation occurring in supercritical water above 425°C in less than 7 seconds reactor residence time. The following important facts support the proposed hierarchy of products depicted in Figure 4.23:

- 1) The evolution of ethylene signified the first signs of TDG conversion and therefore suggests that the C-S bonds are broken as a first step in TDG decomposition.
- 2) Hydrogen sulfide accounted for essentially all reacted sulfur at subcritical temperatures but solid sulfur substituted for the H₂S yield at higher temperatures. This implies that sulfur initially goes to hydrogen sulfide which may then undergo thermal degradation to solid sulfur. It is also possible that H₂S reacts with residual SO₂ to form sulfur via the following Claus process (Shreve and Brink, 1977).



Figure 4.23 Plausible Reaction Pathways and Hierarchy of Products of TDG Reactions in Sub- and Supercritical Water.



3) The lack of any alcohols (i.e., ethylene glycol, ethanol, methanol) suggests that the hydroxyl groups on TDG quickly reacted or rearranged under conditions explored. One result of that rearrangement may be acetaldehyde.

4) The products that make up the hydrolysis spectrum are similar to those found in HD mustard agent pyrolysis studies (Williams, 1947) and therefore suggest that TDG may be undergoing a pyrolytic thermal decomposition rather than a conversion due to reactions with water.

5) Added oxygen during oxidation experiments only effected the hydrolysis products of TDG as a result of essentially complete conversion before reaching the reactor. Therefore, hydrolysis and oxidation occurred in series for the conditions we explored; hydrolysis decomposed thiodiglycol into an initial array of products and oxidation converted those products to typical, more refractory intermediates found in SCWO reactions.

This proposed hierarchy of products or mechanistic pathway is in general agreement with the observations made by Turner at the University of Texas with a few minor differences. In his study, ethanol and sulfite were identified as additional products. We did not analyze our effluents for sulfite although it is possible that it was present in minor amounts as the result of an incomplete oxidation of sulfur. We had the ability to detect ethanol but did not find it in any effluents. Turner did not specifically analyze for acetaldehyde although he proposed that it may have been produced but thermally decomposed to CO and CH₄.

The observations made here do not agree with the observations made from the extensive study of mustard hydrolysis (Harvey et al., 1994), but the two reactions were examined in two drastically different temperature regimes and OH⁻ concentrations. Mustard hydrolysis was studied at temperatures of 90°C and below. Although

conversion of mustard was rapid and complete, in no case was there evidence of C-S bond breaking and the product spectrum was much more diverse (Harvey et al., 1994). It is likely that the higher temperatures (200 - 525°C) of our study are responsible for breaking C-S bonds and reducing the variety of products observed.

CHAPTER 5

Conclusions and Recommendations

5.1 Conclusions

5.1.1 Methylene Chloride

Kinetics and Corrosion: Conversions of methylene chloride (CH_2Cl_2) under hydrolysis and oxidation conditions were very similar. Most of the CH_2Cl_2 breakdown occurred in the hydrolysis environment of the organic preheater coil. The rate of CH_2Cl_2 destruction does not appear to be affected by the concentration or even presence of oxygen, although it may be affected by the concentration of CH_2Cl_2 . Significant corrosion was confirmed within the Hastelloy C-276 organic preheater coil in a hot but subcritical region, resulting in the failure and replacement of the tubing on four occasions.

Product Identification and Distribution: Major products of both hydrolysis and oxidation were CO, CO_2 , HCHO, CH_3OH , HCl, and H_2 , with small amounts of CH_4 above 562°C . Trace amounts of chloromethane, 1,1-dichloroethylene, cis-1,2-dichloroethylene, trans-1,2-dichloroethylene, chloroform, and trichloroethylene were detected in the gas phase effluent. The presence of oxygen resulted in a shift in the product distribution to more CO and CO_2 with less HCHO, CH_3OH and H_2 . At lower temperatures, HCHO and HCl are the only major products. A greater percentage of gaseous products and a greater variety of products were observed as temperature increased up to 550°C . By 600°C , however, the effluent was mostly CO_2 under oxidation conditions.

Mechanistic Insights: The collective evidence from hydrolysis and oxidation experiments, including kinetics, product spectra and distributions, and corrosion behavior, suggests a possible network of reaction pathways for CH₂Cl₂ oxidation in our system. The major steps include: CH₂Cl₂ + H₂O → HCHO (or CH₃OH) + HCl → CO + H₂O → CO₂; the last two steps involving reaction with O₂.

5.1.2 Thiodiglycol

Soluble Organic Feed Method: Under supercritical conditions, thiodiglycol (TDG) degradation occurred rapidly with and without oxidant. In some cases, the results of low temperature but supercritical hydrolysis reactions did not agree with similar experiments conducted at the University of Texas. There was evidence that TDG decomposed in the hydrolysis/pyrolysis environment of the organic preheater coil before reaching the reactor. However, subcritical hydrolysis/pyrolysis experiments showed that TDG did not degrade at temperatures less than 300°C and reactor residence times ≤ 100 seconds. Initial kinetic results for subcritical hydrolysis/pyrolysis of TDG show an activation energy of 178±22 kJ/mol, but the limited data could not determine an order with respect to TDG.

Direct Organic Feed Method: Testing of a direct organic feed method revealed several design challenges. Mixing of the pure organic micro-flow stream with the bulk supercritical water stream was problematic, possibly due in part to the pulsed nature of the water feed pump versus the pulse-less organic feed pump. The relatively large size of the mixing cross and the positioning of the feed streams within that cross may also be responsible for the observed mixing problems. The pure organic stream may have prematurely degraded in the cooled injection nozzle, possibly due to relatively long exposure times to sufficiently high temperatures. Different cooling water flow rates in the cooled nozzle did not seem to affect TDG decomposition but increasing the organic

flow rate, thus reducing the time spent in the cooled nozzle, did significantly reduce the TDG conversion measured in the effluent.

Product Identification and Distribution: The following gas phase products were identified in hydrolysis and oxidation experiments: C₂H₄ (the major hydrolysis gas phase product), CO, CO₂, CH₄, C₂H₆, and H₂S. A more sensitive FID and ECD analysis of the gas phase revealed other unidentified peaks which most likely correspond to compounds in trace amounts. Acetaldehyde was the only major liquid phase product in hydrolysis effluents, and oxidation liquid effluents contained only sulfuric acid as a major product. Trace amounts of acetic acid, formic acid, thioxane and thiodiglycol sulfoxide were also identified. Supercritical hydrolysis experiments produced a suspended solid phase which was identified as elemental sulfur.

Mechanistic Insights: The collective evidence of kinetics, product spectra and distributions, and results of previous investigations of TDG and similar compounds suggests a possible reaction pathway and hierarchy of products. TDG appears to first decompose under subcritical hydrolysis/pyrolysis conditions with a breaking of the C-S bonds, producing primarily C₂H₄, acetaldehyde, and H₂S. Subsequent reactions can then produce acetic acid, formic acid, CH₄, CO, CO₂, and elemental sulfur. Side reactions can produce higher molecular weight compounds, such as thioxane, in trace amounts.

5.2 Recommendations

5.2.1 Methylene Chloride

1. *Determination of degradation in the preheater coil.* Work should continue as planned to determine the temperature-time history of the organic feed in the preheater under all run conditions. This study is necessary to process current data in determining kinetic parameters for the breakdown of CH_2Cl_2 in the complete reactor system.

2. *Subcritical experiments.* Experiments at subcritical temperatures are needed to further examine CH_2Cl_2 degradation in water. CH_2Cl_2 concentrations should be varied along with an examination of different hydroxide ion concentrations as a probe into its possible role as a reactant.

3. *SCWO experiments with added caustic.* Detailed kinetic experiments are necessary to examine the affects of added caustic to waste feeds such as methylene chloride. Commercial SCWO processes call for adding caustic to feeds containing heteroatoms to neutralize mineral acids produced. Reactions of wastes in the presence of caustic must be explored to optimize commercial SCWO process designs.

5.2.2 Thiodiglycol

1. *Expanded subcritical experiments:* The first step in completing the TDG study is to collect more data, including several replicate experiments, at subcritical temperatures. The existing organic solution feed system and plug-flow apparatus can be used to conduct more experiments in the temperature range of 250 - 350°C. A full array of

experiments are required to better define kinetic parameters for TDG degradation in this regime. Reactor residence times can be varied from 30 seconds to 3 minutes and concentrations can be varied over orders of magnitude based on TDG's complete miscibility in water. Reactions in the preheater coil must also be considered in determining hydrolysis/pyrolysis kinetic parameters using the organic solution feed method. Detailed kinetic experiments of TDG subcritical hydrolysis/pyrolysis reactions should also be investigated using the CSTR apparatus in our laboratory to compare results.

2. *Surface area effects:* It is possible that supercritical water hydrolysis of TDG may be affected by the walls of the reactor as well as by elemental sulfur depositing on tubing walls. A set of experiments should be explored using reactors with different surface to volume ratios as well as experiments where different solvents are used to systematically clean reactor walls. A packed reactor in our lab could be used to increase the surface to volume ratio, and the CSTR apparatus could be used to decrease the surface to volume ratio.

3. *SCWO experiments with pre-mixed oxidant and organic feed streams:* Many commercial SCWO process configurations pre-mix oxidant and organic feed streams prior to heating and reacting them. This procedure would probably reduce elemental sulfur production, but increase the chance of corrosion in the preheater coils. Although this pre-mixing study would probably not reveal valuable kinetic information, it could lead to important insights into other facets of SCWO research. For instance, our research group is now well-equipped analytically to study high destruction efficiencies and more accurate elemental balance closures through the sensitive analysis of a variety of products in both gas and liquid effluents.

5.2.3 Direct Organic Feed Method

Several steps can be taken to improve the design of the direct organic feed system:

- 1. Use a pulse-less water feed pump.* This is essential to thorough mixing of the pure organic stream with the water/oxygen stream.
- 2. Determine the temperature-time history of the pure organic in the cooled nozzle.* These measurements are needed to optimize cooling water flow rates and residence times of the organic in the nozzle.
- 3. Reduce the internal volume of the organic line in the cooled nozzle.* Adding a thermocouple inside of this line in our present cooled nozzle will greatly reduce its internal volume but tubing with even smaller inner diameters should be employed.
- 4. Optimize the design of the mixing cross.* Organics which are stable at supercritical temperatures may not need a cooled nozzle, which would then allow for the use of a much smaller mixing crosses. However, for the design which must include a cooled nozzle, a thorough analysis of mixing must be performed. Fluid dynamics programs like FIDAP should be employed to help determine the best mixing arrangement.

APPENDICES

Appendix A: Tabulated Experimental Data

Data obtained from the hydrolysis and oxidation of thiodiglycol are contained in the following tables. Not all measured and calculated quantities are listed for each experiment, but all experiments are included and enough data is given to allow calculation of quantities not listed, if such information is desired.

All original experimental data is contained in lab notebooks and files in MIT's Building 66, Room 66-053.

Table A.1 Experimental Data for TDG Hydrolysis and Oxidation Scoping Runs.^a
Organic solution feed. $P \cong 250$ bar. Intervals shown are estimated 95% confidence.

Run No.	Run ^b Type	Temp °C	[TDG] ₀ $\times 10^4$ mol/L	[O ₂] ₀ $\times 10^3$ mol/L	τ seconds	Conversion %
399	Hyd	425±2	5.78±.32		7.4±0.4	15.5±9.5
400	Oxd	425±2	5.50±.98	3.55±.11	7.5±0.4	88.1±7.8
401	Hyd	500±2	4.27±.55		7.1±0.5	95.3±1.6
402	Oxd	500±1	4.66±.23	3.41±.10	7.1±0.4	83.3±7.8
403	Hyd	600±1	4.53±.66		7.2±0.4	100.0±0.0

^a Detailed analyses of effluents were not performed and, therefore, carbon and sulfur balances are not listed. Also, TDG concentrations were determined by GC/FID analysis for these experiments.

^b Hyd - Hydrolysis
Oxd - Oxidation

Table A.2 Experimental Data for TDG Hydrolysis Runs with Reactor Bypass.
Organic solution feed. $P \cong 250$ bar. Intervals shown are estimated 95% confidence.

Run No.	Temp °C	τ seconds	$[\text{TDG}]_0 \times 10^4 \text{ mol/L}$	Conversion %	Carbon Balance %	Sulfur Balance %
469	424 ± 6	0.6 ± 0.1	5.59 ± 0.39	8.3 ± 8.7	92.7 ± 8.7	91.9 ± 8.7
470	524 ± 2	0.6 ± 0.1	5.19 ± 0.44	100.0 ± 0.0	85.8 ± 7.5	68.3 ± 13.5
471	450 ± 3	0.6 ± 0.1	5.23 ± 0.22	7.2 ± 4.9	100.1 ± 5.0	92.9 ± 4.9
472	474 ± 2	0.6 ± 0.1	5.08 ± 0.38	17.8 ± 7.3	92.8 ± 7.4	82.4 ± 7.3
473	500 ± 2	0.6 ± 0.1	4.94 ± 0.42	42.0 ± 10.0	93.0 ± 10.5	96.1 ± 10.7
474	200 ± 1	9.4 ± 0.5	25.9 ± 1.37	-1.1 ± 5.5	101.2 ± 5.5	101.5 ± 5.5
475	300 ± 1	9.3 ± 0.5	26.3 ± 0.60	2.1 ± 3.6	98.3 ± 3.6	98.3 ± 3.6

Table A.3 Experimental Data for TDG Hydrolysis and Oxidation Runs with Direct Organic Feed.^a P \cong 255 bar. Reactor residence time \cong 7.5 seconds. Intervals shown are estimated 95% confidence.

Run No.	Run ^b Type	Temp °C	[TDG] ₀ ×10 ⁴ mol/L	[O ₂] ₀ ×10 ³ mol/L	Conversion %	Carbon Balance %	Sulfur Balance %
489	Hyd	451 ± 1	5.51 ± 0.43		89.7 ± 15.0	113.1 ± 25.0	78.1 ± 18.0
490	Oxd	451 ± 1	5.28 ± 0.31	3.82 ± 0.15	99.9 ± 0.04	82.4 ± 11.7	77.3 ± 11.0
491	Hyd	476 ± 1	5.18 ± 0.39		99.9 ± 0.06	100.9 ± 20.2	63.4 ± 12.6
492	Hyd	526 ± 1	5.24 ± 0.37		99.9 ± 0.13	97.3 ± 17.3	67.8 ± 18.3
493	Oxd	526 ± 1	5.11 ± 0.28	3.65 ± 0.16	100.0 ± 0.02	97.3 ± 5.9	100.8 ± 6.9
494	Hyd	501 ± 1	5.54 ± 0.95		99.9 ± 0.03	98.2 ± 17.7	64.3 ± 20.6
495	Oxd	501 ± 1	5.39 ± 0.31	3.84 ± 0.14	100.0 ± 0.04	89.3 ± 6.3	77.0 ± 14.7
496	Oxd	476 ± 1	4.95 ± 0.27	3.52 ± 0.12	99.9 ± 0.08	91.3 ± 5.1	82.9 ± 5.4
497	Hyd	425 ± 1	5.40 ± 0.49		99.2 ± 0.35	102.4 ± 20.9	59.3 ± 11.0
498	Oxd	425 ± 1	5.08 ± 0.28	3.60 ± 0.12	98.0 ± 0.89	71.0 ± 11.3	87.9 ± 8.8
499	Hyd	451 ± 1	5.25 ± 0.42		99.9 ± 0.30	94.1 ± 18.0	61.8 ± 18.4
500	Oxd	451 ± 1	5.05 ± 0.26	3.60 ± 0.10	100.0 ± 0.06	82.6 ± 5.5	106.1 ± 7.1
501	Hyd	451 ± 1	6.04 ± 0.56		99.7 ± 0.04	64.2 ± 19.7	50.6 ± 6.8
502	Oxd	450 ± 1	5.36 ± 0.30	3.82 ± 0.14	99.9 ± 0.11	83.8 ± 7.3	107.0 ± 13.5
503	Hyd	425 ± 1	5.39 ± 0.51		99.7 ± 0.11	88.3 ± 40.6	47.4 ± 15.5

^a Runs 501, 502 and 503 had a cooling water flow rate through the cooled-nozzle of \sim 30 mL/min. All other runs had a cooling water flow rate of \sim 3 mL/min.

^b Hyd - Hydrolysis
Oxd - Oxidation

Table A.4 Experimental Data for TDG Hydrolysis Scoping Runs with Direct Organic Feed.^a P \cong 246 bar. Confidence intervals are not shown because of the limited number of measurements taken at each temperature. [TDG]₀ is calculated from syringe pump flow rate setting. Conversion is generally based on one measurement.

Run No.	Temp °C	[TDG] ₀ ×10 ³ mol/L	τ seconds	Conversion %	Comments
504-1	101	2.53	122	3.8	
504-2	152	2.55	122	20.6	
504-3	202	2.56	123	11.8	
504-4	252	2.53	122	-14.6	
504-5	302	2.54	122	18.4	Conversion confirmed by C ₂ H ₄ in gas phase
504-6	353	2.62	127	32.4	More C ₂ H ₄ in gas phase
504-7	425	5.10	7.4	47.0	Pure Org Flow 10x greater than Runs 497 and 503

^a Detailed analyses of effluents were not performed and, therefore, carbon and sulfur balances are not listed.

Table A.5 Experimental Data for TDG Hydrolysis and Oxidation Runs with Soluble Organic Feed.^a P ≅ 255 bar. Reactor residence time ≅ 6 seconds. Intervals shown are estimated 95% confidence.

Run No.	Run ^b Type	Temp °C	[TDG] ₀ ×10 ⁴ mol/L	[O ₂] ₀ ×10 ³ mol/L	Conversion %	Carbon Balance %	Sulfur Balance %
505	Hyd	451 ± 1	5.70 ± 0.35		100.0 ± 0.1	85.9 ± 10.3	86.1 ± 7.8
506	Oxd	451 ± 1	5.54 ± 0.22	3.78 ± 0.19	100.0 ± 0.0	81.0 ± 7.4	86.4 ± 4.8
507	Hyd	426 ± 1	5.69 ± 0.42		99.9 ± 0.0	82.4 ± 7.7	54.3 ± 6.4
508	Oxd	426 ± 1	5.25 ± 0.20	3.63 ± 0.17	97.6 ± 1.5	65.7 ± 4.3	72.6 ± 4.9
509	Hyd	400 ± 1	5.75 ± 0.35		69.7 ± 2.5	85.8 ± 4.6	78.6 ± 5.9
510	Oxd	400 ± 1	5.71 ± 0.28	4.24 ± 0.18	97.7 ± 1.5	68.7 ± 5.0	68.4 ± 5.2
521	Hyd	500 ± 1	5.20 ± 0.57		100.0 ± 0.0	99.5 ± 10.7	89.1 ± 13.9
522	Oxd	500 ± 1	4.98 ± 0.14	3.65 ± 0.12	100.0 ± 0.0	96.8 ± 3.3	94.7 ± 3.7
523	Hyd	525 ± 1	6.07 ± 0.42		100.0 ± 0.0	98.7 ± 8.1	74.0 ± 7.3
524	Oxd	524 ± 1	5.45 ± 0.24	3.83 ± 0.17	100.0 ± 0.0	94.6 ± 4.2	93.0 ± 5.6
525	Hyd	475 ± 1	5.25 ± 0.47		100.0 ± 0.0	98.3 ± 10.2	86.0 ± 11.7
526	Oxd	475 ± 1	4.95 ± 0.18	3.56 ± 0.15	100.0 ± 0.0	92.4 ± 3.9	89.8 ± 5.1

^a Runs 509 and 510 were conducted with the feed pump at its maximum setting. Poor performance at this maximum setting may explain why residence times and feed concentrations are off from target values.

^b Hyd - Hydrolysis
Oxd - Oxidation

Table A.6 Experimental Data for TDG Hydrolysis Runs at Subcritical Temperatures. Organic solution feed. $P \cong 250$ bar. Intervals shown are estimated 95% confidence.

Run No.	Temp °C	τ seconds	[TDG] ₀ ×10 ³ mol/L	Conversion %	Carbon Balance %	Sulfur Balance %
511	200 ± 1	101.0 ± 4.6	2.53 ± 0.03	-0.7 ± 1.6	100.8 ± 1.6	100.7 ± 1.6
512	301 ± 1	100.5 ± 4.5	2.43 ± 0.03	1.5 ± 1.7	101.6 ± 1.8	98.6 ± 1.7
513	250 ± 1	99.9 ± 4.6	2.46 ± 0.03	-0.6 ± 1.6	100.9 ± 1.6	100.6 ± 1.6
514	351 ± 1	104.1 ± 5.0	2.48 ± 0.06	28.3 ± 2.6	95.7 ± 3.5	94.9 ± 3.0
515	276 ± 1	99.9 ± 4.5	2.47 ± 0.03	-1.0 ± 1.4	102.8 ± 1.4	101.1 ± 1.4
516	326 ± 1	101.5 ± 4.6	2.45 ± 0.03	9.9 ± 1.3	100.3 ± 1.7	90.4 ± 1.3

Table A.7 Experimental Data for TDG Hydrolysis Runs at Subcritical Temperatures: Residence Time Variations. Organic solution feed. $P \cong 255$ bar. Intervals shown are estimated 95% confidence.

Run No.	Temp °C	τ seconds	[TDG] ₀ ×10 ³ mol/L	Conversion %	Carbon Balance %	Sulfur Balance %
514	351 ± 1	104.1 ± 5.0	2.48 ± 0.06	28.34 ± 2.6	95.7 ± 3.5	94.9 ± 3.0
517	351 ± 1	37.5 ± 1.7	2.55 ± 0.04	11.25 ± 4.6	98.1 ± 4.6	105.5 ± 4.8
518	351 ± 1	71.8 ± 3.3	2.53 ± 0.05	21.03 ± 3.8	99.3 ± 4.4	102.6 ± 4.4
519	351 ± 1	136.6 ± 7.3	2.60 ± 0.09	41.42 ± 6.9	95.2 ± 7.8	94.6 ± 7.4
520	351 ± 1	179.4 ± 10.2	2.57 ± 0.11	55.14 ± 10.3	100.0 ± 12.4	89.5 ± 11.4

Appendix B: Nomenclature

A	Arrhenius preexponential factor
C_i	concentration of species i
d	tubing diameter
D	diffusivity
D_m	molecular diffusivity
E_a	Arrhenius activation energy
$H_i(T,P)$	Henry's law constant for species i
k	reaction rate constant
k^*	apparent first-order rate constant
K_w	ionic dissociation constant
L	tubing length
P	total pressure
r	tubing radius
R	universal gas constant
R_i	reaction rate for species i
v	velocity
x_i	liquid-phase mole fraction of species i
X	conversion
y_i	gas-phase mole fraction of species i

Greek Letters

ϵ	dielectric constant
ϕ_i	fugacity coefficient of species i
μ	viscosity
ρ	density
τ	reactor residence time

REFERENCES

- Aikens, D. A., Bailey, R. A., Moore, J. A., Giachino, G. G., Tomkins, R. P. T. (1984) *Principles and Techniques for an Integrated Chemistry Laboratory*. Prospect Heights, Illinois: Waveland Press, Inc.
- Albright, L.F., Crynes, B.L., Corcoran, W.H. (1983) *Pyrolysis: Theory and Practice*. New York: Academic Press, Inc.
- Altshuller, A.P., Miller, D.L., Sleva, S.F. (1961) "Determination of Formaldehyde in Gas Mixtures by the Chromotropic Acid Method." *Analytical Chemistry* 33(4), 621.
- Armellini, F.J. (1993) "Phase Equilibria and Precipitation Phenomena of Sodium Chloride and Sodium Sulfate in Sub- and Supercritical Water." Doctoral Thesis, Department of Chemical Engineering, Massachusetts Institute of Technology, Cambridge, MA.
- Armellini, F.J., Tester, J.W., Hong, G.T. (1994) "Precipitation of sodium chloride and sodium sulfate in water from sub- to supercritical conditions: 150 to 500°C, 100 to 300 bar." *Journal of Supercritical Fluids* 7, 147-158.
- Azatyan, V.V. (1972) "Study of gas-phase reactions in a jet, with allowance being made for longitudinal diffusion." *Doklady Akad. Nauk SSSR* 203(1), 137-140.
- Barner, H.E., Huang, C.Y., Johnson, T., Jacobs, G., Martch, M.A., Killilea, W.R. (1991) "Supercritical water oxidation: An Emerging Technology." Presented at AICHE, June 9, 1991, and accepted for publication in *J. Haz Mat.*
- Benson, B. B., Krause, D. Jr., and Peterson, M.A. (1979) "The solubility and isotopic fractionation of gases in dilute aqueous solution. I. Oxygen." *J. Solution Chem.* 8(9), 655-690.
- Bird, R.B., Stewart, W.E., Lightfoot, E.N. (1960) *Transport Phenomena*. New York, NY: John Wiley & Sons, Inc.
- Blank, M.R. (1992) "A survey: destruction of chemical agent simulants in supercritical water oxidation." Los Alamos National Laboratory, Los Alamos, NM, Report No. AFTT/CI/CIA-92-063.

- Bossle, P.C., Ellzy, M.W., Martin, J.J. (1993) "Detection of thiodiglycol and its sulfoxide and sulfone analogues in environmental waters by high performance liquid chromatography." Report No. ERDEC-TR-035; U.S. Army Chemical and Biological Defense Agency, Aberdeen Proving Ground, MD.
- Brelvi, S.W. and O'Connell, J.P. (1972) "Corresponding states correlations for liquid compressibility and partial molal volumes of gases at infinite dilution in liquids." *AIChE J.* **18**(6), 1239-1243.
- Bricker, C.E. and Vail, W.A. (1950) "Microdetermination of Formaldehyde with Chromotropic Acid." *Analytical Chemistry* **22**(5), 720.
- Brooks, M.E. and Parker, G.A. (1979) "Incineration/pyrolysis of several agents and related chemical materials contained in identification sets." Report #ARCSL-TR-79040, Chemical Systems Laboratories, Research Division.
- Buelow, S.T., Dyer, R.B., Atenolo, J.H., Wander, J.D. (1990) "Advanced techniques for soil remediation of propellant components in supercritical water." Los Alamos National Laboratory, Los Alamos, NM, Report No. LA-UR-90-1338.
- Buelow, S.T., Dyer, R.B., Harradine, D.M., Robinson, J.M., Funk, K.A., McInroy, R.E., Sanchez, J.A., Spontrelli, T. (1992) "Destruction of explosives and rocket fuels by supercritical water oxidation." Los Alamos National Laboratory, Los Alamos, NM, Report No. LA-CP-92-281.
- Chuang, S.C. and Bozzelli, J.W. (1986) "Conversion of Chloroform to HCl by Reaction with Hydrogen and Water Vapor." *Environ. Sci. Technol.* **20**, 568.
- Cleland, F.A. and Wilhelm, R.H. (1956) "Diffusion and reaction in viscous-flow tubular reactor." *AIChE J.* **2**(4), 489-497.
- Connolly, J.F. (1966) "Solubility of hydrocarbons in water near the critical solution temperatures." *J. Chem. Eng. Data* **11**(1), 13-16.
- Cutler, A.H., Antal, M.J. Jr., Jones, M. Jr. (1988) "A critical evaluation of the plug-flow idealization of tubular-flow reactor data." *Ind. Eng. Chem. Res.* **27**(4), 691-697.
- Dietrich, M. J., Randall, T.L., Canney, P.J. (1985) "Wet Air Oxidation of Hazardous Organics in Wastewater." *Environ. Prog.*, **4**(3), 171.

- Downey, K.W., Hazlebeck, D.A., Roberts, A.J., Larese, J.P., Snow, R.H. (1994) "Corrosion and chemical agent destruction investigations of the supercritical water oxidation of hazardous military wastes." Presented at the AIChE 1994 Annual Meeting in the Supercritical Fluids Session, November 13-18.
- Dudziak, K.H., Franck, E.U., (1966) "Messungen der Viskosität des Wassers bis 560°C und 3500 bar." *Ber. Bunsenges. Phys. Chem. Phys.* 70(9-10), 1120.
- Ember, L.R. (1990) "Chemical Weapons Disposal; Daunting Challenges Still Ahead." *Chem. & Eng. News* 68(33), 9-19.
- Fells, I. and Moelwyn-Hughes, E.A. (1958) "The Kinetics of the Hydrolysis of Methylene Dichloride." *J. Chem. Soc.* 1326.
- Franck, E.U. (1976) "Properties of water." In *High Temperature, High Pressure Electrochemistry in Aqueous Solutions* D. de G. Jones and R.W. Staehle, eds. Houston, TX : National Association of Corrosion Engineers, pp. 109-116.
- Franck, E.U., Rosenqweig, S., Christoforakos, M., (1990) "Calculation of the dielectric constant of water to 1000°C and very high pressures." *Ver. Bunsenges. Phys. Chem.* 94, 199.
- Gaisinovich, M.S. and Ketov, A.N. (1969) "High-temperature Hydrolysis of Carbon Tetrachloride and Phosgene in the Gaseous Phase." *Russ. J. Inorg. Chem.* 14(9), 1218.
- Gilbert, B.C., Larkin, J.P., Norman, R.O.C. (1973) "Electron spin resonance studies. Part XXXVII. Oxidation of β -hydroxy-sulphides by the hydroxyl radical and structural features of sulphur-conjugated radicals." *J.C.S. Perkin II*, 272.
- Gloyna, E.F. (1989) "Supercritical water oxidation-deep well technology for toxic wastewaters and sludges." The University of Texas, Austin, TX, Tech. Report No. W-89-1
- Greenberg, A.E., Clesceri, L.S., Eaton, A.D. eds. (1992) *Standard Methods for the Examination of Water and Wastewater, 18th Edition*. Washington, D.C.: APHA, AWWA, and WEF.
- Haar, L., Gallagher, J.S., Kell, G.S. (1984) *NBS/NRC Steam Tables*. New York: Hemisphere Publishing Corp.

- Harris, J.M. and McManus, S.P. (1985) "Nucleophilic decontamination agents." Final Report from Department of Chemistry, University of Alabama to U.S. Army Research Office, Research Triangle Park, NC.
- Harvey, S.P. et al. (1994) "Agent Neutralization: I. Hydrolysis of Sulfur Mustard." Report to the Office of the Program Manager, Chemical Demilitarization. U.S. Edgewood Research, Development and Engineering Center, Aberdeen Proving Ground, MD.
- Heger, K., Uematsu, M. Franck, E.U. (1980) "The static dielectric constant of water at high pressures and temperatures to 500 MPa and 550°C." *Ber. Bunsenges. Phys. Chem.* **84**, 758.
- Helling, R.K. (1986) "Oxidation kinetics of simple compounds in supercritical water: carbon monoxide, ammonia, and ethanol." Doctoral thesis, Department of Chemical Engineering, Massachusetts Institute of Technology, Cambridge, MA.
- Helling, R.K. and Tester, J. W. (1987) "Oxidation kinetics of carbon monoxide in supercritical water." *Energy & Fuels* **1**, 417-423.
- Helling, R.K. and Tester, J. W. (1988) "Oxidation of simple compounds and mixtures in supercritical water: carbon monoxide, ammonia and ethanol." *Environ. Sci. Technol.* **22**(11), 1319-1324.
- Hoke, J.B., Gramiccioni, G.A., Balko, E.N. (1992) "Catalytic Hydrodechlorination of Chlorophenols." *Applied Catalyst B: Environmental.* **1**(4), 285.
- Holgate, H.R. (1993) "Oxidation chemistry and kinetics in supercritical water: hydrogen, carbon monoxide, and glucose." Doctoral Thesis, Department of Chemical Engineering, Massachusetts Institute of Technology, Cambridge, MA.
- Holgate, H.R., Meyer, J.C., Tester, J.W. (1995) "Glucose hydrolysis and oxidation in supercritical water." *AIChE Journal* **41**(3), 637-648.
- Holgate, H.R. and Tester, J.W. (1993) "Fundamental kinetics and mechanisms of hydrogen oxidation in supercritical water." *Combust. Sci. and Tech.* **88**, pp.369-397.
- Holgate, H.R., Webley, P.A., Tester, J.W., and Helling, R.K. (1992) "Carbon monoxide oxidation in supercritical water: The effects of heat transfer and the water-gas shift reaction on observed kinetics." *Energy & Fuels* **6**(5), 586-597.
- Hong, G.T. (1991) "Process for oxidation of materials in water at supercritical temperatures." Intl. Patent Appl. WO 91/11394.

- Hong, G.T., Fowler, P.K., Killilea, W.R., and Swallow, K.C. (1987) "Supercritical water oxidation: Treatment of human waste and system configuration tradeoff study." SAE Technical Paper Series #87144, 17th Intersociety Conference on Environmental Systems, Seattle, WA, July 13-15.
- Hossain, S.U. and Blaney, C.A. (1991) "Method for removing polychlorinated dibenzodioxins and polychlorinated dibenzofurans from paper mill sludge." United States patent # 5,075,017, December 24.
- Houser, T.J. and Liu, X. (1994a) "The Removal of Organic Heteroatoms by Supercritical Water." *Proceedings of the 3rd International Symposium on Supercritical Fluids* 3, 75.
- Houser, T.J. and Liu, X. (1994b) "Reactions involving supercritical water and organoheteroatoms." Presented at the AIChE 1994 Annual Meeting in the Supercritical Fluids Session, November 13-18.
- Huang, C. (1992) "Apparatus and method for supercritical water oxidation." US Patent, #5,100,560.
- Huang, C., Barner, H.E., Killilea, W.R., Hong, G.T. (1992) "Method for supercritical water oxidation." Intl. Patent Appl. WO 92/21621.
- Huang, S., Daehling, K., Carleson, T.E., Abdel-Latif, M., Taylor, P., Wai, C., Propp, A. (1989) "Electrochemical Measurements of Corrosion of Iron Alloys in Supercritical Water." *ACS Symposium Series 406: Supercritical Fluid Science and Technology*; K.P. Johnston and J.M.M. Penninger, eds. Washington, D.C.: American Chemical Society, pp. 287-300.
- Hung, S.L. and Pfefferle, L.D. (1989) "Methyl Chloride and Methylene Chloride Incineration in a Catalytically Stabilized Thermal Combuster." *Environ. Sci. Technol.* 23(9), 1085.
- Japas, M.L. and Franck, E.U. (1985) "High pressure phase equilibria and PVT-data of the water-oxygen system including water-air to 673 K and 250 MPa." *Ber. Bunsenges. Phys. Chem.* 89, 1268-1275.
- Jeffers, P.M., Ward, L.M., Woytowitch, L.M., Wolfe, N.L. (1989) "Homogeneous Hydrolysis Rate Constants for Selected Chlorinated Methanes, Ethanes, Ethenes, and Propanes." *Environ. Sci. Technol.* 23(8), 965.

- Jin, L., Shah, Y.T., Abraham, M.A. (1990) "The Effect of Supercritical Water on the Catalytic Oxidation of 1,4-Dichlorobenzene." *J. Supercritical Fluids* 3, 233.
- Jolly, G.S., McKenney, D.J., Singleton, D.L., Paraskevopoulos, G., Bossard, A.R. (1986) "Rates of OH radical reactions: Rate-constant and mechanisms for the reaction of hydroxyl radicals with formic acid." *J. Phys. Chem.* 90, 6557-6562.
- Josephson, J. (1982) "Supercritical fluids." *Environ. Sci. Technol.* 16(10), 548A-551A.
- Killilea, W R., Swallow, K. C., Hong, G. T. (1992) "The fate of nitrogen in supercritical water oxidation." *J. Supercritical Fluids* 5(1), 72-78.
- Krader, T. and Franck, E.U. (1987) "The ternary system H₂O-CH₄-NaCl and H₂O-CH₄-CaCl₂ to 800 K and 250 MPa." *Ber. Bunsenges. Phys. Chem.* 91, 627-634.
- Kramers, H. and Westerterp, K.R. (1963) *Elements of Chemical Reactor Design and Operation*. New York, Academic Press, Inc.
- Lamb, W.J., Hoffman, G.A., Jonas, J. (1981) "Self-diffusion in compressed supercritical water." *J. Chem. Phys.* 74(12), 6875.
- Lee, D.S., Gloyna, E.F., Li, L. (1990) "Efficiency of H₂O₂ and O₂ in Supercritical Water Oxidation of 2,4-Dichlorophenol and Acetic Acid." *J. Supercritical Fluids* 3(4), 249.
- Li, R., Savage, P.E., Szmukler, D. (1993) "2-Chlorophenol Oxidation in Supercritical Water: Global Kinetics and Reaction Products." *AIChE J.* 39(1), 178.
- Lide, D.R. ed. (1993) *CRC Handbook of Chemistry and Physics, 74th Edition*. Boca Raton, FL: CRC Press, Inc.
- Liepa, M. A. (1988) "A Kinetic Study of the Oxidation of Model Chlorinated Hydrocarbons Catalyzed by Chromia Supported on γ -Alumina." Doctoral Thesis, Department of Chemical Engineering, Massachusetts Institute of Technology, Cambridge, MA.
- Lundin, S.J. ed. (1991) *Verification of Dual-use Chemicals under the Chemical Weapons Convention: The Case of Thiodiglycol*. New York: Oxford University Press.
- MacNaughton, M.G. and Brewer, J.H. (1994) "Environmental Chemistry and Fate of Chemical Warfare Agents." Final Report for SWRI Project #01-5864, Southwest Research Institute, San Antonio, TX.

- Marrone, P.A., Lachance, R.P., DiNaro, J.L., Phenix, B.D., Meyer, J.C., Tester, J.W., Peters, W.A., Swallow, K.C. (1995) "Methylene chloride oxidation and hydrolysis in supercritical water." In *ACS Symposium Series: Supercritical Fluids Science and Technology*, K. Hutchinson and N. Foster, eds. Washington, D.C.: American Chemical Society, in press.
- Marshall, W.L., Franck, E.U. (1981) "Ion product of water substance, 0-1000 °C, 1-10,000 bars. New international formulation and its background." *J. Phys. Chem. Ref. Data* 10(2), 295.
- Meyer, J.C. (1993) "Oxidation Chemistry and Kinetics of Model Compounds in Supercritical Water: Glucose, Acetic Acid, and Methylene Chloride." Masters Thesis in the Department of Chemical Engineering, Massachusetts Institute of Technology, Cambridge, MA.
- Meyer, J.C., Marrone, P.A., Tester, J.W. (1995) "Acetic Acid Oxidation and Hydrolysis in Supercritical Water." accepted for publication in *AIChE J.*
- Mitton, D.B., Orzalli, J.C., Latanision, R.M. (1994) "Corrosion Phenomena Associated with SCWO Systems." *Proceedings of the 3rd International Symposium on Supercritical Fluids* 3, 43.
- Modell, M. (1982) "Processing methods for the oxidation of organics in supercritical water." United States patent #4,338,199, July 6.
- Modell, M. (1985a) "Processing methods for the oxidation of organics in supercritical water." United States patent #4,543,190, September 24.
- Modell, M. (1985b) "Gassification and liquefaction of forest products in supercritical water." In *Fundamentals of Thermochemical Biomass Conversion*, R.P. Overend, T. A. Milne, and L.K. Mudge, eds. New York: Elsevier Applied Science Publishers, pp. 95-119.
- Modell, M. (1989) "Supercritical-water oxidation." In *Standard Handbook of Hazardous Waste Treatment and Disposal*, H. M. Freeman, ed. New York, NY: McGraw-Hill, pp. 8.153-8.168.
- Modell, M., Larson, J., and Sobczynski, S. F. (1992) "Supercritical water oxidation of pulp mill sludges." *Tappi J.* June, 195-202.

- Modell, M., Gaudet, G. G., Simson, M., Hong, G.T., and Biemann, K. (1982) "Supercritical water: testing reveals new process holds promise." *Solid Wastes Management*, August.
- Modell, M., Kuharich, E.F., Rooney, M.R. (1993) "Supercritical water oxidation process and apparatus of organics with inorganics." Intl Patent Appl. WO 93/00304.
- Mohan, H. and Mittal, J.P. (1991) "Electron transfer reactions in aqueous solutions of 2,2'-thiodiethanol: A pulse radiolysis study." *Radiat. Phys. Chem.* 38(1), 45-50.
- Moore, J. C., Battino, R., Rettich, T. R., Handa, Y. P., and Wilhelm, E. (1982) "Partial molar volumes of 'gases' at infinite dilution in water at 298.15K." *J. Chem. Eng. Data* 27, 22-24.
- Norton, T.S. (1990) "The combustion chemistry of simple alcohol fuels." Doctoral thesis, Department of Mechanical and Aerospace Engineering, Princeton University, Princeton, NJ.
- Ogata, Y. and Sawaki, Y. (1963) "Kinetics of the catalytic hydrogen peroxide oxidation of thiodiglycol in aqueous solutions." *Chem. Soc. Japan Bulletin* 36(11), 1453-1459.
- Perry, R. H., Green, D., and Maloney, J.O., eds. (1984) *Perry's Chemical Engineers' Handbook, Sixth Edition*. New York: McGraw-Hill.
- Ploos van Amstel, J.J.A. and Rietema, K. (1970) "Na₂O₂ oxidation von Abwässerschläm. Teil I: Oxidation von Glucose als Modellschubstanz." *Chem.-Ing.-Tech.* 42(15), 981-990.
- Poirier, R.V. and Carr, R.J. Jr. (1971) "The use of tubular flow reactors for kinetic studies over extended pressure ranges." *J. Phys. Chem.* 75(10), 1593-1601.
- Press, W.H., Flannery, B.P., Teukolsky, S.A., and Vetterling, W.T. (1986) *Numerical Recipes: The Art of Scientific Computing*. New York: Cambridge University Press.
- Ramayya, S. V. and Antal, M.J. Jr. (1989) "Evaluation of systematic error incurred in the plug flow idealization of tubular flow reactor data." *Energy & Fuels* 3, 105-108.
- Randall, T. L., and Knopp, P. V. (1980) "Detoxification of Specific Organic Substances by Wet Oxidation." *J. Water Poll. Control Fed.*, 52, 221.
- Reid, E.E. (1960) *Organic Chemistry of Bivalent Sulfur: Volume II*. New York: Chemical Publishing Co., Inc.

- Reid, R.C., Prausnitz, J.M., and Poling, B.E. (1987) *The Properties of Gases and Liquids, Fourth Edition*. New York: McGraw-Hill.
- Rettich, T.R., Battino, R., and Wilhelm, E. (1982) "Solubility of gases in liquids. 15. High-precision determination of Henry coefficients for carbon monoxide in liquid water at 278 to 323K." *Ber. Bunsenges. Phys. Chem.* **86**, 1128-1132.
- Rettich, T.T., Handa, Y.P., Battino, R., and Wilhelm, E. (1981) "Solubility of gases in liquids. 13. High-precision determination of Henry's constants for methane and ethane in liquid water at 275 to 328K." *J. Phys. Chem.* **85**, 3230-3237.
- Rice, S.F., Steeper, R.R., LaJeunesse, C.A. (1993) "Destruction of Representative Navy Wastes Using Supercritical Water Oxidation." Report No. SAND 94-8203 UC-402; Sandia National Laboratories, Livermore, CA.
- Rice, S.F., LaJeunesse, C.A., Hanush, R.G., Aiken, J.D., Johnston, S.C. (1994) "Supercritical water oxidation of colored smoke, dye, and pyrotechnic compositions." Report No. SAND 94-8209 UC-402; Sandia National Laboratories, Livermore, CA.
- Rohrbaugh, D.K., Yang, Y-C., Ward, J.R. (1989) "The characterization of sulfonium chlorides by gas chromatography/mass spectrometry and the degradation of 2-chloroethyl sulfide derivatives." *Phosphorous, Sulfur, and Silicon.* **44**, 17-25.
- Ross, S.D. (1946) "The rate of oxidation of thiodiglycol and triethylamine by hydrogen peroxide." *J. Am. Chem. Soc.* **68**, 1484-5.
- Savage, P.E., Gopalan, S., Mizan, T.I., Martino, C.J., Brock, E.E. (1995) "Reactions at supercritical conditions: Applications and fundamentals." submitted for publication in the *AIChE Journal*.
- Shanableh, A. and Gloyna, E.F. (1991) "Supercritical water oxidation - wastewaters and sludges." *Water Sci. Technol.* **23**(1-3), 389-398.
- Shaw, H., Wang, Y., Yu, T., Cerkanowicz, A.E. (1993) "Catalytic Oxidation of Trichloroethylene and Methylene Chloride." *ACS Symposium Series 518: Emerging Technologies in Hazardous Waste Management III*, D.W. Tedder and F.G. Pohland, eds.; Washington, D.C.: American Chemical Society, pp. 358-379.

- Shaw, R.W., Brill, T.R., Clifford, A.A., Eckert, C.A., and Franck, E.U. (1991) "Supercritical water: a medium for chemistry." *Chem. Eng. News* 69(5), 26-39.
- Shreve, R.N. and Brink, J.A. (1977) *Chemical Process Industries, 4th Edition*. New York: McGraw-Hill Book Company.
- Silverstein, R.M., Bassler, G.C., and Morrill, T.C. (1991) *Spectrometric Identification of Organic Compounds, Fifth Edition*. New York: John Wiley and Sons.
- Staszak, C.N., Malinowski, K.C., Killilea, W.R. (1987) "The Pilot-Scale Demonstration of the MODAR Oxidation Process for the Destruction of Hazardous Organic Waste Materials." *Environ. Prog.* 6(1), 39.
- Swallow, K.C., Killilea, W.R., Malinowski, K.C., and Staszak, C. (1989) "The MODAR process for the destruction of hazardous organic wastes-field test of a pilot-scale unit." *Waste Management* 9, 19-26.
- Tester, J.W., Holgate, H.R., Armellini, F.J., Webley, P.A., Killilea, W.R., Hong, G.T., and Barner, H.E. (1993) "Oxidation of hazardous organic wastes in supercritical water: A review of process development and fundamental research." *ACS Symposium Series 518: Emerging Technologies in Hazardous Waste Management III*, D.W. Tedder and F.G. Pohland, eds. Washington, D.C.: American Chemical Society, pp. 35-76.
- Tester, J.W., Webley, P.A., and Holgate, H.R. (1992) "Revised global kinetic measurements of methanol oxidation in supercritical water." *Ind. Eng. Chem Res.*, 32(1), 236-239.
- Thomason, T.B. and Modell, M. (1984) "Supercritical water destruction of aqueous wastes." *Haz. Waste* 1(4), 453-467.
- Thomason, T.B., Hong, G.T., Swallow, K.C., and Killilea, W.R. (1990) "The MODAR supercritical water oxidation process." In *Innovative Hazardous Waste Treatment Technology Series, Volume 1: Thermal Processes*, H.M. Freeman, ed. Lancaster, PA: Technomic Publishing, pp. 31-42.
- Thornton, T.D. and Savage, P.E. (1990) "Phenol oxidation in supercritical water." *J. Supercritical Fluids* 3(4), 240-248.

- Timberlake, S.H., Hong, G.T., Simson, M., and Modell, M. (1982) "Supercritical water oxidation for wastewater treatment; preliminary study of urea destruction." SAE Technical Paper Series #820872, 12th Intersociety Conference on Environmental Systems, San Diego, CA, July 19-21.
- Titmas, J.A. (1986) "Method and apparatus for conducting chemical reactions at supercritical conditions." U.S. Patent #4,594,164.
- Tödheide, K. (1972) "Water at high temperatures and pressures." *Water: A Comprehensive Treatise*, F. Franks, ed. New York: Plenum Press, Inc., pp. 463-514.
- Tödheide, K. and Franck, E.U. (1963) "Das Zweiphasengebiet und die kritische Kurve im System Kohlendioxid-Wasser vis zu Drucken von 3500 bar." *Z. Phys. Chem. N.F.* **37**, 387-401.
- Townsend, S.H., Abraham, M.A., Huppert, G.L., Klein, M.T., Paspek, S.C. (1988) "Solvent effects during reactions in supercritical water." *Ind. Eng. Chem. Res.* **27**, 143.
- Turner, M.D. (1993) "Supercritical water oxidation of dimethyl methylphosphonate and thiodiglycol." Doctoral Thesis, University of Texas at Austin. Austin, TX.
- Tsang, W. and Hampson, R.F. (1986) "Chemical kinetic data base for combustion chemistry. Part I. Methane and related compounds." *J. Phys. Chem. Ref. Data* **15**(3), 1087-1279.
- Uematsu, M. and Franck, E.U. (1980) "Static dielectric constant of water and steam." *J. Phys. Chem. Ref. Data* **9**(4), 1291-1306.
- Walker, R.E. (1961) "Chemical reaction and diffusion in a catalytic tubular reactor." *Phys. Fluids* **4**(10), 1211-1216.
- Webley, P.A. (1989) "Fundamental oxidation kinetics of simple compounds in supercritical water." Doctoral Thesis, Department of Chemical Engineering, Massachusetts Institute of Technology, Cambridge, MA.
- Webley, P.A. and Tester, J.W. (1988) "Fundamental kinetics and mechanistic pathways for oxidation reactions in supercritical water." SAE Technical Paper Series #881039, 18th Intersociety Conference on Environmental Systems, San Francisco, CA, July 11-13.

- Webley, P.A. and Tester, J.W. (1989) "Fundamental kinetics of methanol oxidation in supercritical water." *ACS Symp. Ser. 406: Supercritical Fluid Science and Technology*, K.P. Johnston and J.M.L. Penninger, eds. Washington, D.C.: American Chemical Society, pp. 259-275.
- Webley, P.A. and Tester, J.W. (1991) "Fundamental kinetics of methane oxidation in supercritical water." *Energy & Fuels* 5, 411-419.
- Webley, P.A., Holgate, H.R., Stevenson, D.M., and Tester, J.W. (1990) "Oxidation kinetics of model compounds of metabolic waste in supercritical water." SAE Technical Paper Series #901333, 20th Intersociety Conference on Environmental Systems, Williamsburg, VA, July 9-12.
- Webley, P.A., Tester, J.W., and Holgate H.R. (1991) "Oxidation kinetics of ammonia and ammonia-methanol mixtures in supercritical water in the temperature range 530-700°C at 246 bar." *Ind. Eng. Chem. Res.* 30(8), 1745-1754.
- West, P.W. and Sen, B. (1956) "Spectrophotometric Determination of Traces of Formaldehyde." *Z. Anal. Chem.* 153, 177.
- Wightman, T.J. (1981) "Studies in supercritical wet air oxidation." Masters Thesis, Department of Chemical Engineering, University of California at Berkeley, Berkeley, CA.
- Wilhelm, E., Battino, R., and Wilcock, R.J. (1977) "Low-pressure solubility of gases in liquid water." *Chem. Rev.* 77(2), 219-262.
- Williams, A.H. (1947) "The thermal decomposition of 2:2'-dichlorodiethyl sulphide." *J. Chem. Soc.* 318-320.
- Wilmanns, E.G. and Gloyna, E.F. (1990) "Supercritical water oxidation of volatile acids." Center for Research in Water Resources, Bureau of Engineering Research, University of Texas at Austin, Technical Report CRWR 218.
- Yang, H.H. and Eckert, C.A. (1988) "Homogeneous Catalysis in the Oxidation of p-Chlorophenol in Supercritical Water." *Ind. Eng. Chem. Res.* 27, 2009.
- Yang, Y-C., Ward, J.R., Luteran, T. (1986) "Hydrolysis of mustard derivatives in aqueous acetone-water and ethanol-water mixtures." *J. Org. Chem.* 51, 2756-2759.
- Young, P. C. (1982) "A Kinetic Study of the Catalytic Oxidation of Dichloromethane." Masters Thesis, Massachusetts Institute of Technology, Cambridge, MA.